



THE HONG KONG  
POLYTECHNIC UNIVERSITY

香港理工大學

Pao Yue-kong Library

包玉剛圖書館

---

## Copyright Undertaking

This thesis is protected by copyright, with all rights reserved.

**By reading and using the thesis, the reader understands and agrees to the following terms:**

1. The reader will abide by the rules and legal ordinances governing copyright regarding the use of the thesis.
2. The reader will use the thesis for the purpose of research or private study only and not for distribution or further reproduction or any other purpose.
3. The reader agrees to indemnify and hold the University harmless from and against any loss, damage, cost, liability or expenses arising from copyright infringement or unauthorized usage.

### IMPORTANT

If you have reasons to believe that any materials in this thesis are deemed not suitable to be distributed in this form, or a copyright owner having difficulty with the material being included in our database, please contact [lbsys@polyu.edu.hk](mailto:lbsys@polyu.edu.hk) providing details. The Library will look into your claim and consider taking remedial action upon receipt of the written requests.



**The Hong Kong Polytechnic University**

**Department of Civil and Structural Engineering**

**Development of a Framework for Real-time 3D Positioning  
and Visualization of Construction Resources**

**BY**

**XIONG LIANG**

**A THESIS SUBMITTED IN PARTIAL FULFILLMENT OF THE REQUIREMENTS FOR THE  
DEGREE OF DOCTOR OF PHILOSOPHY**

**January 2011**

## **CERTIFICATE OF ORIGINALITY**

I hereby declare that this thesis is my own work and that, to the best of my knowledge and belief, it reproduces no material previously published or written nor material that has been accepted for the award of any other degree or diploma, except where due acknowledgement has been made in the text.

\_\_\_\_\_ (Signed)

Xiong Liang (Name of student)

## **Abstract**

With the development of automated data collection technologies, construction resources can be tracked and positioned with ease and high accuracy. On the other hand, 3D computer graphics technologies have rapidly evolved to maturity with much reduced application cost. However, the lack of an approach to integrating real-time site data and 3D virtual design models has handicapped application of emerging technologies to the benefit of the construction industry.

Real-time 3D positioning and visualization of construction resources entails frequently updating the position and orientation of 3D models of site objects based on positioning and sensor data fed back from site in real time. This provides construction engineers with accurate spatial information about building elements being handled, and construction equipment in operation. The frequently updated 3D models also produce sufficient and accurate virtual references for locating and positioning building components and construction equipment in the field.

This research has developed a framework that consists of data models, algorithms and techniques to facilitate real-time 3D positioning and visualization of construction resources enabled by resource tracking on the jobsite. The construction resources are generally divided into two categories, namely: solid objects and articulated systems.

A “points to matrix” algorithm is developed to compute the position and orientation parameters for a solid object on site. In contrast with the solid object, construction equipment normally consists of a set of rigid bodies connected by joints, which is termed as a kinematic chain. The relative motion and constraints between successive bodies of the chain make the real-time 3D visualization a challenge, which requires

minimizing the number of sensors as needed on practical applications in construction. The Denavit-Hartenberg (DH) technique which is widely used in robotics research is introduced and adapted for computing the relative motions of various components in the articulated equipment system based on a minimal quantity of input parameters.

Considering the dynamic nature of construction industry, where new construction methods and equipment are being continuously adopted, coding the proposed methodologies in the computer system in an “ad hoc” manner entails substantial efforts for programming and system development, thus making application of the proposed methodology prohibitively expensive and practically infeasible. A graphic network modeling technique which is used in mechanical simulation systems is adapted to model the real-time 3D positioning and visualization applications.

To summarize, this research has contributed three aspects of new knowledge in the field of construction industry. First, instead of using expensive devices, the 3D position of solid objects can be analytically fixed by tracking the least amount of control points. Second, the 3D position of articulated construction equipment can be analytically fixed by analyzing point coordinates and joint movement parameters. Last, the possibility of applying the developed methodologies in real-time 3D visualization of microtunneling operations has been evaluated. The kinematic chain of the tunnel boring machine (TBM) is modeled without the need of programming. The positioning of TBM cutter head which is not visible in most TBM guidance systems can be visualized in computer 3D graphics. Thus, a TBM operator in a remote control station can make more informed decisions as regards how to steer the TBM drilling in the complicated underground space along the as-designed tunnel alignment.

The method for positioning and visualization of single solid object has been successfully validated by numerical analysis and laboratory experiments. The analytical method for positioning and visualization of articulated system has been validated by simulating a backhoe excavator in a computer environment, where the location of the backhoe' tracks is computed by using the "points to matrix" algorithm, and the positioning states of the cabin, boom, stick and bucket are deduced by using the DH technique.

## **Publications**

Liang, X., Lu, M. and Zhang, J.P. (2011) “On-site visualization of building component erection enabled by integration of four-dimensional modeling and automated surveying” *Automation in Construction*, Elsevier,20(3), 236-246.

Liang X., Lu M. “3D Visualization for Tunnel Boring Machine Steering and Alignment Control in Microtunneling”, *Construction Research Congress*, Banff, Canada, 2010.

Liang X., Lu M. and Zhang J.P. “3D Visualization of Articulated Micro-Tunnel Boring Machine during Pipe-jacking Operations”. *10th International Conference on Construction Applications of Virtual Reality*, Sendai, Miyagi, Japan, 2010

Liang, X., Lu, M. “Managing the Urban Underground Infrastructure Development through Automated Data Collection and Visualization” *Proceeding of 2nd International Postgraduate Conference on Infrastructure and Environment*, Hong Kong, China SAR, 2010.

Liang X., Lu M. and Zhang J.P. “Parametric 4D Modeling for Real-time Visualization of Microtunneling Operations” *First International Conference on Sustainable Urbanization*, Hong Kong, China SAR, 2010.

Liang X., Lu M. and Zhang J.P. “Integration of As-built and As-designed Models for 3d positioning control and 4D Visualization during Construction”. *9th International Conference on Construction Applications of Virtual Reality*, Sydney, Australia, 2009.

Liang X., Lu M., Zhang J.P. and Hu Z.Z. “A Case Study of Dynamic Construction Site Facilities Modeling in a 4D Environment”. *12th International Conference on Computing*

in Civil and Building Engineering, International Conference on Information Technology  
in Construction, Beijing, China, 2008.



## Acknowledgements

I express my sincere gratitude to my supervisor Dr. Ming Lu, for his guidance, suggestions and patience during the course of my doctoral study at the Hong Kong Polytechnic University. Without his mentoring, inspiration and continued support, this work could not have materialized.

I would also like to sincerely thank my co-supervisor, Professor JianPing Zhang of Tsinghua University, for her constructive suggestions, encouragement and support throughout my PhD study.

Thanks and good luck go out to the members of Dr. Lu's research group for their help, including Dr. Fei Dai, Dr. Xuesong Shen, Mr. Sze-Chun Lau, Mr. Hoi-Ching Lam, Mr. Ming-Fung Siu and Mr. Wah-Ho Chan. Special thanks go to Dr. Fei Dai and Dr. Xuesong Shen; we not only had many great meetings and constructive discussions, but also played squash almost every week, which had made my life as a PhD student much more interesting.

I would like to express my deepest gratitude to my parents Farun Liang and Suhua Xiong, my sister Lijuan Liang, my parents-in-law Jianmin Wu and Shuiyin Zou, my sister-in-law Xiaofang Wu, and my entire family for their continuous support, encouragement, understanding, and affection.

Most of all, I would like to thank my wife Lifang Wu for her love, companion and support during the most difficult time of my doctoral study. Special thanks to my little girl Atina who would come to the world almost at the same time as I finished this dissertation. Her arrival gives me a lot of inspiration and motivation.

Last but not least, thanks to the financial support provided by the Natural Science Foundation of China (National Key Technology R&D Program in the 11th Five Year Plan of China No. 2007BAF23B02) and The Hong Kong Polytechnic University through the Niche Area Research Grant (A/C No. BB89).

# Table of Contents

CERTIFICATE OF ORIGINALITY.....	I
ABSTRACT .....	II
PUBLICATIONS .....	V
ACKNOWLEDGEMENTS .....	VII
TABLE OF CONTENTS .....	IX
LIST OF FIGURES.....	XIV
LIST OF TABLES.....	XVII
<b>CHAPTER 1 INTRODUCTION .....</b>	<b>1</b>
1.1 INTRODUCTION.....	1
1.2 IMPORTANCE OF THE RESEARCH ACTIVITY .....	2
1.2.1 <i>3D Positioning of structural components during construction</i> .....	3
1.2.2 <i>Guidance to construction equipment operators</i> .....	6
1.2.3 <i>Effective use of large volume of site data</i> .....	8
1.2.4 <i>Leverage the application of 3D/4D modeling</i> .....	9
1.3 POSITIONING AND VISUALIZATION OF CONSTRUCTION RESOURCES .....	10
1.4 RESEARCH OBJECTIVES .....	15
1.4.1 <i>Detailed objectives of conducting this research</i> .....	16
1.5 METHODOLOGY.....	19
1.6 DISSERTATION OUTLINE .....	21
<b>CHAPTER 2 FUNDAMENTALS OF 3D POSITIONING AND VISUALIZATION OF CONSTRUCTION</b>	
<b>RESOURCES 25</b>	
2.1 3D POSITIONING.....	25
2.1.1 <i>Location</i> .....	25
2.1.2 <i>Orientation</i> .....	27

2.2	3D VISUALIZATION .....	29
2.2.1	<i>3D geometric modeling</i> .....	31
2.2.2	<i>Kinematic analysis</i> .....	33
2.3	THE UPDATE RATE FOR A REAL-TIME SYSTEM IN CONSTRUCTION APPLICATIONS .....	34
2.4	CLASSIFICATION OF CONSTRUCTION RESOURCES .....	36
2.5	ARTICULATED SYSTEM .....	38
2.5.1	<i>Kinematic Chain</i> .....	38
2.5.2	<i>Degree of freedom</i> .....	40
2.6	SUMMARY .....	41
<b>CHAPTER 3</b>	<b>REAL-TIME 3D POSITIONING AND VISUALIZATION OF SOLID OBJECTS .....</b>	<b>43</b>
3.1	INTRODUCTION .....	43
3.2	IMPORTANCE OF THE RESEARCH .....	44
3.2.1	<i>Industry practical needs</i> .....	44
3.2.2	<i>Streamlining the 3D design and on-site construction</i> .....	45
3.2.3	<i>Facilitating the spatial integration in construction</i> .....	45
3.3	OVERVIEW OF PROPOSED METHODOLOGY .....	47
3.4	THE DATA MODELS .....	48
3.5	SURVEYING TRACKING POINTS .....	52
3.6	TRANSFORMATION .....	54
3.6.1	<i>Numerical Example</i> .....	57
3.7	COMPUTING ROTATION ANGLES .....	59
3.8	COMPUTER PROTOTYPE DEVELOPMENT .....	62
3.9	LABORATORY TEST .....	66
3.9.1	<i>Computation by using the proposed algorithm</i> .....	70
3.9.2	<i>Comparing the calculated results with the measured results</i> .....	74
3.9.3	<i>Visualization of the computing results</i> .....	75
3.10	SUMMARY .....	77
<b>CHAPTER 4</b>	<b>REAL-TIME 3D POSITIONING AND VISUALIZATION OF ARTICULATED SYSTEM .....</b>	<b>79</b>

4.1	INTRODUCTION.....	79
4.2	IMPORTANCE OF THE RESEARCH .....	81
4.2.1	<i>Improving the performance of construction equipment operations</i> .....	81
4.2.2	<i>Important component in construction automation system</i> .....	82
4.3	OVERVIEW OF THE PROPOSED METHODOLOGY .....	82
4.4	THE GENERIC DATA MODELS FOR ARTICULATED SYSTEM .....	85
4.4.1	<i>Data models for backhoe</i> .....	87
4.5	KINEMATIC MODELING .....	89
4.5.1	<i>Frames assignment</i> .....	89
4.5.2	<i>Representation of frame position and orientation using DH parameters</i> .....	93
4.6	3D POSITIONING ANALYSIS.....	96
4.6.1	<i>Raw data from joint sensors</i> .....	96
4.6.2	<i>Computing the rotation angles by laws of trigonometry</i> .....	97
4.6.3	<i>Principles of forward kinematics</i> .....	98
4.6.4	<i>The location of the base frame</i> .....	100
4.7	VALIDATION.....	100
4.7.1	<i>Validation on 2D experiments</i> .....	102
4.7.2	<i>Validation on 3D experiments</i> .....	107
4.8	SUMMARY .....	116
<b>CHAPTER 5 GRAPHIC NETWORK MODELING FOR 3D POSITIONING AND VISUALIZATION OF CONSTRUCTION RESOURCES.....</b>		<b>118</b>
5.1	INTRODUCTION.....	118
5.2	BACKGROUND .....	119
5.2.1	<i>Simulink environment</i> .....	120
5.3	METHODOLOGY.....	121
5.3.1	<i>Built-in graphic blocks</i> .....	121
5.3.2	<i>Custom graphic blocks</i> .....	123
5.3.3	<i>Modeling process</i> .....	125

5.4	APPLICATION .....	127
5.5	SUMMARY .....	132
<b>CHAPTER 6</b>	<b>APPLICATION POSSIBILITY IN POSITIONING TUNNEL BORING MACHINES .....</b>	<b>134</b>
6.1	INTRODUCTION.....	134
6.2	BACKGROUND .....	135
6.2.1	<i>The practical industrial needs.....</i>	<i>135</i>
6.2.2	<i>Kinematics of MTBM .....</i>	<i>137</i>
6.2.3	<i>Virtual reality in construction applications.....</i>	<i>138</i>
6.3	PREPARATION FOR THE EVALUATION .....	139
6.3.1	<i>Preparation of input data .....</i>	<i>140</i>
6.3.2	<i>3D Geometric modeling.....</i>	<i>147</i>
6.3.3	<i>Kinematic modeling.....</i>	<i>148</i>
6.3.4	<i>“Points to matrix” transformation .....</i>	<i>150</i>
6.4	POTENTIAL BENEFITS AND LIMITATIONS .....	150
6.4.1	<i>Positioning and visualization of MTBM’s position and orientation.....</i>	<i>151</i>
6.4.2	<i>Positioning and visualization of cutter head control system .....</i>	<i>153</i>
6.4.3	<i>Limitations and future work .....</i>	<i>155</i>
6.5	FUTURE DEVELOPMENT OF VISUALIZATION SYSTEM .....	156
6.6	SUMMARY .....	158
<b>CHAPTER 7</b>	<b>CONCLUSIONS .....</b>	<b>160</b>
7.1	CONTRIBUTIONS .....	160
7.2	DIRECTIONS FOR FUTURE RESEARCH .....	163
7.2.1	<i>Interaction between solid objects and articulated systems .....</i>	<i>164</i>
7.2.2	<i>Automated as-built modeling.....</i>	<i>164</i>
7.2.3	<i>Considering dynamics.....</i>	<i>165</i>
<b>APPENDIX A.</b>	<b>MATLAB FUNCTION OF THE “POINT TO MATRIX” CUSTOM BLOCK .....</b>	<b>166</b>
<b>APPENDIX B.</b>	<b>DATA COLLECTED BY THE TOTAL STATION .....</b>	<b>169</b>

REFERENCES: .....172

# List of Figures

FIGURE 1-1: THE REAL CASE OF LARGE-SCALE STRUCTURAL STEEL COMPONENTS ASSEMBLY.....	3
FIGURE 1-2: POSITIONING LARGE-SCALE STRUCTURAL STEEL COMPONENTS DURING ASSEMBLY.....	4
FIGURE 1-3: THE REAL-TIME 3D POSITIONING AND VISUALIZATION TECHNIQUES FOR LARGE-SCALE STRUCTURAL COMPONENTS ASSEMBLY.....	5
FIGURE 1-4: FREQUENTLY UPDATING THE COMPUTER GENERATED VIRTUAL SCENES TO REFLECT THE REAL WORLD BUILDING COMPONENT MOVEMENT.....	6
FIGURE 1-5: REAL-TIME 3D POSITIONING AND VISUALIZATION OF TBM FOR SUPPORTING OPERATORS TO MAKE DECISIONS...	7
FIGURE 1-6: MAPPING THE REAL CONSTRUCTION SITE ENVIRONMENT TO VIRTUAL REALITY ENVIRONMENT TO SUPPORT CONSTRUCTION ENGINEERING AND MANAGEMENT TASKS.....	16
FIGURE 1-7: THE METHODOLOGY APPLIED TO CONDUCT THIS RESEARCH .....	19
FIGURE 1-8: THE ITERATION PROCESS FOR DEVELOPMENT OF THE PROPOSED DATA MODELS .....	21
FIGURE 1-9: GRAPHICALLY REPRESENTATION OF THE DISSERTATION OUTLINE .....	23
FIGURE 2-1: THE LOCATION OF A SOLID OBJECT.....	26
FIGURE 2-2: THE ORIENTATION OF A SOLID OBJECT .....	28
FIGURE 2-3: THREE TYPES OF JOINTS COMMONLY USED IN CONSTRUCTION EQUIPMENT .....	39
FIGURE 2-4: ROBOCRANE DEVELOPED BY NIST .....	40
FIGURE 3-1: OVERVIEW OF THE PROPOSED METHODOLOGY FOR REAL-TIME 3D POSITIONING AND VISUALIZATION OF SOLID SITE OBJECTS.....	47
FIGURE 3-2: THE PRODUCT DATA MODEL FOR A TYPICAL BUILDING PROJECT.....	50
FIGURE 3-3: DECOMPOSING A PRODUCT MODEL INTO CONSTRUCTION LEVEL OF DETAILS .....	51
FIGURE 3-4: INCORPORATING THE ASSEMBLY DETAILS IN THE DATA MODEL: EXAMPLE AND DATA STRUCTURE .....	52
FIGURE 3-5: THE INITIALIZATION OF TOTAL STATION LOCATION FOR POSITIONING A STEEL COLUMN; NUMERAL IDs IN THE FIGURES IDENTIFY: (1) TOTAL STATION (2) FIXED CONTROL POINTS (3) PRISM ATTACHED ON A TRACKING POINT .....	53
FIGURE 3-6: AN ILLUSTRATIVE 2D EXAMPLE.....	58
FIGURE 3-7: THE RIGHT HAND RULE FOR SPECIFYING THE POSITIVE DIRECTION OF THE ROTATIONS ABOUT THE THREE AXES...	60
FIGURE 3-8: THE SOFTWARE ARCHITECTURE OF 4D-POS CON .....	63



FIGURE 3-9: CONCEPTUALIZATION OF THE APPLICATION OF 4D-PosCON SYSTEM ON A CONSTRUCTION SITE DURING STRUCTURAL STEEL INSTALLATION .....	64
FIGURE 3-10: PSEUDO CODE SPECIFYING EXECUTION PROCEDURE OF 4D-PosCON .....	64
FIGURE 3-11: GRAPHICAL USER INTERFACE OF 4D-PosCON.....	66
FIGURE 3-12: THE SET UP OF THE LABORATORY TEST: (A) LEICA TCA 1000 TOTAL STATION CONNECTED TO A LAPTOP COMPUTER USING RS232 CABLE; (B) THREE REFLECTIVE TAPES ADHERED TO TRACKING POINTS ON A BLACK BOX; (C) AS-DESIGNED STATE (TIME EVENT T <sub>0</sub> ) OF THE BOX IMPORTED INTO 4D-PosCON .....	67
FIGURE 3-14: SURVEYING DATA AND COMPUTING RESULTS FOR FOUR POSITIONING STATES OF THE BOX .....	69
FIGURE 3-16: VISUALIZATION OF THE ROTATION DEVIATIONS ON THE BOX.....	76
FIGURE 4-1: THE LOGICAL FLOW CHART OF THE PROPOSED METHODOLOGY .....	83
FIGURE 4-2: A GENERIC DATA MODELS FOR ARTICULATED SYSTEM .....	87
FIGURE 4-3: THE 3D MODEL OF A TYPICAL BACKHOE .....	88
FIGURE 4-4: THE DATA MODEL OF THE BACKHOE AND THE PROBLEMS WILL BE ADDRESSED BY KINEMATIC MODEL.....	89
FIGURE 4-5: FRAME ASSIGNMENT ON A BACKHOE .....	90
FIGURE 4-6: ASSIGNMENTS OF AXIS X <sub>2</sub> IN THE CASE THAT <b>z<sub>1</sub></b> IS PARALLEL TO <b>z<sub>2</sub></b> .....	92
FIGURE 4-7: TOP VIEW OF BACKHOE SHOWING THE FRAMES ASSIGNED .....	92
FIGURE 4-8: THE RIGHT HAND RULE ON THE DIRECTION OF AXIS Y .....	92
FIGURE 4-9: ILLUSTRATION OF DH PARAMETERS FROM FRAME F <sub>i-1</sub> TO FRAME F <sub>i</sub> .....	94
FIGURE 4-10: DH PARAMETERS OF THE BACKHOE EXAMPLE .....	95
FIGURE 4-11: SENSORS FOR REVOLUTE AND PRISMATIC JOINTS .....	97
FIGURE 4-12: TRANSLATE THE LINEAR ENCODER DATA TO THE DH PARAMETERS .....	98
FIGURE 4-13: A TWO DIMENSIONAL ARTICULATED SYSTEM .....	102
FIGURE 4-14: THE ROTATION ANGLES CAN BE COMPUTED FROM LINEAR ENCODER DATA.....	105
FIGURE 5-1: THE PARAMETERS DIALOG OF BODY BLOCK .....	126
FIGURE 5-2: THE PARAMETERS DIALOG OF REVOLUTE JOINT BLOCK .....	126
FIGURE 5-3: THE CONFIGURATIONS OF THE BACKHOE EXCAVATOR .....	128
FIGURE 5-4: MODELING THE BACKHOE EXCAVATOR USING BODY BLOCKS AND JOINT BLOCKS.....	129
FIGURE 5-5: THE PARAMETERS DIALOG OF GROUND BLOCK. ....	129
FIGURE 5-6: EXTEND THE KINEMATIC MODEL WITH CUSTOM BLOCKS TO LINK THE REAL-TIME DATA .....	130

FIGURE 5-7: THE DATA MODEL DEVELOPED FOR REAL-TIME 3D POSITIONING AND VISUALIZATION OF BACKHOE EXCAVATOR .....	131
FIGURE 5-8: 3D VISUALIZATION BY LINKING THE COMPUTATION RESULT WITH THE ROHT DATA MODEL.....	132
FIGURE 6-1: THE COMMONLY USED VISUALIZATION APPROACH FOR MTBM REMOTE CONTROL .....	136
FIGURE 6-2: THE KINEMATIC CHAINS OF MTBM.....	138
FIGURE 6-3: OVERVIEW OF THE APPLICATION PROCEDURE .....	140
FIGURE 6-4: THE CONFIGURATION OF THE POINT COORDINATES COLLECTION SYSTEM .....	142
FIGURE 6-5: THE STATIC 3D MODELS FOR A MICRO-TUNNELING PROJECT .....	148
FIGURE 6-6: THE KINEMATIC MODEL OF MTBM IN SIMULINK ENVIRONMENT.....	149
FIGURE 6-7: CODING THE “POINTS TO MATRIX” TRANSFORMATION ALGORITHM IN USER-DEFINED APPLICATION BLOCKS ...	150
FIGURE 6-8: THE DATA FLOW AND VISUALIZATION RESULT OF THE FIRST EXPERIMENT .....	153
FIGURE 6-9: THE DATA FLOW AND VISUALIZATION RESULTS OF THE SECOND EXPERIMENT .....	154
FIGURE 6-10: THE MODULES AND DATA FLOW OF NEXT GENERATION 4D SYSTEM FOR REAL-TIME 3D VISUALIZATION OF CONSTRUCTION OPERATIONS.....	157

## List of Tables

TABLE 2-1: CLASSIFICATION OF CONSTRUCTION RESOURCES .....	37
TABLE 3-1: TRANSFORMATION OF THE COORDINATES FROM TOTAL STATION CS TO BOX CS .....	71
TABLE 3-2: THE CALCULATED RESULTS AND THE MEASURED RESULTS .....	74
TABLE 4-1: DH PARAMETERS OF THE BACKHOE EXAMPLE .....	96
TABLE 4-2: DH PARAMETERS OF THE BACKHOE EXAMPLE .....	104
TABLE 4-3: THE INPUT CONFIGURATION OF THE ARTICULATED SYSTEM:.....	109
TABLE 4-4: THE INPUT DATA FOR THE SIX EXPERIMENTS .....	109
TABLE 4-5: THREE EXPERIMENTS AND THE ACTUAL RESULTS BY THE LAW OF TRIGONOMETRY.....	109
TABLE 4-6: THE CALCULATED RESULTS FROM THE PROPOSED METHODOLOGY.....	113
TABLE 4-7: THE CALCULATED RESULTS FROM THE PROPOSED METHODOLOGY.....	114
TABLE 4-8: VALIDATION BY VISUALIZING THE ACTUAL POSE AND THE CALCULATED TARGET POINT “E” .....	114
TABLE 5-1: GRAPHIC ELEMENTS FOR KINEMATIC MODELING OF CONSTRUCTION EQUIPMENT.....	122
TABLE 5-2: THE THREE TYPES OF MATLAB FUNCTION BLOCKS FOR DEVELOPING CUSTOM BLOCKS .....	124
TABLE 6-1: THE COORDINATES OF TARGET POINTS .....	142

# ***Chapter 1***

## ***Introduction***

### **1.1 Introduction**

The purpose of this research is to find methods that can be easily adopted by construction practitioners to model real construction site operations into a virtual reality environment with sufficient accuracy in 3D spatial relationships as well as sufficient updating frequency in accordance to application requirements in the construction engineering and management domain. The fundamental question addressed in this research is how construction practitioners, who may not have the skill of programming and software development, can easily embrace advanced reality capturing and 3D computer graphic technologies to position and visualize various construction resources (building elements, equipment, material, and crews etc.) in 3D and at the time they are moving/working in the field. Construction resources are positioned in 3D not only in terms of three coordinate values (x, y and z) but also in terms of the pose of those resources in the 3D space.

The end result of the research effort consists of a set of formalized 3D positioning data models, data transformation algorithms, and motion modeling methodologies, which facilitate (1) mapping the real-time site sensor data into a formalized 3D positioning

data model for single solid construction site objects, such as large-scale structural steel components of high-rise buildings; (2) mapping the real-time site sensor data to a formalized 3D positioning data model for construction equipment with articulated mechanical systems, such as backhoes and tunnel boring machines; and (3) integration of formalized 3D positioning data models with the computer generated virtual environment, such as 4D CAD and virtual reality tools, to realize real-time visualization of construction operations.

## **1.2 Importance of the research activity**

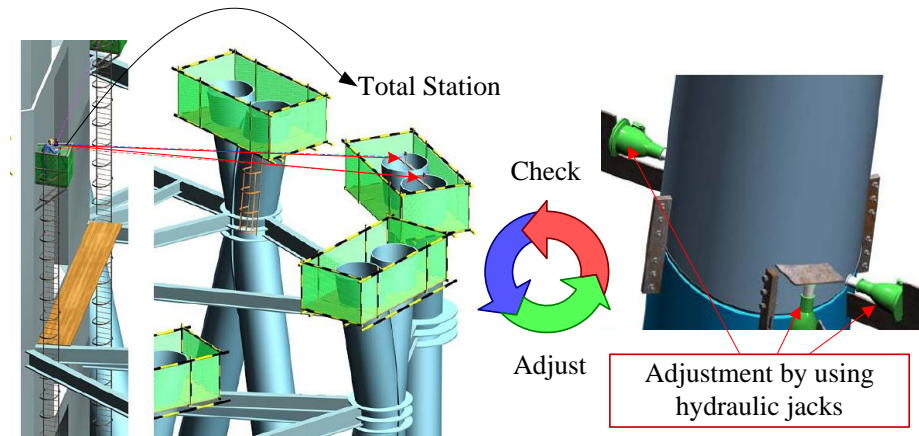
The fundamental rationale of conducting this research lies mainly in following facts: (1) a number of significant application values can be gained by incorporating real-time 3D positioning and visualization techniques in construction practices, such as surveying integrated construction, tele-operation of construction equipment, and alignment control during tunnelling and pipe-jacking; (2) although the integration of advanced computer and information technologies, such as 3D/4D CAD, in construction practices has brought innovations to the construction industry, there is still a wide gap between the real construction site and the virtual design environment. The real-time 3D positioning and visualization technologies may partially fill the gap, leveraging the application of state-of-the-art computer and information technologies to improve construction practices.

### ***1.2.1 3D Positioning of structural components during construction***

A large number of construction operations performed in the field require accurate positioning of structural components (pipe sections, prefabricated wall, beam, and column etc.) as per design (Bernold 2002). The photos in Figure 1-1 show the procedure of assembling large-scale structural steel components in a high-rise building project. As observed by the contractor, the accurate positioning of these components during their erection processes (the weight of each ranging from 30 ton to 100 ton) is the most time-consuming and costly task, as specialist surveying crew and equipment are required to ensure very accurate pose control during erection. Normally, for each column segment, the crew needs to adjust its pose several times. Furthermore, the temperature between day time and night is so different that geometric dimensions and shapes of these steel components can be significantly affected. Thus workers may need to wait until the evening to adjust the position and pose of these building components so as to minimize the temperature effect.



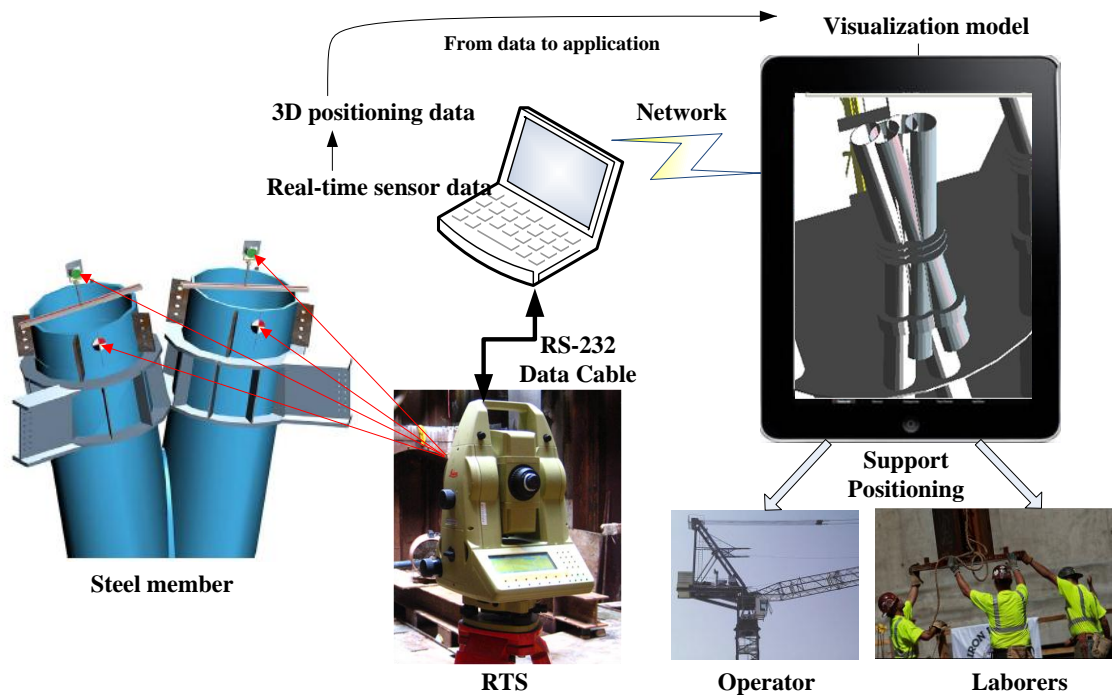
**Figure 1-1: The real case of large-scale structural steel components assembly**



**Figure 1-2: Positioning large-scale structural steel components during assembly**

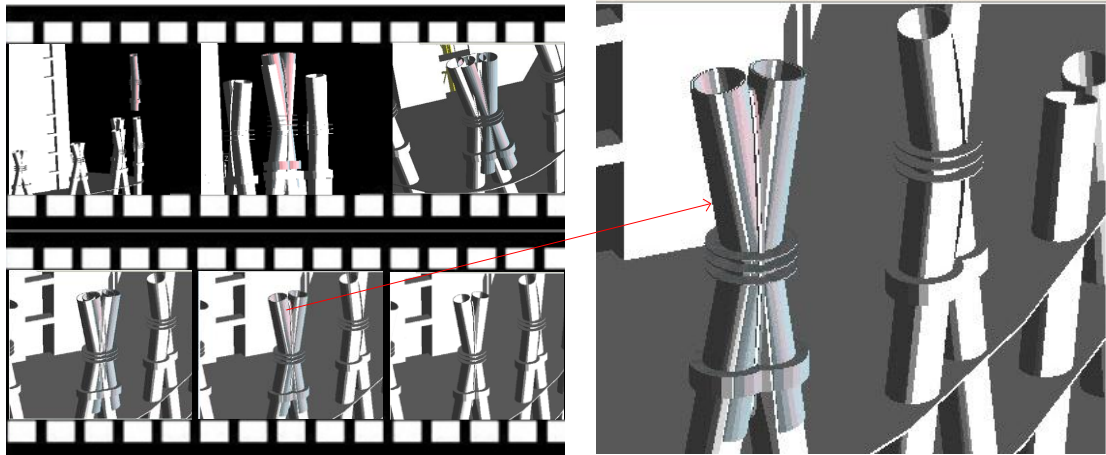
Figure 1-2 illustrates the state-of-the-art technique for positioning structural steel column segments as per design. The steel column segment being assembled is positioned based on checking a number of reference points by using instruments such as theodolites, levels, total stations. These are labour intensive tasks jointly performed by installation workers, crane operators, site engineers and surveyors. The positioning procedure (fixing the element temporarily, checking its location with a measuring device, adjusting it, and then checking it again) is very time-consuming and highly repetitive, considering the large quantity of structural components to be assembled on a typical project. Furthermore, obtaining coordinate values (x, y, z) of reference points only is insufficient to achieve accurate 3D orientation, which is vital to ensuring structural safety for buildings featuring nonconventional structure design, for instance, a structure with a double curved profile. Since point coordinate values do not directly indicate the rotation angles of the building component in the 3D space, and small deviations on the point coordinate values may result in large orientation errors.

Real-time 3D positioning building components being assembled and visualizing them in a computer generated virtual reality environment offers substantial benefits to improve current construction practices. Figure 1-3 illustrates the concept of real-time 3D positioning and visualization of large-scale building components during installation operations. The coordinate values of reference points surveyed by a robotic total station (RTS) are processed into 3D positioning data, which are then fed to the computer graphic engine to update the pose of the computer generated 3D geometry model on a real-time basis. As shown in Figure 1-4, the virtual scenes are linked with the steel component movement in the real world during construction operations.



**Figure 1-3: The real-time 3D positioning and visualization techniques for large-scale structural components assembly**





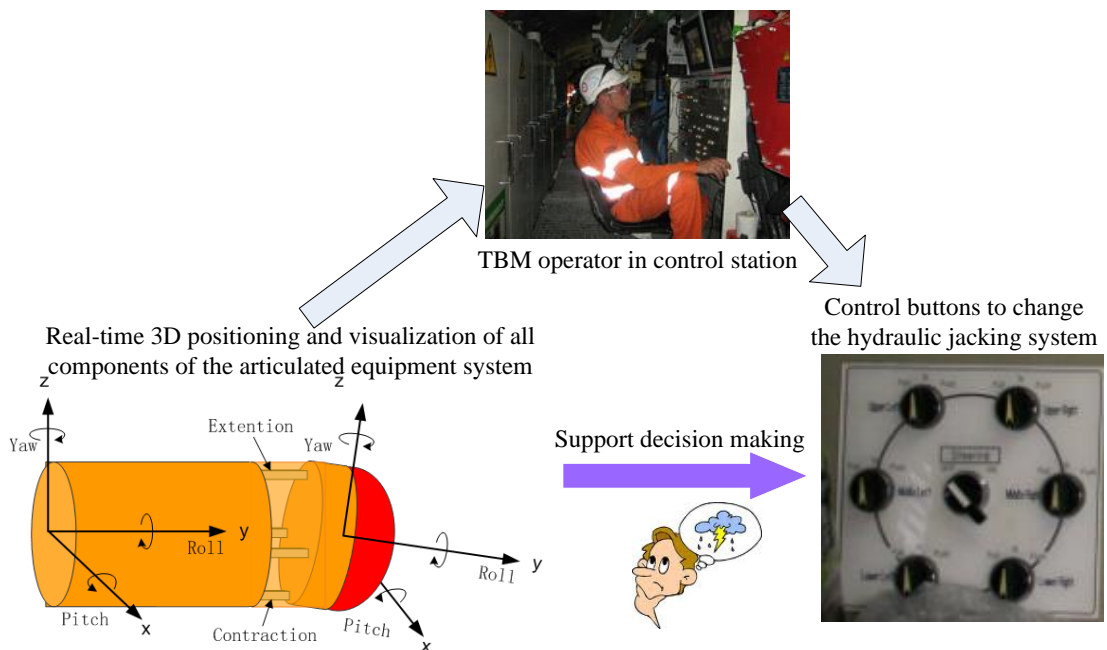
**Figure 1-4: Frequently updating the computer generated virtual scenes to reflect the real world building component movement**

The above 3D positioning and visualization techniques enable surveying-integrated construction as follows: the as-designed model in the virtual reality environment provides a cost-effective and information-intensive virtual reference, to which the building component being tracked is gradually approaching; when they converge in the virtual environment, it indicates that the building component is placed as per design in the real world. With this integration, productivity and quality of installation operations can be significantly improved by enhancing spatial perception and situational awareness of the crew.

### ***1.2.2 Guidance to construction equipment operators***

Vision is the main source of information that equipment operators count on for positioning and obstacle avoidance (Hirabayashi et al. 2006). However, on a dynamic construction site, the vision can be blocked frequently by numerous obstacles such as materials, temporary or permanent facilities, equipment, and even workers. In particular,

the visual information is extremely limited in underground construction environments, such as micro-tunneling. Using real-time site data to update the computer generated 3D virtual scenes of the construction site is a promising approach to enhancing spatial perception and situational awareness of a tunnel boring machine (TBM) operator.



**Figure 1-5: Real-time 3D positioning and visualization of TBM for supporting operators to make decisions**

As shown in Figure 1-5, the 3D model of a TBM is updated by using the real-time data sourced from an automated TBM guidance system. Operators count on the visual information to make decisions on steering the TBM at a remote control station. Since the as-designed tunnel alignment can be easily merged into the virtual reality environment, TBM operators can identify any alignment deviations as soon as they occur in the field. The 3D pose of all parts of the articulated TBM mechanical system

can be visualized on the fly, thus operators can easily find the most efficient way to correct alignment deviations.

### ***1.2.3 Effective use of large volume of site data***

Many researchers have found that visualization is an effective way to represent and communicate a large volume of information. Visual information is more effective and efficient to understand and communicate than using texts and numerals. Furthermore, a more effective use of the real-time information depends on how the data is visualized (Cheng and Teizer 2010), as the visualization can help people retrieve, analyze and interpret information from a large volume of data.

The rapid advancement and wide application of automated data collection technologies have made construction sites more intelligent and integrated than decades ago. As envisioned by the Fully Integrated and Automated Technology (FIATCH) consortium, construction resources such as materials, components, tools, equipment, and even people will become elements of a fully sensed and monitored environment (Lytle and Saidi 2007). However, currently the large volume of sensor data makes the construction site a data-rich, but information-poor environment, thereby resulting in the failure of judicious handling of important situations at a given point in time (Rojas and Lee 2007). 3D positioning and visualization of the construction resources can facilitate people to

retrieve information from the large volume of sensor data by representing the information in 3D computer graphics in real time.

#### ***1.2.4 Leverage the application of 3D/4D modeling***

With the advance of computer technology, more and more construction projects have embraced 3D/4D models in design and management processes (Hartmann and Fischer 2007; Mahalingam et al. 2010; Staub-French 2007). The benefits which can be potentially gained from applications of 3D/4D models have been documented by many researchers. However, we enlist many project managers' views on limitations of such technology that have motivated the present research. One common observation is that the cost of 4D modeling is very high, but it is only used on one or two occasions in the early stages of project development, e.g. to facilitate the communication of contractors' bid proposals with owners. Then the 4D models are often shelved without follow-up applications. This observation was also echoed by Hartman et al. (2008) who analyzed twenty-six case studies of 3D/4D model applications on construction projects. They reported that practitioners mostly used the models in one application area only (Hartmann et al. 2008).

The research on integration of 3D/4D models in construction practices should address the more widespread use of 3D/4D models throughout the lifecycle of a project (Hartmann et al. 2008). 3D positioning and visualization of construction resources is a

straightforward way to extend the existing 3D/4D models to facilitate various critical construction engineering tasks in the field, thus significantly broadening the application of 3D/4D models in construction practices.

### **1.3 Positioning and visualization of construction resources**

Positioning and visualization are two different but closely related technologies. A construction resource such as a prefabricated column can be, without visualization, positioned by numeric values in a coordinate system. Similarly, without the positioning data the resource can be visualized in 3D computer graphics using its geometric data. However, visualization without positioning data can only reflect geometric shapes, without informing where it is and the status/pose at a particular point of time. On the other hand, positioning without computer generated visualization requires people to imagine the actual situation in their mind, which can be mentally challenging and insufficient given the complexity of the situation.

In construction, the integration of the two technologies has been studied by some researchers. Bernold conceptualized the spatial integrated construction by merging spatial design data with the 3D model of working equipment during the process of implementing the design (Bernold 2002). Seo et al. developed a graphical control interface for tele-operations that can update the graphical representation of equipment

and the work environment in real time (Seo et al. 2000). The National Institute of Standards and Technology (NIST)'s Construction Methodology and Automation Group developed a robot crane and associated visualization software named as "JobSight", which was used to display pose and planned trajectory of the robot crane (Lytle and Saidi 2007).

The benefits of visualization and positioning integration in real time are apparent, however, the research efforts have largely focused on evaluation, validation, or verification of the technical feasibility in specific application scenarios. There is a lack of research in understanding the relationship between the two technologies, and also a lack of methodologies which can be adapted to various construction applications in order to facilitate the integration of the two technologies (Chin et al. 2008).

With the development of advanced positioning technologies, such as Global Positioning System (GPS), total station, and laser scanner etc., researchers have developed methods for locating construction resources for quality, safety and productivity improvement. For example, locating construction materials by using GPS (Caldas et al. 2006; Ergen et al. 2007b), identification and localization of construction components by using Radio-Frequency Identification (RFID) (Song et al. 2006; Torrent and Caldas 2009). The present research differs from those efforts in that it not only concerns about the

location of construction resources but also the real time determination and visualization of their pose/orientation on the site.

Site data captured by positioning technologies underlie techniques developed for 3D positioning and visualization of construction resources, while positioning technologies applicable to construction sites vary in functionality, accuracy, cost and difficulty of deployment. Hence, a rigorous evaluation of these technologies is important to conduct the current research.

GPS is available worldwide to provide position of latitude, longitude and altitude to any object equipped with a GPS receiver. GPS is particularly appropriate for outdoor applications, such as tracking user's positions in open sites (Behzadan et al. 2008). However, GPS signals transmitted from the satellites can be easily blocked and deflected on a construction site (Torrent and Caldas 2009), compromising the reliability and accuracy in positioning resources on site. The positioning accuracy provided by commonly available GPS is in order of a few meters, while high precision GPS solutions with achievable accuracy in centimeters [such as real time kinematics (RTK) GPS] are expensive in terms of application cost, entailing complicated system setup and calibration (Lu et al. 2007).

Ultra-wideband (UWB) is a more recent commercially available radio frequency technology that operates at very low energy levels for short-range high-bandwidth data communication on a wide spectrum of radio frequencies. It can be used for precision locating and tracking of construction laborers, equipment, and materials in semi-open areas (Teizer et al. 2008). Although UWB has the advantages of “see-through-the-wall” positioning with higher accuracy and lower uncertainty [0-50 cm according to (Khoury and Kamat 2009)], it is a relatively expensive technology and requires significant time and effort to deploy the hardware (the hub and receivers) around the coverage area (Khoury and Kamat 2009).

Radio-Frequency Identification (RFID) is one of the most explored and matured technologies with successful applications in identification and localization of construction components (Song et al. 2006; Torrent and Caldas 2009), progress management (Chin et al. 2008) and construction quality inspection and management (Wang 2008). RFID does not require (1) line-of-sight, (2) close proximity, (3) individual readings, or (4) direct contact. A RFID tag features data entry and access at any time, as well as data storage capability (Kiziltas et al. 2008). The main factor that impedes the application of RFID for positioning structural components during installation lies in its low positioning accuracy, which can only indicate approximate locations of building components on site (Song et al. 2007).



Laser scanning is another reality capturing technology that uses a laser scanner to capture vast amounts of measurements of points (point clouds) in the target object and its vicinity (Kiziltas et al. 2008). Nevertheless, it is computationally intensive and difficult to filter various sources of noises and to register multiple scans in generation of a more comprehensive, accurate set automatically (Cho et al. 2002; Kiziltas et al. 2008).

Photogrammetry originates from the discipline of surveying and is capable of extracting input data from two-dimensional photo images and mapping them onto a three-dimensional space (Dai and Lu 2010). However its accuracy is largely dependent on the quality of the camera used, the quality of the photos taken and the functionality of the photo-processing software applied. For an off-the-shelf digital camera with fixed focal length and eight megapixel image resolution, the achievable accuracy level was found to be in the order of one to two centimeters in comparison with a conventional measurement tape (Dai and Lu 2010).

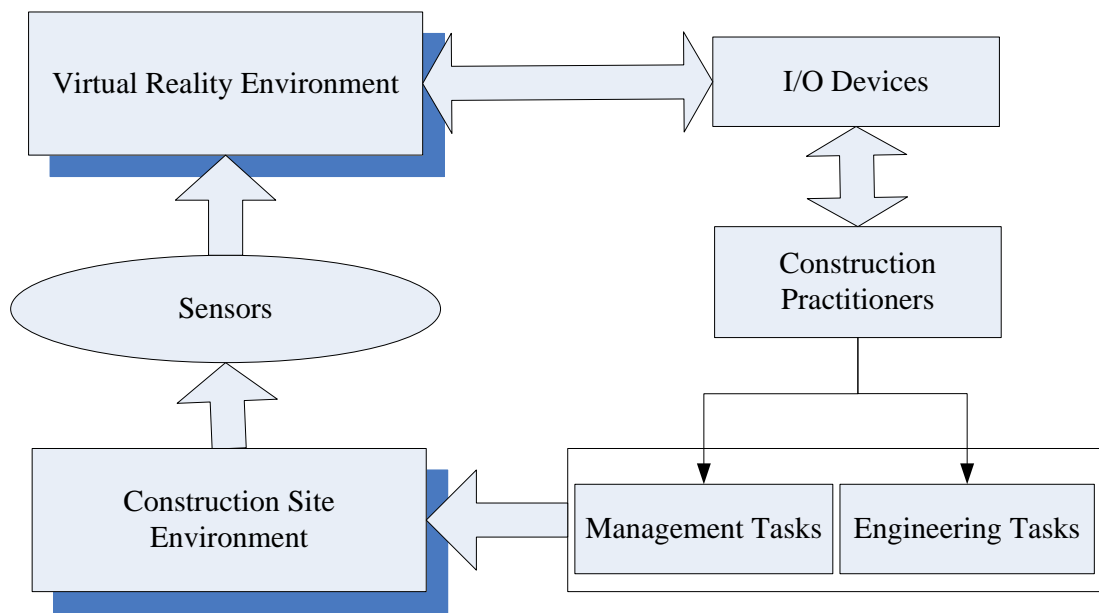
Total station is a kind of high precision surveying instrument, which has replaced transits and theodolites and increasingly becomes the predominant instrument used in surveying practices (Ghilani and Wolf 2008). A modern robotic total station functions like a surveying robot, which is capable of automatic target tracking as controlled by pre-programmed surveying procedures. With the programmable interface provided, the coordinates of a limited quantity of points can be automatically collected in a certain

frequency and with high accuracy in order of a few millimeters, making a robotic total station ideal for positioning control during the installation of building components. From our site investigation on a high rise building (the “West Tower” in Guangzhou, China) in 2007-2008, it was observed total stations were used to position large-scale structural steel components in construction operations.

#### **1.4 Research objectives**

Real-time 3D positioning and visualization of construction resources working in the field is a complex and challenging proposition. Firstly, it is necessary to accurately represent the real position and movement of construction resources. These data cannot be modeled in computer systems through a human-machine interface. Thus, appropriate positioning techniques are required to track the movements of site objects in real-time and to capture sufficient data automatically for later analysis and modeling. Secondly, In order to visualize construction resources, it is necessary to model their geometry profile in 3D, either directly by 3D CAD tools or through automated as-built modeling techniques like laser scanner and Photogrammetry etc. Lastly, mapping algorithms and technologies are needed to link positioning data with the 3D geometric model in the virtual environment.

To summarize, the main objective of this research is to find methods to map the real construction site environment to the virtual reality environment in real time. As shown in Figure 1-6, the fundamental question addressed in this research is how to effectively and efficiently link the two environments through the integration of positioning/sensor technologies and techniques for 3D/4D computer graphics, so that users can rely on the real-time updated virtual reality environment to facilitate the execution of construction engineering and management tasks performed in a real construction site.



**Figure 1-6: Mapping the real construction site environment to virtual reality environment to support construction engineering and management tasks**

### ***1.4.1 Detailed objectives of conducting this research***

Notwithstanding potential application values could be gained by incorporating 3D positioning and visualization techniques in construction practices, several challenges must be addressed so as to realize system development and solution application in the

construction field. Thus, tackling the following difficulties leads to identification of particular objectives for conducting this current research.

#### ***1.4.1.1 The gaps between positioning technologies and 3D positioning data***

As discussed in Section 2, each positioning/sensor technology has its own limitations. Thus, generally, a single positioning technology cannot directly provide the full set of 3D positioning data as required for positioning and visualization integration in a 4D environment. For example, a total station can determine coordinate values of the points marked on a solid object, but the coordinates of points data itself does not inform the orientation angles of the object. Conversely, a gyroscope or inclinometer can gauge the orientation angles of the object but the angle data itself cannot provide the coordinate values of the object's location.

There are also many constraints on the construction site, that it is sometimes difficult to deploy the positioning equipment/instrument for 3D positioning some construction resources or some part of a resource. For example, in micro-tunneling and pipe-jacking operations, it is very difficult to deploy instruments in the confined tunnel space in order to position the cutter head of the tunnel boring machine.

#### ***1.4.1.2 The dynamic nature of construction industry***

Due to the dynamic nature of construction industry, new construction methods and new equipment are continuously adopted. Yet, practical applications for 3D positioning and

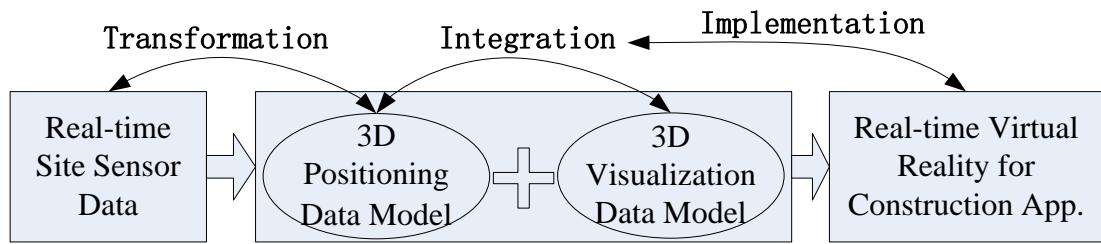
visualization of construction resources are still conducted in an “ad hoc” manner, which needs substantial programming and software development efforts; on the other hand, the developed system cannot be easily adapted to other projects using different construction methods and equipment. Thus, generally speaking, the cost to develop a 3D positioning and visualization system for a specific project or one application scenario is prohibitively high to inhibit wide practical applications.

#### ***1.4.1.3 Construction product is unique***

In the manufacturing industry, a product will be repeatedly produced by the same set of resources. “Ad hoc” approach is feasible to rapidly customize the system for 3D positioning and visualization of products or resources involved in the production process. The system development cost for each product can be sufficiently low considering the large number of products to be produced. However, it is impractical to adopt the above approach for 3D positioning and visualization of construction resources.

Different with manufacturing, every construction product (building, bridge, and infrastructure) is unique, and requires a large number of special resources, and these requirements may vary considerably on different projects. Normally, the cost to develop a system for 3D positioning and visualization of construction resources are too high if it can only be applied on one construction project.

## 1.5 Methodology



**Figure 1-7: The methodology applied to conduct this research**

The Figure 1-7 outlines the research methodology applied to this research. There are mainly three steps, namely, (1) transformation of the real-time site sensor data to the 3D positioning data model; (2) integration of the 3D positioning data model with the 3D visualization model; and (3) implementation of integrated models in a real-time virtual reality environment for construction applications.

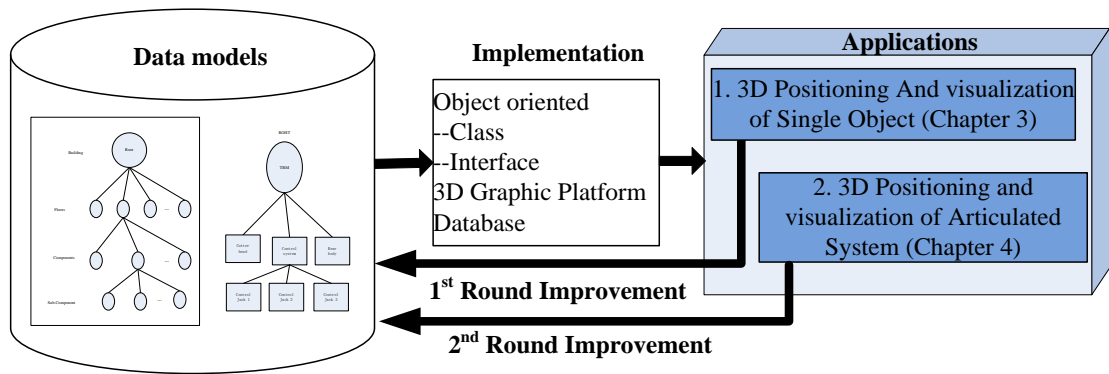
- Transformation of data captured from a construction site

The coordinate values (x, y, z) of points tagged on a solid building product are the most commonly available data on construction site, which can be collected by using automated reality capturing techniques. Algorithms that transform these coordinate values to position data (location and pose) of the solid object on the site for accurate 3D visualization in the virtual computer environment need be developed.

- Development of 3D positioning data model and 3D virtual reality visualization model

Due to the inherent complexity and the associated large volumes of data in the field, data models for real-time 3D positioning and visualization of construction resources cannot be developed in one round. In this research, an iterative process, which means the act of repeating a process with the aim of approaching a desired goal, is proposed in order to achieve an incremental improvement on the data models. Each repetition of the process is called “iteration”, and the results of the first iteration will be used as the start point for the next iteration.

Figure 1-8 shows the “iteration” methodology: at the beginning of iteration, an initial data models for 3D positioning and visualization is designed based on practical application requirements perceived from construction projects. Then the data models are implemented in a computer system by using programming technologies including: object oriented programming, 3D graphic platform, and database. After that, the developed system and data models are validated and verified in laboratory experiments and real site applications. Last, feedback and lessons learned are incorporated in the next iteration for refining data models.



**Figure 1-8: The iteration process for development of the proposed data models**

## 1.6 Dissertation Outline

This dissertation is a compilation of scientific manuscripts that document the developed framework for real-time 3D positioning and visualization of construction resources.

Figure 1-9 graphically illustrates the dissertation outline. The Chapter 1 introduces the importance of the research activity and clarifies the definition and scope of the present research in terms of real-time 3D positioning and visualization of construction resources as well as the difference with previous related research efforts.

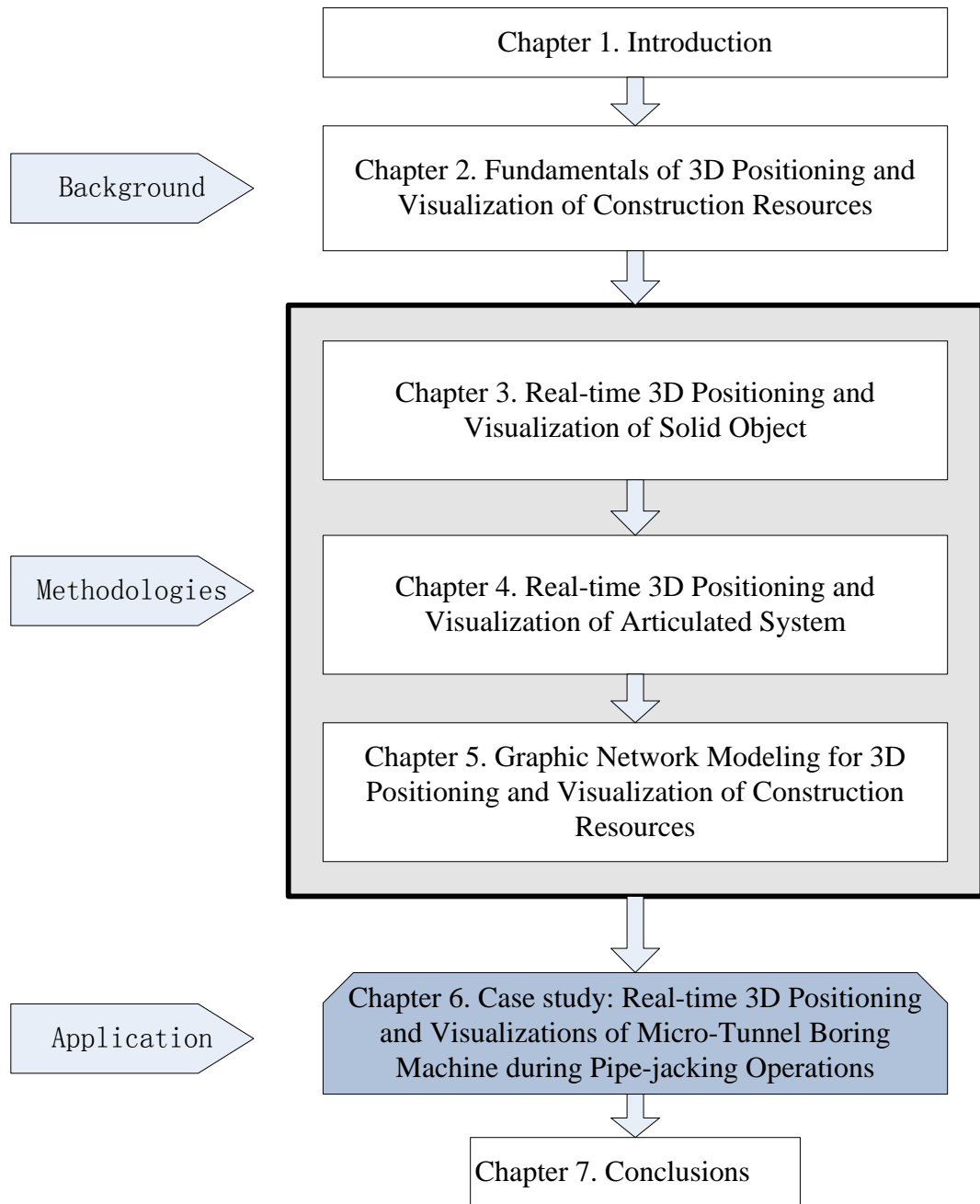
Chapter 2 describes the fundamental knowledge required to realize real-time 3D positioning and visualization of construction resources in a computer generated virtual world. This chapter is also designed to provide readers, who may not possess a background in computer science, the basic knowledge about 3D computer graphics for better understanding of the following chapters.

Chapters 3 to 4 describe technologies step by step, which are used to realize the real-time 3D positioning and visualization framework proposed. Chapter 3 describes the



algorithm and methodology for real-time 3D positioning and visualization of single solid site object. The structural steel building components undergoing assembly operations on a building site serve as the test bed for validation and verification of the proposed methodology. The 3D animation is generated in a near real-time manner to exactly reflect the 3D position and orientation of the building component being tracked on the real construction site.

Chapter 4 introduces the methodology for efficient real-time 3D positioning and visualization of articulated systems, which are abstract representation of major construction equipment working on site. The methodology can deduce the pose of all components of the system with respect to the base frame by using a minimal quantity of sensor data. The location of the base frame can be determined using the technique discussed in Chapter 3. Thus the 3D model of articulated system can be placed at their virtual working location at a particular time with an accurate 3D pose.



**Figure 1-9: Graphically representation of the dissertation outline**

Chapter 5 introduces the graphic network modeling technique that facilitates the implementation of the methodologies described in Chapter 3 and Chapter 4 with user-friendly, basic model elements. This technique can eliminate the programming work when applying the proposed methodology for real-time 3D positioning and visualization of construction equipment working in the field.

Based on the real application requirement, namely, the steering of a micro-tunnel boring machine during pipe-jacking operations, Chapter 6 discusses the possibility of applying the proposed methodologies in positioning tunnel boring machines for alignment control and TBM steering. Chapter 7 summarizes contributions and achievements of this research.

## ***Chapter 2***

### ***Fundamentals of 3D Positioning and Visualization of Construction Resources***

#### **2.1 3D positioning**

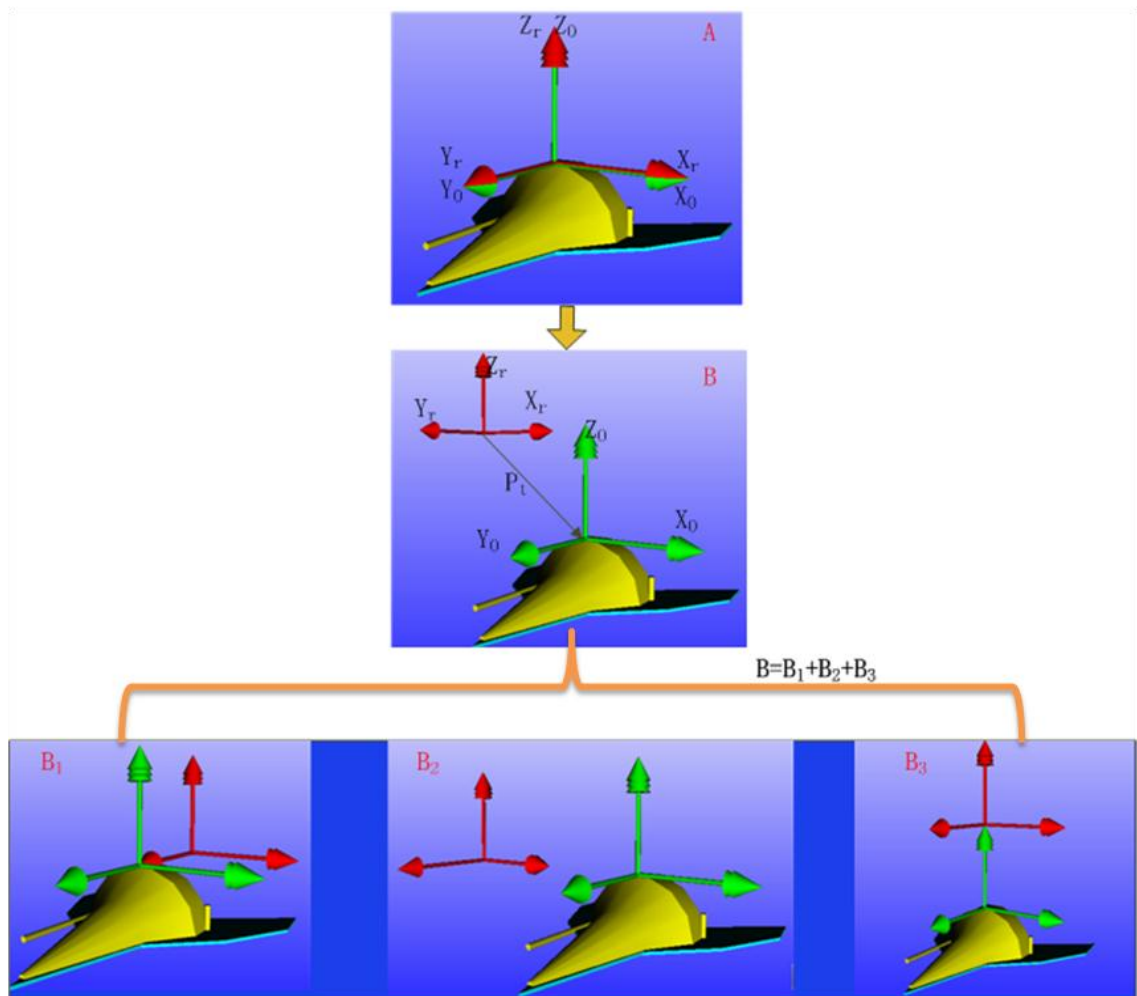
In construction, different people interpret differently the terms “positioning” or “locating”. In particular, the terms have been used in literature to refer to any activities to capture the spatial information of construction personnel, material, equipment and the buildings.

The spatial information has always been a topic of concern in construction engineering and management domain. In effect, numerous research activities may be appropriately termed as positioning or locating, such as localization of construction components and materials (Ergen et al. 2007a; Ergen et al. 2007b; Song et al. 2006; Torrent and Caldas 2009), personnel (Behzadan et al. 2008; Khoury and Kamat 2009), and construction equipment (Bernold 2002; Navon et al. 2004; Papachristou et al. 2010).

Different with above research, the term 3D positioning in this research not only indicates where an object is (location) but also about its pose (orientation). The following will formalize this term by using geometric method.

##### ***2.1.1 Location***

In geometry, the position of an object in the 3D space is always referenced to a fixed 3D coordinate frame, such as the geodetic frame. A 3D coordinate frame uses three numbers, or coordinates, to uniquely determine the position of a point. Normally, a construction site local coordinate frame will be used for positioning construction objects. In Figure 2-1, the red color frame is the reference frame for positioning the object, whose axes are noted as  $X_r$ ,  $Y_r$  and  $Z_r$  respectively.



**Figure 2-1: The location of a solid object**

An object can be located by three coordinate values (x, y, and z). However, in order to define the location of the object unambiguously, a frame must be attached on the object.

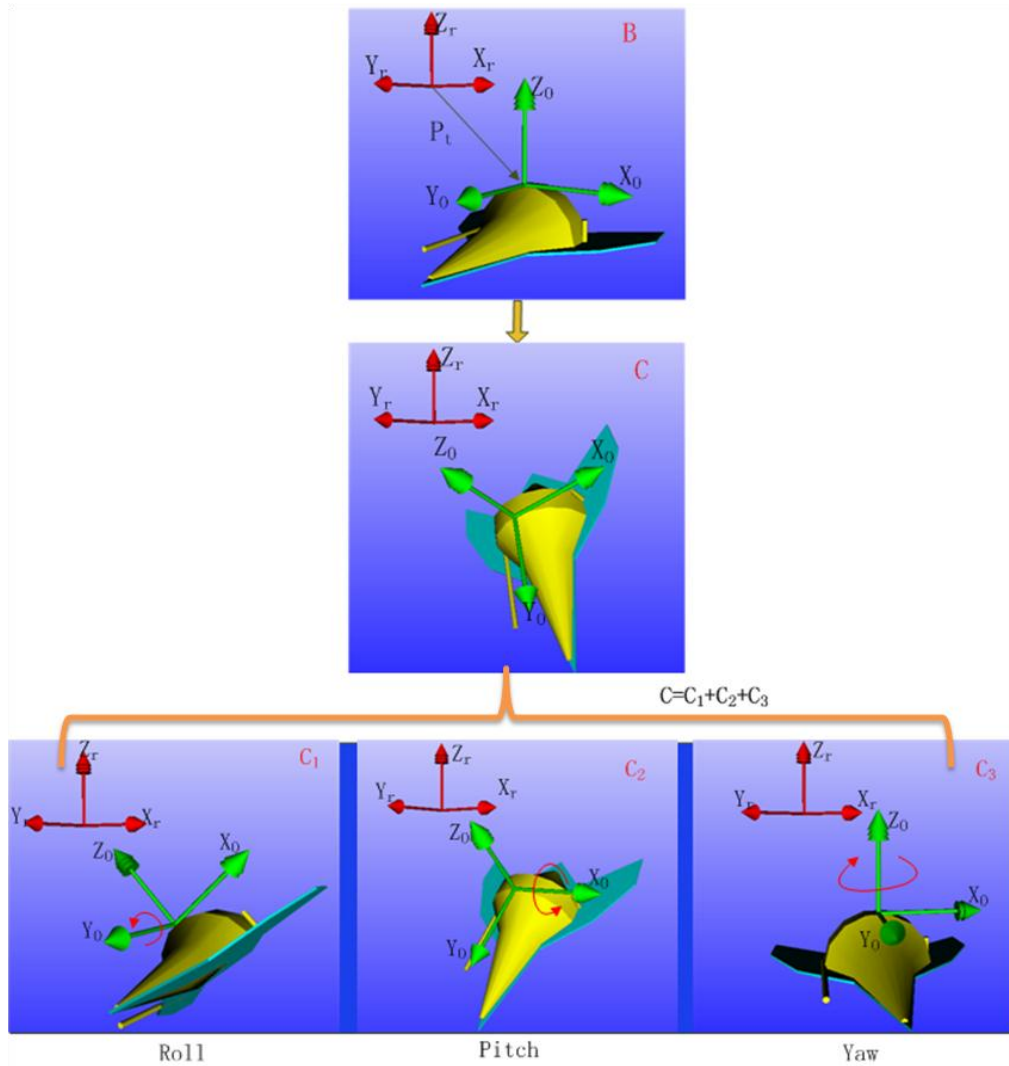
The attached frame is usually called object frame which represents the object's 3D position. The attachment means the frame and the object are fixed together without any relative movement.

As shown in Figure 2-1, the green color frame is attached on the object. The vector between the origin of reference frame (red color) and the origin of object frame indicates the object location relative to the red color frame. The coordinate values of the origin point of object frame represent the location of the object.

Initially, the object is located at the origin of reference frame, the location can be represented as  $x=0$ ,  $y=0$ , and  $z=0$  (snapshot "A" of Figure 2-1). The object is then moved to the location shown in snapshot "B" of Figure 2-1, which can be decomposed into three independent movements along the three axes, namely the axis X, Y and Z.

### **2.1.2 Orientation**

The objects can be located on the site with respect to the fixed reference frame by use of three coordinate values ( $x$ ,  $y$ , and  $z$ ). However, the location of an object described by the coordinate values tells only half of the story. As shown in Figure 2-2, the objects in the five snapshots have same locations, however, their pose are totally different. Thus the orientation of the object must also be specified to solely describe the object's position in 3D space.



**Figure 2-2: The orientation of a solid object**

In 3D geometry, the orientation can be expressed by three rotation angles about the reference frame's three axes. The three angles are generally represented as alpha (about X), beta (about Y), and gamma (about Z) in the literature of mechanics (Manseur 2006).

While in navigation and aviation, they are denoted as Roll, Pitch and Yaw as shown in Figure 2-2. Construction resources will generally move around in the field, which is similar with the aircraft moving in the space. Thus we will use the notation of Roll, Pitch and Yaw to describe the orientation of construction resources in this research. As

shown in Figure 2-2, the pose of the object in snapshot C can be represented as three sequential rotations from the pose in snapshot B.

To summarize, in this research, the 3D position of a solid object equals location plus orientation:

$$3D \text{ Position of solid object} = \text{Location} + \text{orientation} \quad (1)$$

## 2.2 3D visualization

A solid object can be clearly and unambiguously positioned in 3D space by the three coordinate values plus the three angles that the object frame rotate about the reference frame. However, the six numeric numbers cannot be directly used for rendering the 3D graphics in computer. In order to understand the process of visualizing the 3D object in computer, the complex proposition of 3D computer graphics should be firstly explored.

The term of “computer graphics” first coined by William Fetter in 1960 (Carlson, 2003) is used to describe the discipline of producing pictures or images using a computer, including (1) modeling - creation, manipulation, and storage of geometric data; (2) rendering – converting a scene to an image, or the process of transformations, rasterization, shading, illumination, and animation of the image (CompHist.org 2004).

As a branch of the discipline, the three-dimensional (3D) computer graphics use a 3D representation of geometric data to calculate and render 2D views on the computer



display screen. These views can be displayed dynamically according to the user input (e.g. through navigation and manipulation interface) to provide users with 3D perceptions.

The process of creating 3D computer graphics can be sequentially divided into three basic phases: (1) 3D modeling which describes the process and method of creating the shape of real world objects in computer, (2) kinematics analysis, which describes the motion and placement of objects in the 3D space along a timeline, and (3) rendering, which produces an image of 3D objects on the display screen (usually referred to as a frame in computer graphics). The three phases are very complex subjects in computer science. The purpose of this chapter is to provide readers a basic knowledge of 3D computer graphics for better understanding of the following chapters.

The following sections in the chapter will focus on introducing the first two phases, since they are the fundamentals of modeling construction operations in the virtual computer world. The third phase has been extensively addressed in the computer science field. In addition, there are many existing rendering algorithms and tools [i.e. an open source 3D graphic toolkit named as “OpenSceneGraph” (OSG-Community 2010)] for efficiently rendering 3D scenes. These tools can be directly adopted in the development of various visualization systems.

### ***2.2.1 3D geometric modeling***

3D modeling is concerned with mapping objects in the real world into computer digital world which is essentially mathematic representations (3D models) of the real world. The mathematic representations, however, can only partially reflect the characteristics of the real world. For example, the 3D models can describe objects' appearance but may not represent their physical behaviors. Thus it is important to understand what contents the 3D models have, and how they can be constructed with affordable efforts.

#### ***2.2.1.1 The contents of 3D models***

The contents of 3D models can be generally divided into two categories.

- Geometric data

The shapes of objects are described by the geometric data which are essentially a set of Cartesian coordinates organized and stored in different data structures. For example, the exterior of the objects can be represented using polygonal mesh or Non-Uniform Rational B-Splines (NURBS). Both of them are essentially defined by the coordinates of points. The points called vertices are connected by line segments to form a polygonal mesh, while the NURBS surfaces are defined by spline curves, which are controlled by several points. The geometric data normally will not be changed since they are modeled and stored in computer.

- Property data

The appearance of an object is not only described by its shapes but also by color, transparency, and texture etc. Furthermore, in order to place an object in the 3D virtual space, its position and orientation must be specified. In this research, these different types of data are uniformly treated as property data which can be changed by various systems to cater for specific applications, e.g. 4D tools can change the color and transparency of the 3D building component objects expressing the building evolving process, and the positioning system discussed in Chapter 4 changes the position and orientations of the building component objects reflecting their pose during erection operations.

#### ***2.2.1.2 3D modeling methods***

Nowadays, the 3D modeling techniques are maturing rapidly in regard to both software and hardware technologies. The 3D modeling techniques can be divided into two categories, namely, software based and hardware based. There are numerous commercial 3D CAD tools available for creating 3D model using primitives or parametric modeling technique, such 3DMAX, Maya, SketchUp etc. The hardware enabled 3D modeling techniques are based on the reality capturing techniques, such as 3D laser scanner and cameras. In the construction engineering, some researchers have studied the rapid 3D modeling of construction site objects, i.e. integration of sensors and

CAD models (Cho and Haas 2003), and Photogrammetry (Dai and Lu 2008). As envisioned by researchers, 3D modeling efforts will be reduced tremendously in the near future with the development of new software and hardware, which will facilitate the wide applications of 3D techniques in construction industry.

### ***2.2.2 Kinematic analysis***

A 3D object can be represented as a geometric model which can be rendered in computer graphics. The model is a static 3D model with its initial 3D position. When an object's 3D position changes, the 3D model must be transformed to the new position.

Kinematics is the study of the motion of objects without consideration of the causes leading to the motion (Beggs 1983). The motion of an object is described in computer by the location changes in two time frames. The kinematic analysis is about using mathematics to calculate the movement of a real world object.

In the previous 3D positioning section, we use six parameters to describe the position changes between two snapshots which can be viewed as the movement of the object in two time events. However, in order to render the correct graphics, all the data in the 3D models must be transformed to the new status. Basically, the coordinates of all the points in the 3D model should be transformed to the new coordinates. This is achieved by using a  $4 \times 4$  homogeneous transformation matrix (Grigore and Coiffet 2003). In linear algebra, a point's three coordinate values can be represented by a three

dimensional vector ( $\bar{x}$ ). The homogeneous transformation matrix is used to transform the vector to a new vector that represents the new location of that point:

$$\bar{x}' = T\bar{x} \quad (2)$$

where  $T$  is the  $4 \times 4$  homogeneous transformation matrix which can be represented as following:

$$T = \begin{bmatrix} \cos \theta \cos \varphi & -\sin \varnothing \sin \theta \cos \varphi + \cos \varnothing \sin \varphi & \cos \varnothing \sin \theta \cos \varphi + \sin \varnothing \sin \varphi & \Delta x \\ \cos \theta \sin \varphi & \sin \varnothing \sin \theta \sin \varphi + \cos \varnothing \cos \varphi & -\cos \varnothing \sin \theta \sin \varphi + \sin \varnothing \cos \varphi & \Delta y \\ -\sin \theta & \sin \varnothing \cos \theta & \cos \varnothing \cos \theta & \Delta z \\ 0 & 0 & 0 & 1 \end{bmatrix} \quad (3)$$

where  $\varnothing, \theta$ , and  $\varphi$  are three rotation angles, namely, roll, pitch and yaw; and  $\Delta x, \Delta y$  and  $\Delta z$  are the location changes between the two time events.

If the elements of the matrix are expressed using functions of time, then the matrix represents the motion of an object in the two time frames. Multiplying the three coordinate numbers of a point at the first time frame (before moving) by the transformation matrix will yield the point coordinates at the second time frame (after moving). Different notations can be used to construct the transformation matrix, e.g. the Roll-Pitch-Yaw (RPY) notation will be used in Chapter 3 and Denavit-Hartenberg (DH) notations will be used in Chapter 4. The notations are different with respect to the defined rotation axes.

### **2.3 The update rate for a real-time system in construction applications**

In different application contexts, the term “real-time” may have different connotations. The study of hardware and software systems that are subject to a “real-time constraint”, i.e. operational deadlines from an event to a system response, is kind of a real-time problem. However, there are no specified requirements on the update rate for a system to be a real-time system, since the time for operational deadline is scenario or context dependent.

A real time hardware/software system may be one where its application can be considered to be mission critical. The anti-lock brakes on a car are a simple example of a real-time computing system. The real-time constraint in this system is the short time, i.e. within one second, in which the brakes must be released to prevent the wheel from locking.

Real-time systems can be said to have failed if they are not responsive before their deadline where their deadline is relative to an event. Real-time is sometimes misunderstood to be high-performance, but this is not always the case. For example, a massive super computer executing a scientific simulation may offer impressive performance, yet it is not executing a real-time computation. Conversely, once the hardware and software for an anti-lock braking system has been designed to meet its required deadlines, no further performance gains are necessary.

In this research, the real-time also means the time for finishing an operation before its deadline. For example, if the building components positioning operation conducted by workers usually requires ten minutes, the positioning system is a type of real-time system if it can provide the positioning data within minutes. However, if the positioning of building components is automatically conducted by robots, the real-time positioning system may have to provide the positioning data within millisecond. Lytle et al. reported the research conducted by the National Institute of Standards and Technology (NIST) Construction Metrology and Automation Group, in which the positioning system can provide millimeter-level position data at an approximate 5Hz update rate (Lytle et al. 2004).

To summarize, whether a system/technology is real-time does not depends on the update rate but on the application scenario or context.

## **2.4 Classification of construction resources**

Various construction resources with 3D geometric shapes are involved on a typical construction project, including the elements of construction products (i.e. elements of buildings, tunnels and bridges), construction equipment (i.e. backhoe, Tunnel boring machine, Cutting machine, Roller) and temporary structures (i.e. scaffolds and formworks) etc. These construction resources can be generally classified into two

categories considering the complexity of 3D positioning and visualization, namely solid object and articulated system.

Table 2-1 gives examples of the two types of construction resources. The solid objects are resources that can be treated as one solid body, such as prefabricated concrete units, steel pipe sections. The articulated system contains a set of rigid bodies connected by joints that constrains their relative movements, for example, a backhoe contains five rigid bodies: track, cabin, boom, stick and bucket.

Table 2-1: Classification of construction resources

Types	examples	Application purposes	Granularity
Solid object	Steel pipe/ Reinforcement/ Prefabricated concrete unit/ Mobile working tower/ Hand tools	Tracking resources for management/logistic purpose Positioning during assembly	Location Location + Orientation
	Backhoe/ Tunnel boring machine/ Personnel/ Mobile Crane/ Construction Vehicles	Locating equipment Tele-operation Automated construction	Location Location + Orientation Location + Orientation

For each category, the granularity of 3D positioning is also affected by the application purposes. For example, if the purpose of tracking steel components is for logistics and management, only the location information is needed. However, if the purpose is for positioning the steel components during assembly, both the location and orientation should be considered.



The technologies for 3D positioning of solid objects are the basis for the 3D positioning of articulated systems. Compared with solid objects, It is much more complex for 3D positioning of articulated systems, which needs the 3D position information of each solid body. The following section will introduce the fundamental knowledge of articulated system.

## **2.5 Articulated system**

### ***2.5.1 Kinematic Chain***

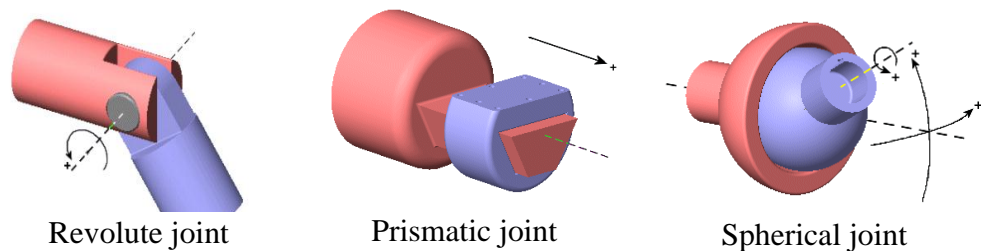
It is relatively simple to describe the 3D position of a single solid object. However, to describe the motion of a set of rigid bodies connected by joints that constrains their relative movements (articulated system), the term “kinematic chain” is defined as the assembly of rigid body segments connected by joints.

#### ***2.5.1.1 The rigid body***

A rigid body is an idealization of a solid body in which deformation is neglected. For example, the components of construction equipment can be regarded as a rigid body, because their deformations can be neglected without affecting the analysis result. Similarly, the building components are usually treated as rigid bodies in the visualization of the assembly operations.

#### ***2.5.1.2 Joints***

A joint is the mechanism that connects two rigid bodies in contact with each other. The nature of the relative motion between a pair of successive rigid bodies is determined by the type of connecting joint. Three types of joints are most commonly used in construction equipment, namely, revolute joint, prismatic joint, and spherical joint. As shown in Figure 2-3, the revolute joint allows one rigid body to rotate relative to the other rigid body about a common axis. The prismatic joint allows one rigid body to translate relative to the other rigid body along a parallel vector. The spherical joint equals three revolute joints with the three rotation axes intersecting at a common point.



**Figure 2-3: Three types of joints commonly used in construction equipment**

### ***2.5.1.3 Classification of kinematic chains***

The kinematic chains can be generally divided into two categories, namely, open chain and closed chain (Khalil and Dombre 2002). A closed kinematic chain contains at least one closed loop, while an open kinematic chain has not this kind of loop. Among the closed kinematic chain family, the parallel kinematic chain is widely used in robotic system. A parallel kinematic chain typically consists of a moving platform that is connected to a fixed base by several limbs. Figure 2-4 shows a robotic crane named

RoboCrane developed by American National Institute of Science and Technology (NIST)(Wavering 1998). It is a kind of Stewart platform using six cables to connect the work platform. The principal advantage of the RoboCrane over conventional crane systems is the improved control of the position and orientation of the load (Wavering 1998).



**Figure 2-4: RoboCrane developed by NIST**

### ***2.5.2 Degree of freedom***

The degree of freedom (DoF) is an important concept in kinematic chain analysis. As discussed above, six parameters are needed to determine the location of an object (rigid

body). Thus a rigid body without any connection to other rigid bodies has six degrees of freedom. Before counting the degrees of freedom, the concept of constraints on the joints should be introduced. As illustrated in Figure 2-3, the revolute joint only allows one degree of freedom between the two rigid bodies. Thus the revolute joint has five constraints (6-1=5). Similarly, the prismatic joint has five constraints and the spherical joint has three constraints. The degree of freedom of a kinematic chain consists of  $n$  rigid bodies and  $m$  joints can be calculated by the following equation:

$$F = 6(n - 1) - \sum_{i=1}^m u_i \quad (4)$$

Where,  $u_i$  is the number of constraints on the joint  $i$ .

The degree of freedom is also crucial in the real-time 3D positioning and visualization, because it gives the number of input parameters required for calculating the pose of the construction equipment.

## 2.6 Summary

This chapter first describes the terminology of 3D positioning in this research, which defines the 3D positioning of construction resources as a combination of the location and the orientation. Then the fundamental knowledge of 3D visualization technologies is provided for better understanding of the following chapters. The following chapters will elaborate on the methodologies proposed towards the realization of the real-time

3D positioning and visualization of the two types of construction resources classified in this chapter.

## ***Chapter 3***

### ***Real-time 3D Positioning and Visualization of Solid Objects***

#### **3.1 Introduction**

Solid objects on site are resources that can be treated as one solid body, such as a prefabricated concrete unit, a steel column and a working platform. The real-time 3D positioning and visualization of solid objects on site is the first step towards the real-time mapping of real world construction sites into a computer generated virtual world.

Building components are important construction resources that can be generally treated as solid objects. This chapter will first introduce the importance of real-time 3D positioning and visualization of the building components during assembly operations.

Then a generic methodology for real-time 3D positioning and visualization of solid objects is briefly introduced. The methodology can be easily adapted to the real-time 3D positioning and visualization of building components during erection operations on site.

The methodology is enabled by integration of a newly proposed data model compatible with the automated on-site reality capturing technology. 3D animation can be generated in a real-time manner to exactly reflect the 3D position and orientation of a solid object on a real construction site. The data model, the reality capturing technology and the

transformation algorithm that comprise the methodology will be elaborated in Section 4, 5, 6 and 7, respectively.

Based on the new methodology, a software system called 4D-PosCon is prototyped with user-friendly graphic user interfaces designed to cater for the practical needs identified from site studies. Finally, laboratory experiments are conducted to verify the feasibility and the effectiveness of the proposed methodology, and conclusions drawn in the end for this chapter.

## **3.2 Importance of the research**

### ***3.2.1 Industry practical needs***

Locating and positioning building components in the three dimensional space on a construction site is the fundamental construction operation (Beliveau et al. 1995). Accurate positioning of bulky building components, such as structural steel members, are labor-intensive, highly repetitive and time consuming tasks, which are normally conducted by laborers exposed in a potentially hazardous environment like an elevated location (Bernold 2002; Lytle et al. 2002).

In an American Institute of Steel Construction report, decreasing the fabrication and erection time for steel frame buildings, while increasing the safety of workforce during construction, were identified as the two crucial issues on automated steel construction.

In particular, the time required to erect a steel frame structure need to be reduced by 25% for the steel construction industry to remain competitive (Lytle et al. 2002). At present, it is imperative to improve positioning control practices during the process of erecting bulky building components, aimed at making improvements on construction productivity, safety and quality.

### ***3.2.2 Streamlining the 3D design and on-site construction***

In recent years more and more construction projects have used three-dimensional/four-dimensional (3D/4D) models to support management tasks (Hartmann et al. 2008). These models contain accurate spatial information of the building products to be constructed. When it comes to the setting of an actual construction field, however, those spatial models have not yet found much value-added application (Bernold 2002). One main reason is that these models lack the integration of “reality” information along with cost-effective methodologies for seamless integration with automated reality capturing technologies (Chin et al. 2008).

### ***3.2.3 Facilitating the spatial integration in construction***

Since the construction process involves various tasks that deal with the creation of physical elements (i.e. prefabricated building elements) which will then be positioned on the site as per design. These construction site physical elements most often require



visual information to understand and communicate their complexity and relationship to existing structures or elements (Shin and Dunston 2008).

Spatial integration in construction refers to research efforts of synthesizing various technologies for spatial data collection in construction operations so as to improve productivity, quality and safety of the construction process. Examples include the integration of real-time position measurements with computer aided design (CAD) (Beliveau et al. 1995), merging spatial design data with the digital model of equipment working on implementing the design (Bernold 2002), and real-time updating the graphical representation of construction equipment and the work environment for tele-operations (Seo et al. 2000).

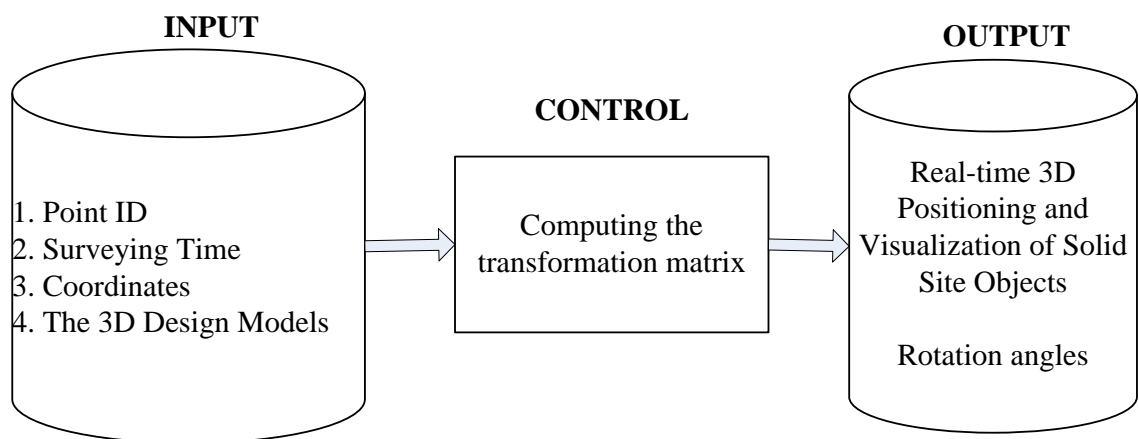
Benefits to be gained from the integration of spatial information in construction operations include: (1) desired positions are provided to operators of equipment and tools on the spot and at the right time, allowing them to be more spatially accurate, (2) the amount of rework is diminished as a result of reduced errors and elimination of blueprints and staking, (3) manpower requirements are significantly reduced for working in dangerous work zones and for position checking (Bernold 2002).

Previous research efforts on spatial integration have been largely focused on integrating spatial information with specific construction equipment models. This research

effectively integrates site spatial information of a building component with its as-designed product model by embracing the proposed data models and surveying technologies. With the increasing adoption of 3D/4D technologies for building product design, this research potentially broadens their application scope by utilizing 3D/4D design information at the construction operation level.

### 3.3 Overview of proposed methodology

The main goal of this research is to realize real-time 3D positioning and visualization of solid site objects so as to reflect their actual position and orientation (pose) during construction operations. To achieve this goal, the proposed methodology relies on the use of surveying data to automatically update the 3D object models. Figure 3-1 gives an overview of the proposed methodology.



**Figure 3-1: Overview of the proposed methodology for real-time 3D positioning and visualization of solid site objects**

The building components are selected as a typical solid site objects in this research.

Thus the 3D design models are represented in the form of 4D models which are

generated in consideration of multiple constraints on site, such as the lifting capacity of the tower crane, construction method and activity sequence.

The surveying data include point identification, surveying time and coordinates of the tracking points which are marked on the building component. The data are processed using a special algorithm to generate the transformation matrix. In the 3D computer graphics, any movement and rotation of a solid object can be encoded in a transformation matrix. The resulting transformation matrix is used to update the 3D model of the building component and mirror its actual motion during installation operations.

Furthermore, by comparing the as-designed model and the actual model of the building product, any deviations between them are determined in terms of position offsets and rotation angles, which facilitate follow-up adjustment operations in erecting the building component.

### **3.4 The data models**

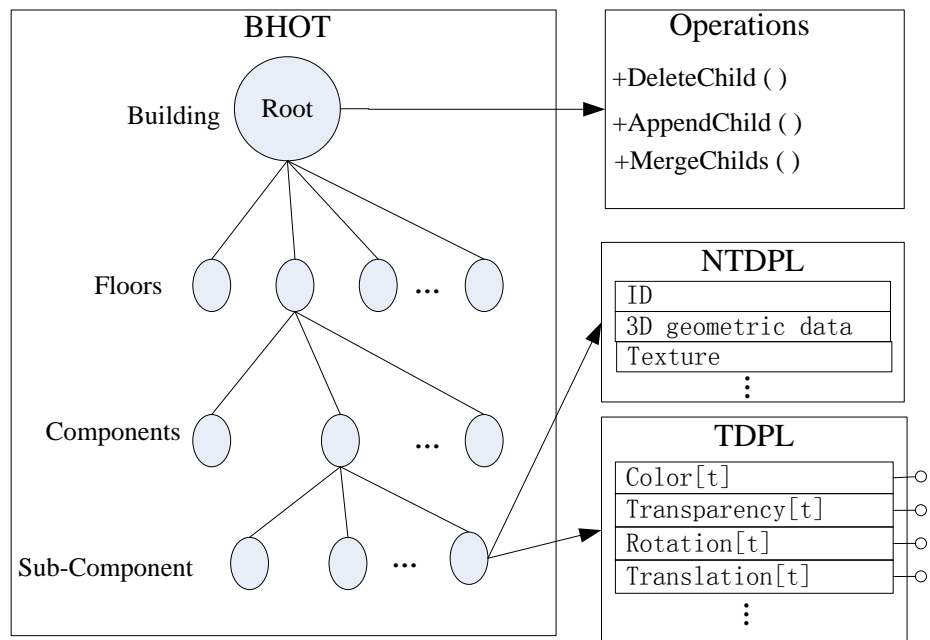
The real world site objects are modeled as 3D computer graphic models (mathematical representations) defined by geometric data and various associated property data such as texture, color and position. There are many ways of storing and organizing these data in an application system.

In computer science, the term “data structure” is utilized to represent the way of storing and organizing data in computer for achieving better algorithmic efficiency (Black 2004). Different kinds of data structures are suited to a diversity of application purposes. Data structure is the key factor in the design of an extensible and scalable application system, which is especially important for the construction operations visualization practices (Kamat and Martinez 2008).

The product of a construction project can always be organized in a hierarchical data model which is a tree-like structure. Figure 3-2 illustrates the product data model for a typical high-rise building project. In the Building Hierarchical Object Tree (BHOT), the root node represents the whole building. The building is firstly decomposed into floors in the second layer, and each floor is then decomposed into components, such as walls, beams, windows and doors.

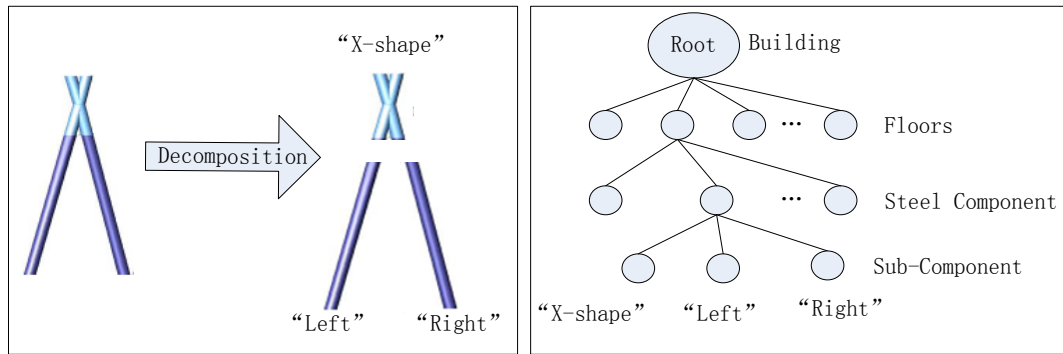
It is noteworthy that when applying the data model for construction process 4D simulation at the pre-construction stage, it is generally not necessary to decompose the building into smaller pieces. The three layer tree structure is sufficient for the application. However, decomposing the product data model into the construction level of details is necessary when applying the data model to support operation level tasks during construction.

Thus the data model should provide three functions to facilitate the decomposition operations in different stages. They are: (1) deleting a child node, (2) merging two child nodes into one node, and (3) appending a tree node. By combining the usage of the three functions, any requirement on the model's level-of-details can be easily handled.



**Figure 3-2: The product data model for a typical building project**

For example, a 3D model of a steel member in a high-rise building is shown in the left hand side of Figure 3-3. The breakdown of a building into components by an architect or a structural engineer is in general design-centric; the three sub-components of the member (namely, the “X-shape” part, the “left” part, and the “right” part) are the results of the construction-centric decomposition, which are generally prepared by site engineers of the contractor, factoring in the weight of each steel component and the lifting capacity of the tower crane deployed on site.

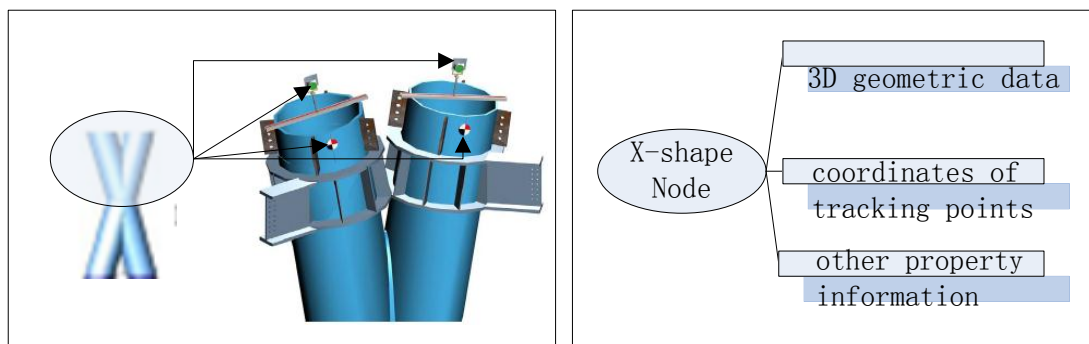


**Figure 3-3: Decomposing a product model into construction level of details**

As shown in Figure 3-2, each node in the tree is linked with two lists which contain the associated data. The first list is named as Non-Time-Dependent-Property-List (NTDPL) which contains the static data, such as the identification number, 3D geometric data, and texture image. The static data generally will not be changed during the whole application periods. While the other list is named as Time-Dependent-Property-List (TDPL) which contains the dynamic data, such as color, transparency, rotation matrix, translation vectors. The dynamic data will be changed in particular applications, e.g. the color and transparency will be changed in the application of 4D simulations, while the rotation matrix and translation vectors will be changed in the application of real-time 3D positioning and visualization of building components for positioning control (which will be discussed in the followings). Thus the TDPL should provide interfaces that enable other modules or systems to update the associated data.

Furthermore, the dimensions of the two lists can be extended, enabling different users to enter particular types of information as needed at different stages for their own application purposes. As shown in Figure 3-4, the design models produced for 4D

project planning generally do not contain sufficient information for erection positioning control. For instance, two prisms and two reflective tags are firmly fixed on the “X-shape” part, the coordinates of which will be tracked and surveyed in erecting the structural steel member. The positions of those control points are designed by engineers on site and generally available shortly before site installation commences. Facilitated by the extensible list data structures, these data are appended to the NTDPL where the 3D geometric models are stored, as shown on the right hand side of Figure 3-4.



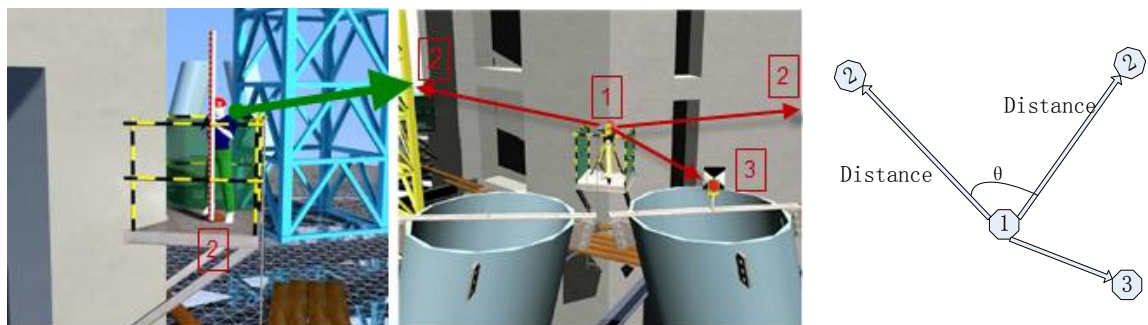
**Figure 3-4: Incorporating the assembly details in the data model: example and data structure**

### 3.5 Surveying tracking points

In the proposed methodology, multiple tracking points are marked on the solid objects, which are automatically surveyed by a robotic total station. The surveying data provide inputs to a special algorithm for determining the position and orientation of the rigid body in the 3D space. This section explains how to collect the point surveying data.

The total station needs to be set up at a known location and initialized before surveying the tracking points. The location of the total station is determined through the following procedures: Prior to the erection of a building component, two control points with known coordinates are established on a construction site. The total station is then placed at a convenient location with line-of-sight to the two control points as well as all the tracking points on the building component being erected.

As illustrated in Figure 3-5, the total station checks the two control points and determines the slope distance, the horizontal angle, and the vertical angle in relation to each control point. As such, the total station can calculate its own position and fix its initial perspective angle by straightforward geometrics. Then a computer controls the total station to lock on the prisms and/or reflective tapes firmly fixed on those tracking points of the building component and to survey their coordinates. Figure 3-5 shows that the total station is initialized for positioning a steel column during its installation on a high-rise building project.



**Figure 3-5: The initialization of total station for positioning a steel column; numeral IDs in the figures identify: (1) total station (2) fixed control points (3) prism attached on a tracking point**



Three types of data are collected in one surveying cycle, namely, the point identification (ID), data collection time (e.g. 30/06/2001 15:30:45), and point coordinates in the format of geodetic latitude, longitude and leveling (e.g. 23.130, 113.269, 310.500). These data are serialized in one package for transfer to the real-time 3D positioning and visualization system through a data communication network.

### 3.6 Transformation

In order to update the position and orientation of a building component model with a limited quantity of tracking points, we need to compute those parameters as needed to display the 3D building component model in alignment with their actual positions and orientations in the real world. These parameters include the translation vector  $\mathbf{T}$  and the rotation matrix  $\mathbf{R}$  given in Equation (1):

$$\mathbf{T} = \begin{bmatrix} \Delta x \\ \Delta y \\ \Delta z \end{bmatrix} \text{ and } \mathbf{R} = \begin{bmatrix} r_{11} & r_{12} & r_{13} \\ r_{21} & r_{22} & r_{23} \\ r_{31} & r_{32} & r_{33} \end{bmatrix} \quad (1)$$

The translation vector  $\mathbf{T}$  is the offsets of a solid object in the 3D space. Next, how to derive the matrix elements  $r_{ij}$  in the rotation matrix  $\mathbf{R}$  by using the collected coordinates of tracking points is elaborated.

First, let us define the mean-coordinates  $(\bar{x}_j, \bar{y}_j, \bar{z}_j)$  of all the points being tracked at time event  $j$  which are expressed by:

$$\bar{x}_j = \frac{\sum_i x_{ji}}{N}, \bar{y}_j = \frac{\sum_i y_{ji}}{N}, \bar{z}_j = \frac{\sum_i z_{ji}}{N} \quad (2)$$

Where,  $N$  is the number of points marked on the building component for erection positioning control purposes, and  $N \geq 3$ ;  $(x_{ji}, y_{ji}, z_{ji})$  is the coordinates of point  $i$  ( $i = 1, 2, \dots, N$ ) tracked at time event  $j$ . In the 3D world, any position and orientation changes in the two time events ( $j = 1$  and  $2$ ) can be represented with a translation and a rotation, obeying the following equation:

$$\begin{bmatrix} x_{2i} - \bar{x}_2 \\ y_{2i} - \bar{y}_2 \\ z_{2i} - \bar{z}_2 \end{bmatrix} = \begin{bmatrix} r_{11} & r_{12} & r_{13} \\ r_{21} & r_{22} & r_{23} \\ r_{31} & r_{32} & r_{33} \end{bmatrix} \begin{bmatrix} x_{1i} - \bar{x}_1 \\ y_{1i} - \bar{y}_1 \\ z_{1i} - \bar{z}_1 \end{bmatrix} \quad (3)$$

The physical meaning of the above Equation (3) is that a vector on a solid object, which links point  $i$  and the mean-coordinate point, rotates about the mean-coordinate point from time event  $i$  to  $j$ . Equation (3) can be simplified into Equation (4):

$$\begin{bmatrix} \dot{x}_{2i} \\ \dot{y}_{2i} \\ \dot{z}_{2i} \end{bmatrix} = \begin{bmatrix} r_{11} & r_{12} & r_{13} \\ r_{21} & r_{22} & r_{23} \\ r_{31} & r_{32} & r_{33} \end{bmatrix} \begin{bmatrix} \dot{x}_{1i} \\ \dot{y}_{1i} \\ \dot{z}_{1i} \end{bmatrix} \text{ or } \dot{\mathbf{x}}_{2i} = \mathbf{R}\dot{\mathbf{x}}_{1i} \quad (4)$$

There are nine unknowns in Equation (4), which can be solved given the coordinates of three or more points. However, considering surveying errors associated with these coordinates data, which are referred to as ill-conditioned spatial marker coordinates by Carman and Milburn (Carman and Milburn 2006), simply solving the rotation matrix by matrix inversion could produce large computation errors. Instead, the least-square approach is recommended to tackle the problem, which considers all the points available to arrive at an optimal solution, which has been intensively applied in biomechanics (Carman and Milburn 2006; Challis 1995).

The first step to solve Equation (4) is to formulate a three by three matrix  $\mathbf{c}$  using the vector  $\hat{\mathbf{x}}_{2i}$  and  $\hat{\mathbf{x}}_{1i}$ , which is called the cross-dispersion matrix or the correlation matrix as follows:

$$\mathbf{c} = \frac{1}{N} \sum_{i=1}^N \hat{\mathbf{x}}_{2i} (\hat{\mathbf{x}}_{1i})^t \quad (5)$$

The next step is to apply the procedure of Singular Value Decomposition (SVD) to the matrix  $\mathbf{c}$ . SVD is a powerful technique for coping with sets of equations or matrices that are either singular or numerically very close to being singular. Applying SVD allows one to diagnose the problem defined in a given matrix, while at the same time finding numerical solutions to it. By using SVD, any  $m \times n$  matrix ( $m \geq n$ ) can be written as the product of a  $m \times n$  column-orthogonal matrix  $\mathbf{u}$ , a  $n \times n$  diagonal matrix  $\mathbf{w}$  with positive or zero elements, and the transpose of a  $n \times n$  orthogonal matrix  $\mathbf{v}$  as follows:

$$\mathbf{c} = \mathbf{u} \cdot \mathbf{w} \cdot \mathbf{v}^t \quad (6)$$

By using the results from the SVD, the rotation matrix can be calculated by the following Equation (7):

$$\mathbf{R} = \mathbf{u} \begin{bmatrix} 1 & 0 & 0 \\ 0 & 1 & 0 \\ 0 & 0 & \det(\mathbf{u}\mathbf{v}^t) \end{bmatrix} \mathbf{v}^t \quad (7)$$

Where,  $\det(\mathbf{u}\mathbf{v}^t)$  is the determinant of matrix  $\mathbf{u}\mathbf{v}^t$ .

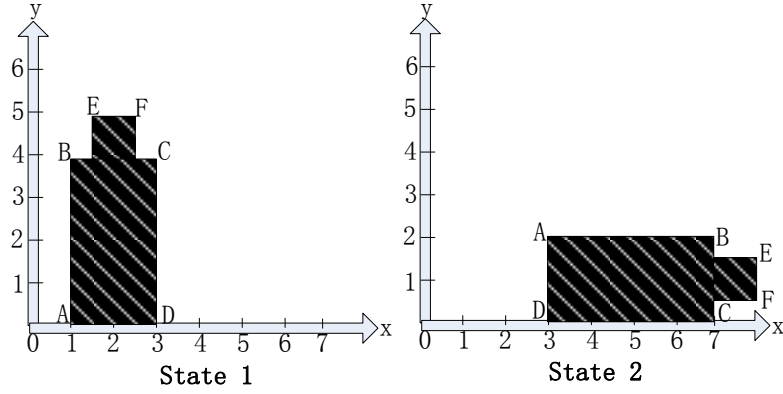
With the rotation matrix  $\mathbf{R}$ , we can readily calculate the coordinates of any other point ( $k$ ) that constitutes the geometric profile of the building component by using Equation (8) :

$$x_{2k} = \mathbf{R}(x_{1k} - \bar{x}_1) + \bar{x}_2 \quad (8)$$

The above approach only requires the input of coordinates for a minimum of three points to update the positioning and orientation of the building component in 3D computer graphics. To simplify the presentation, the following section uses a simple 2D example to illustrate the calculations and verify the methodology.

### ***3.6.1 Numerical Example***

As shown in Figure 3-6 a 2D example is given to illustrate the computation procedure. Note for a 3D problem, the calculation procedure is identical but more complicated to visualize and verify the computation results. In Figure 3-6, on the left hand side is a building component in “State 1”, and the right hand side denotes the “State 2” of the component during installation. The points A, B, C and D are the four tracking points. In order to update the component’s current position and orientation from State 1 to State 2, the coordinates of all the points outlining the component’s profile are needed, including points E and F. In this example, we determine the coordinates of E and F in State 2 by applying the proposed methodology.



**Figure 3-6: An illustrative 2D example**

Step 1: Input the coordinates of the tracking points in State 1 (actually three points are enough, more points collected yield a higher accuracy):

$$A: (1, 0, 0); B: (1, 4, 0); C(3, 4, 0); D(3, 0, 0) \quad (9)$$

Step 2: Input the coordinates collected in State 2:

$$A: (3,2,0); B: (7,2,0); C(7,0,0); D(3, 0, 0) \quad (10)$$

Step 3: Perform calculations:

$$\bar{x}_1 = \frac{1 + 1 + 3 + 3}{4} = 2; \bar{y}_1 = \frac{0 + 4 + 4 + 0}{4} = 2; \bar{z}_1 = \frac{0 + 0 + 0 + 0}{4} = 0$$

$$\hat{x}_{1A} = [-1 \ -2 \ 0]^t; \hat{x}_{1B} = [-1 \ 2 \ 0]^t; \hat{x}_{1C} = [1 \ 2 \ 0]^t; \hat{x}_{1D} = [1 \ -2 \ 0]^t$$

$$\bar{x}_2 = \frac{3 + 7 + 7 + 3}{4} = 5; \bar{y}_2 = \frac{2 + 2 + 0 + 0}{4} = 1; \bar{z}_2 = \frac{0 + 0 + 0 + 0}{4} = 0$$

$$\hat{x}_{2A} = [-2 \ 1 \ 0]^t; \hat{x}_{2B} = [2 \ 1 \ 0]^t; \hat{x}_{2C} = [2 \ -1 \ 0]^t; \hat{x}_{2D} = [-2 \ -1 \ 0]^t$$

$$c = \frac{1}{N} \sum_{i=1}^N \hat{x}_{2i} (\hat{x}_{1i})^t = \begin{bmatrix} 0 & 4 & 0 \\ -1 & 0 & 0 \\ 0 & 0 & 0 \end{bmatrix} \quad (11)$$

SVD:

$$\mathbf{c} = \frac{1}{N} \sum_{i=1}^N \dot{\mathbf{x}}_{2i} (\dot{\mathbf{x}}_{1i})^t = \begin{bmatrix} 0 & 4 & 0 \\ -1 & 0 & 0 \\ 0 & 0 & 0 \end{bmatrix} \quad (12)$$

$$\mathbf{c} = \mathbf{u} \cdot \mathbf{w} \cdot \mathbf{v}^t = \begin{bmatrix} 1 & 0 & 0 \\ 0 & 1 & 0 \\ 0 & 0 & 1 \end{bmatrix} \begin{bmatrix} 4 & 0 & 0 \\ 0 & 1 & 0 \\ 0 & 0 & 0 \end{bmatrix} \begin{bmatrix} 0 & -1 & 0 \\ 1 & 0 & 0 \\ 0 & 0 & 1 \end{bmatrix}^t \quad (13)$$

$$\mathbf{R} = \mathbf{u} \begin{bmatrix} 1 & 0 & 0 \\ 0 & 1 & 0 \\ 0 & 0 & \det(\mathbf{u}\mathbf{v}^t) \end{bmatrix} \mathbf{v}^t = \begin{bmatrix} 0 & -1 & 0 \\ 1 & 0 & 0 \\ 0 & 0 & 1 \end{bmatrix} \quad (14)$$

Step 4: Calculate and verify the coordinates of point E and F in state 2 using equation (8)

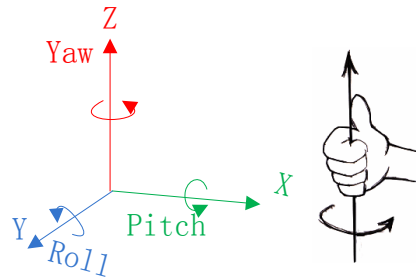
$$\begin{aligned} \mathbf{E}_2 &= \mathbf{R}(\mathbf{E}_1 - \bar{\mathbf{x}}_1) + \bar{\mathbf{x}}_2 = \begin{bmatrix} 0 & -1 & 0 \\ 1 & 0 & 0 \\ 0 & 0 & 1 \end{bmatrix} \begin{bmatrix} 1.5 - 2 \\ 5 - 2 \\ 0 \end{bmatrix} + \begin{bmatrix} 5 \\ 1 \\ 0 \end{bmatrix} = \begin{bmatrix} 8 \\ 1.5 \\ 0 \end{bmatrix} \\ \mathbf{F}_2 &= \mathbf{R}(\mathbf{F}_1 - \bar{\mathbf{x}}_1) + \bar{\mathbf{x}}_2 = \begin{bmatrix} 0 & -1 & 0 \\ 1 & 0 & 0 \\ 0 & 0 & 1 \end{bmatrix} \begin{bmatrix} 2.5 - 2 \\ 5 - 2 \\ 0 \end{bmatrix} + \begin{bmatrix} 5 \\ 1 \\ 0 \end{bmatrix} = \begin{bmatrix} 8 \\ 0.5 \\ 0 \end{bmatrix} \end{aligned} \quad (15)$$

The computation results are consistent with the point coordinates of E and F which can be easily taken in Figure 3-6. The algorithm can be processed by computers on a near real-time basis to enable frequent updating, which is vital to positioning control during building component installation. Note the proposed methodology requires the building component to be a solid object which would incur no marked deformation during erection. This assumption is valid and acceptable in most practical application scenarios.

### 3.7 Computing rotation angles

In order to quantify orientation deviations between the actual and targeted positions, the rotation matrix is further decomposed into three sequential rotations: Roll ( $\phi$ ) Pitch ( $\theta$ ) and Yaw ( $\varphi$ ), which are the terms commonly used in the aerospace field to describe the orientation of a space craft. Roll is the rotation about the axis  $Y$  of the coordinate system.

Pitch is the rotation about the axis  $X$ , and Yaw is the rotation about axis  $Z$ . If the 3D models are generated based on the local north, east, up (NEU) coordinates system, then the east axis is labeled  $Y$ , the north is  $X$  and the up is  $Z$ . Nonetheless, the transformation from one coordinate system to another is needed in case that a different coordinate system is used. The “positive” signs of rotation angles are specifically defined according to the “right hand rule” as given in Figure 3-7.



**Figure 3-7: The right hand rule for specifying the positive direction of the rotations about the three axes**

The rotation matrix in Equation (7) can be decomposed into three rotation matrices as follows:

$$\mathbf{R} = \mathbf{R}_\varnothing \cdot \mathbf{R}_\theta \cdot \mathbf{R}_\varphi \quad (16)$$

$\mathbf{R}_\varphi$  is the rotation about axis  $Z$  (Yaw) with  $\varphi$  degrees which can be given as:

$$\mathbf{R}_\varphi = \begin{bmatrix} \cos \varphi & -\sin \varphi & 0 \\ \sin \varphi & \cos \varphi & 0 \\ 0 & 0 & 1 \end{bmatrix} \quad (17)$$

$\mathbf{R}_\theta$  is the rotation about axis  $X$  (Pitch) with  $\theta$  degrees which can be given as:

$$\mathbf{R}_\theta = \begin{bmatrix} 1 & 0 & 0 \\ 0 & \cos \theta & -\sin \theta \\ 0 & \sin \theta & \cos \theta \end{bmatrix} \quad (18)$$

Where  $\mathbf{R}_\varnothing$  is the rotation about axis  $Y$  (Roll) with  $\varnothing$  degrees which can be given as:

$$\mathbf{R}_\emptyset = \begin{bmatrix} \cos \emptyset & 0 & \sin \emptyset \\ 0 & 1 & 0 \\ -\sin \emptyset & 0 & \cos \emptyset \end{bmatrix} \quad (19)$$

Thus, rotation matrix  $\mathbf{R}$  can be represented as:

$$\mathbf{R} = \begin{bmatrix} \cos \theta \cos \varphi & -\sin \emptyset \sin \theta \cos \varphi + \cos \emptyset \sin \varphi & \cos \emptyset \sin \theta \cos \varphi + \sin \emptyset \sin \varphi \\ \cos \theta \sin \varphi & \sin \emptyset \sin \theta \sin \varphi + \cos \emptyset \cos \varphi & -\cos \emptyset \sin \theta \sin \varphi + \sin \emptyset \cos \varphi \\ -\sin \theta & \sin \emptyset \cos \theta & \cos \emptyset \cos \theta \end{bmatrix} \quad (20)$$

The three angles can be solved by equating the matrix elements in Eq. (20) with their counterparts obtained from Eq. (7):

$$\theta = \begin{cases} (1) & \sin^{-1}(-r_{31}) \\ (2) & \pm \pi - \sin^{-1}(-r_{31}) \end{cases} \quad (21)$$

As given in Equation (21), more than one possible solution can be obtained. However, considering the building component positioning practice, the rotation angle is commonly small. The solution for pitch angle  $\theta$  should be bounded between -90 and 90 degrees, thus the solution should be as:

$$\theta = \sin^{-1}(-r_{31}) \quad (22)$$

For the same reasons, the following equations determine Roll ( $\emptyset$ ) and Yaw ( $\varphi$ ):

$$\emptyset = \tan^{-1}\left(\frac{r_{32}}{r_{33}}\right) \quad (23)$$

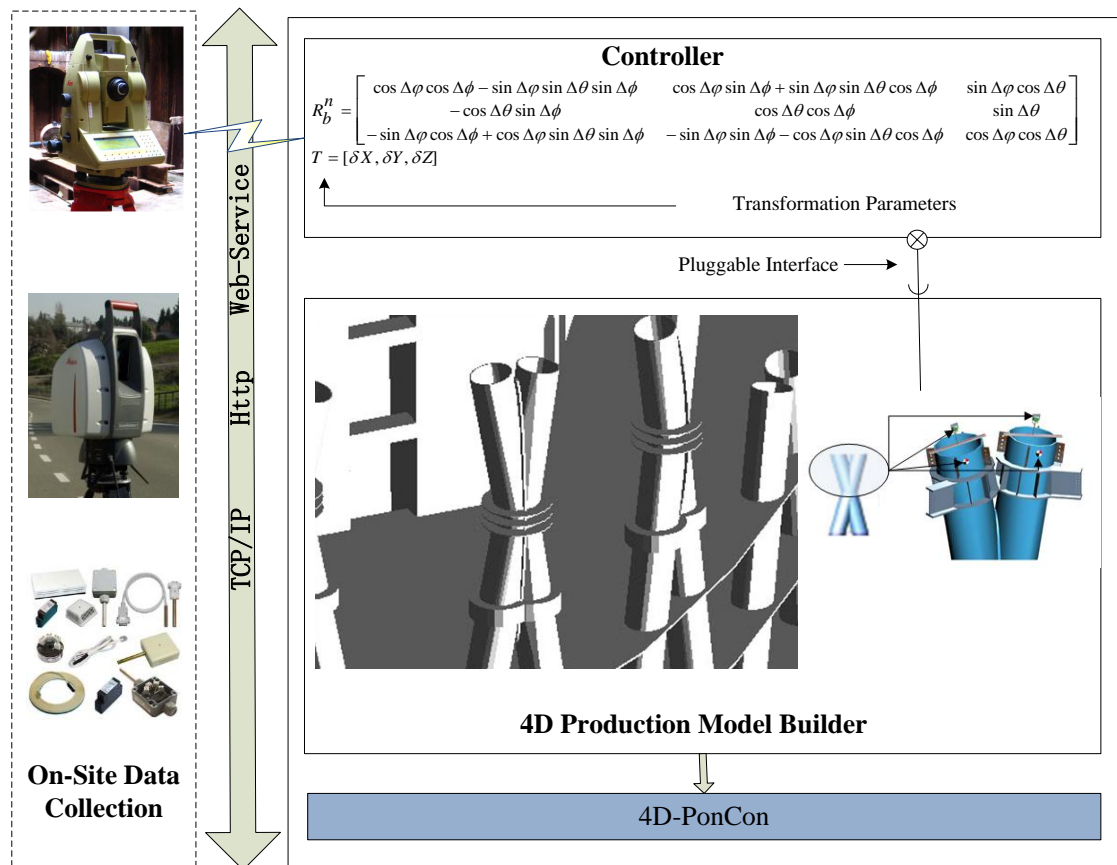
$$\varphi = \tan^{-1}\left(\frac{r_{21}}{r_{11}}\right) \quad (24)$$

As for the 2D numerical example given in previous section, it is determined that the simulated component rotates about axis Z (pointing outward of X-Y plane) with  $\varphi = \tan^{-1}\left(\frac{r_{21}}{r_{11}}\right) = \tan^{-1}\left(\frac{-1}{0}\right) = -90^\circ$  degrees. The negative sign indicates that the rotation direction from State 1 to State 2 is clockwise around point D.



### **3.8 Computer prototype development**

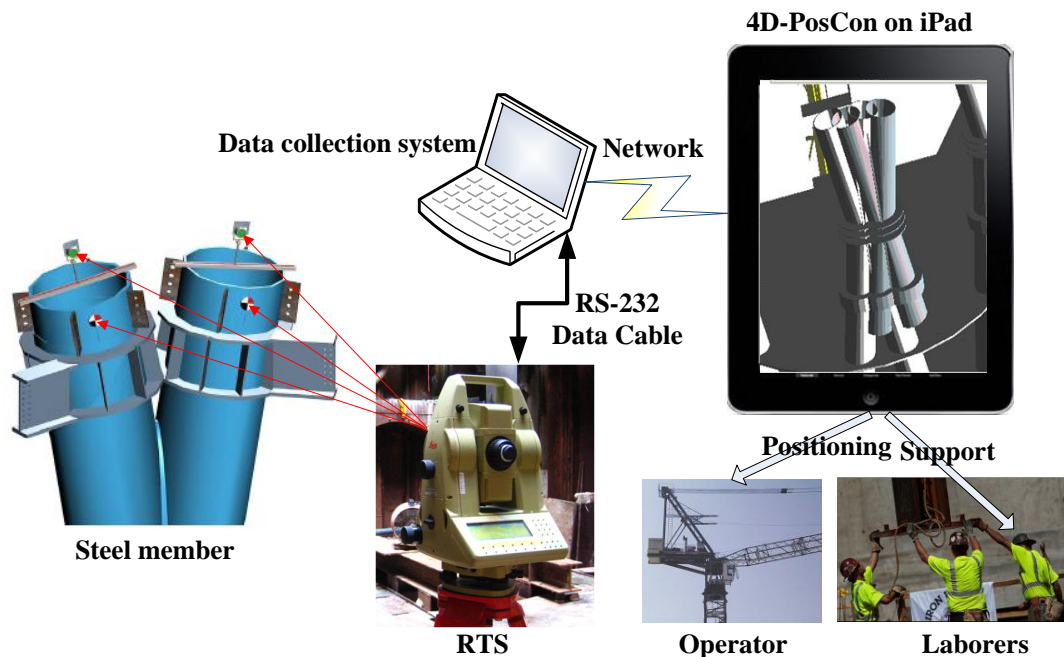
Based on the presented methodology, a software system named as 4D-PosCon (acronym of four dimensional positioning controller) was prototyped, consisting of three modules, namely on-site data collection system, 3D positioning controller, and 4D production model builder. Figure 3-8 illustrates the software architecture of the prototype system. Considering the variety and evolution of on-site data collection technologies, embedding the data collection system in the 4D-PosCon would compromise the system's extensibility. In order to allow for easy integration with alternative on-site data collection technologies in the future, a standalone data collection system, which was developed for operating the robotic total station through a RS-232 data communication cable (Shen et al. 2010), is integrated to materialize the development of 4D-PosCon. Note, the communication between the data collection system and 4D-PosCon needs to be addressed.



**Figure 3-8: The software architecture of 4D-PosCon**

Matured wireless network technologies available for data communication include TCP/IP (Transmission Control Protocol/Internet Protocol), HTTP (Hypertext Transfer Protocol) and Web-Service. They are Internet-based data exchange protocols enabling real-time data communications between different applications. Following a certain protocol, the data collection system and 4D-PosCon can be installed in multiple computers distributed at different places, so that the equipment operators and erection laborers can use 4D-PosCon at their respective working locations. Figure 3-9 conceptualizes the application of the system on a construction site during structural steel installation. In the developed prototype system, the TCP/IP protocol was adopted to

transfer data packets from the data collection system to 4D-PosCon, as ready-to-use TCP/IP programming libraries are provided in the majority of software development kits (SDK) like Java SDK and Microsoft .Net Framework.



**Figure 3-9: Conceptualization of the application of 4D-PosCon system on a construction site during structural steel installation**

- Open a TCP/IP socket to connect DCS using open(IP, Port)
- Listening on the port, and whenever a data package arrive:
  1. Deserialize the data package using Deserialize(Data Array)
  2. Validate and verify the data
- User selected a building component to be tracked
  1. Get the selected object by using the pluggable interface function get(ID)
- Create a copy of the building component object using copy()
  1. Get the as-designed coordinates from the object getCoordinate(PointID)
  2. Compute the kinematic parameters using collected data: kineParameters()
  3. Update the position and orientation of the copied object using update(object)

**Figure 3-10: Pseudo code specifying execution procedure of 4D-PosCon**

The erection positioning controller is designed to translate the raw point-surveying data collected into the transformation matrix based on the proposed methodology. Figure 3-10 gives the pseudo code specifying the execution procedure of the positioning controller: First, a TCP/IP socket is opened to connect with the data collection system

(i.e. the total station) by specifying the particular IP and port addresses. Whenever a data package is received, the controller deciphers the data and validates its format for ensuing computation.

In order to reduce the system's complexity while enhancing its extensibility, the interface technology is applied to allow the positioning controller and 4D production model builder to function independently. In the field of computer science, an interface refers to a point of interaction between different software modules (Blaauw et al. 1997). As such, each module functions independently and relies on interfaces to communicate with other modules through defined methods and associated protocols.

By using the interface technology, different positioning controllers, which correspond with different data collection systems, can be developed, thus eliminating the need to modify the core of the complex 4D graphic platform (i.e. the 4D production model builder). This design strategy is deemed critical to construction engineering software development due to the non-unique and dynamic nature of the construction industry (Kamat and Martinez 2008). In the prototype system, the erection positioning controller uses the pluggable interface to retrieve the 3D model and the tracking point data of the building component being tracked in order to compute the transformation matrix and update the position and orientation of the building component model.

Figure 3-11 shows the graphic user interface (GUI) of the 4D-PosCon system designed to be user-friendly and very intuitive. Users need to enter the IP and Port addresses to connect with the data collection system through the Internet. The next step is to select the model for the building component to be tracked in the 3D view given in the left hand side of Figure 3-11. The selected component is then highlighted and displayed in a small window below. Then, clicking on the “Tracking Select” button at the top right corner of the screen triggers the execution of 4D-PosCon’s controller in accordance with the pseudo code given in Figure 3-10. The 3D view is then updated with the collected surveying data, and the three gauges show the derived three rotation angles between the current state and the final as-designed state of the building component.

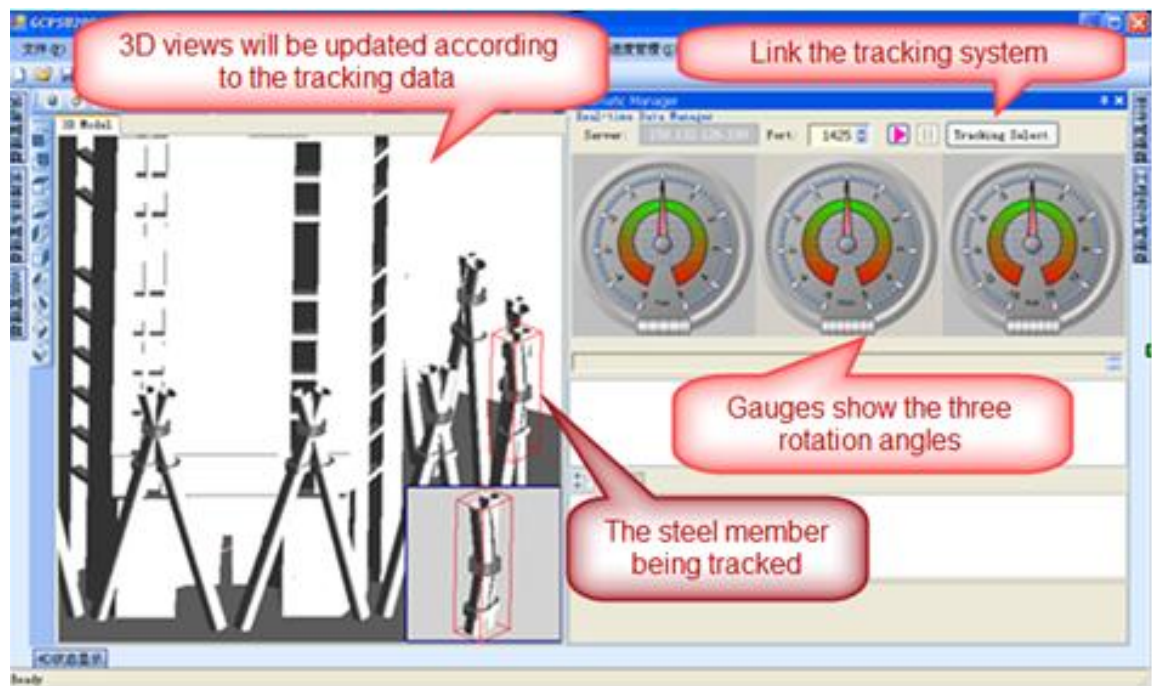
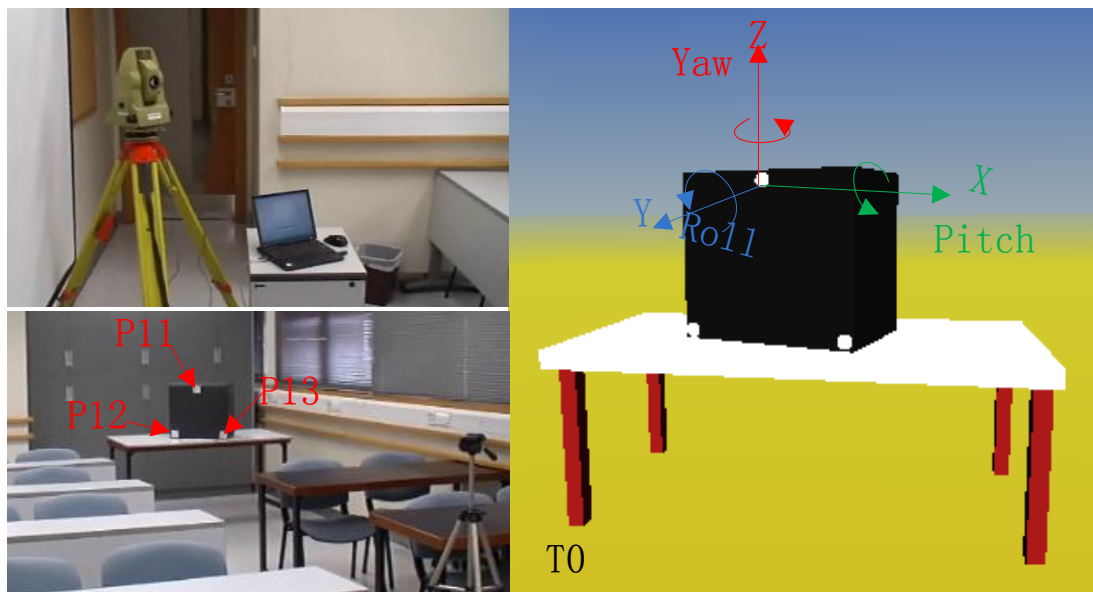


Figure 3-11: Graphical user interface of 4D-PosCon

### 3.9 Laboratory test

It is difficult to validate the methodology for 3D problem by using numerical analysis, since the real data cannot be observed from a Cartesian Coordinates System. In order to validate the methodology on 3D problem, laboratory experiments were designed and carried out. The set up of the test is shown in Figure 3-12. Three reflective tapes were adhered to corresponding tracking points on a black box (510mmX460mmX340mm) that simulated a building component. A Leica TCA 1000 total station was connected to a laptop computer using RS232 cable. The as-designed state (time event T0) of the box was modeled using 3D MAX and then imported into the developed visualization system.



**Figure 3-12: The set up of the laboratory test: (a) Leica TCA 1000 total station connected to a laptop computer using RS232 cable; (b) Three reflective tapes adhered to tracking points on a black box; (c) As-designed state (time event T0) of the box imported into 4D-PosCon**

The laptop computer controlled the point tracking and surveying operations. In one surveying cycle, it took around half a minute to survey the three tracking points in the sequence of P11, P12 and P13. The surveying data are shown in Appendix B. In one

surveying cycle, the box remained stationery, and the interval between two surveying cycles was pre-set as about one minute. However, as shown in Figure 3-13, the robotic total station will automatically search the target points and measure the horizontal and vertical angles and the distance between the target points and the total station. The time needs to search and lock a target point is not consistent since the robotic total station will try many times to search the target points from the initial position. Moreover, during the manipulation of the box, the measured data need to be removed from the data set, thus the time gap between different series of measurements is not consistent.

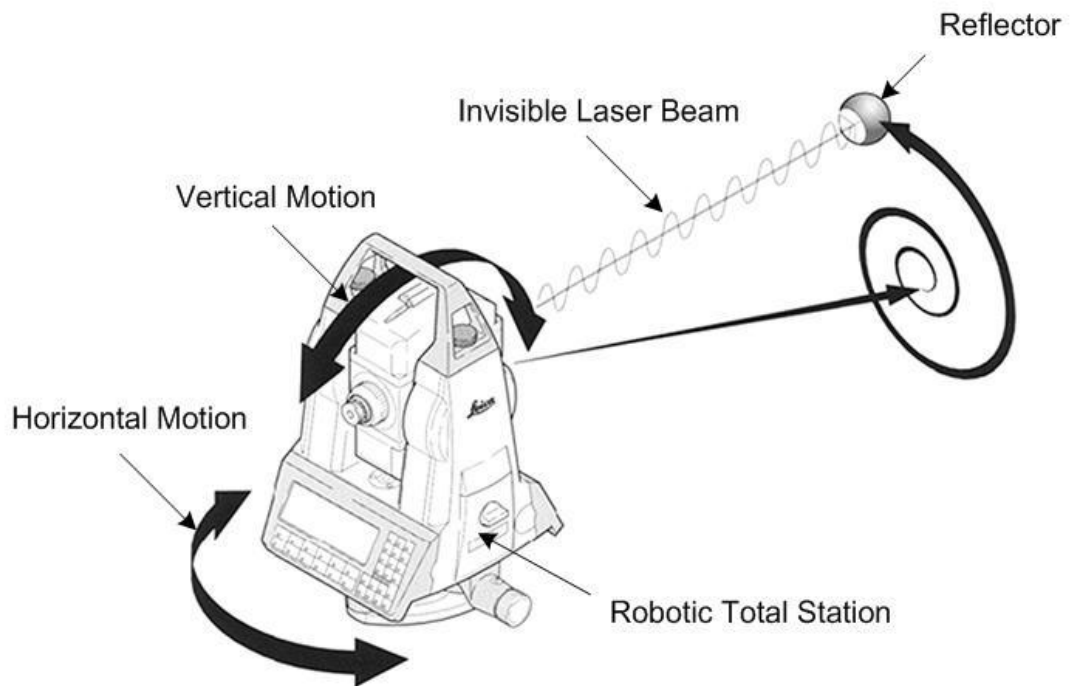


Figure 3-13: The mechanism of automatic target tracking by robotic total station

Figure 3-14 shows the four sets of surveying data, namely, T0: denoting the as-designed positioning state, T1: a simulated actual state with 10 degrees rotation about axis Z (Yaw), T2: a simulated actual state with -10 degrees rotation about axis X (Pitch), T3: a simulated actual state with 6.5 degrees rotation about axis Y (Roll). The raw surveying data contains point identification, surveying time, slope distance, horizontal angle, and vertical angle between each tracking point and the total station.

Point ID & Survey Time			Raw Surveying Data			Coordinates			Computing Results		
Point ID	Date	Time	H <sub>z</sub> Angle	V Angle	Distance	Northing	Easting	Elevation	Yaw	Pitch	Roll
	11	20100520 161336	66.808	90.822	9.254	8.505	3.644	-0.133			
	12	20100520 161407	65.583	93.2	9.259	8.418	3.822	-0.517			
<b>T0</b>	13	20100520 161427	68.19	93.207	9.296	8.617	3.448	-0.52	-61.9904	1.0119	-0.4058
	11	20100520 162421	66.778	90.825	9.251	8.5	3.647	-0.133			
	12	20100520 162431	65.59	93.211	9.222	8.385	3.805	-0.516			
<b>T1</b>	13	20100520 162442	68.088	93.192	9.33	8.642	3.476	-0.52	9.9751	-0.2099	-0.1329
	11	20100520 162746	66.698	90.498	9.331	8.57	3.691	-0.081			
	12	20100520 162755	65.502	92.838	9.268	8.423	3.838	-0.459			
<b>T2</b>	13	20100520 162805	68.105	92.86	9.303	8.621	3.465	-0.464	-0.1712	-10.1105	-0.2341
	11	20100520 163112	66.411	90.69	9.248	8.474	3.7	-0.111			
	12	20100520 163124	65.455	93.186	9.259	8.409	3.84	-0.515			
<b>T3</b>	13	20100520 163134	68.048	92.912	9.289	8.604	3.468	-0.472	-0.3404	0.0961	6.2521

**Figure 3-14: Surveying data and computing results for four positioning states of the box**



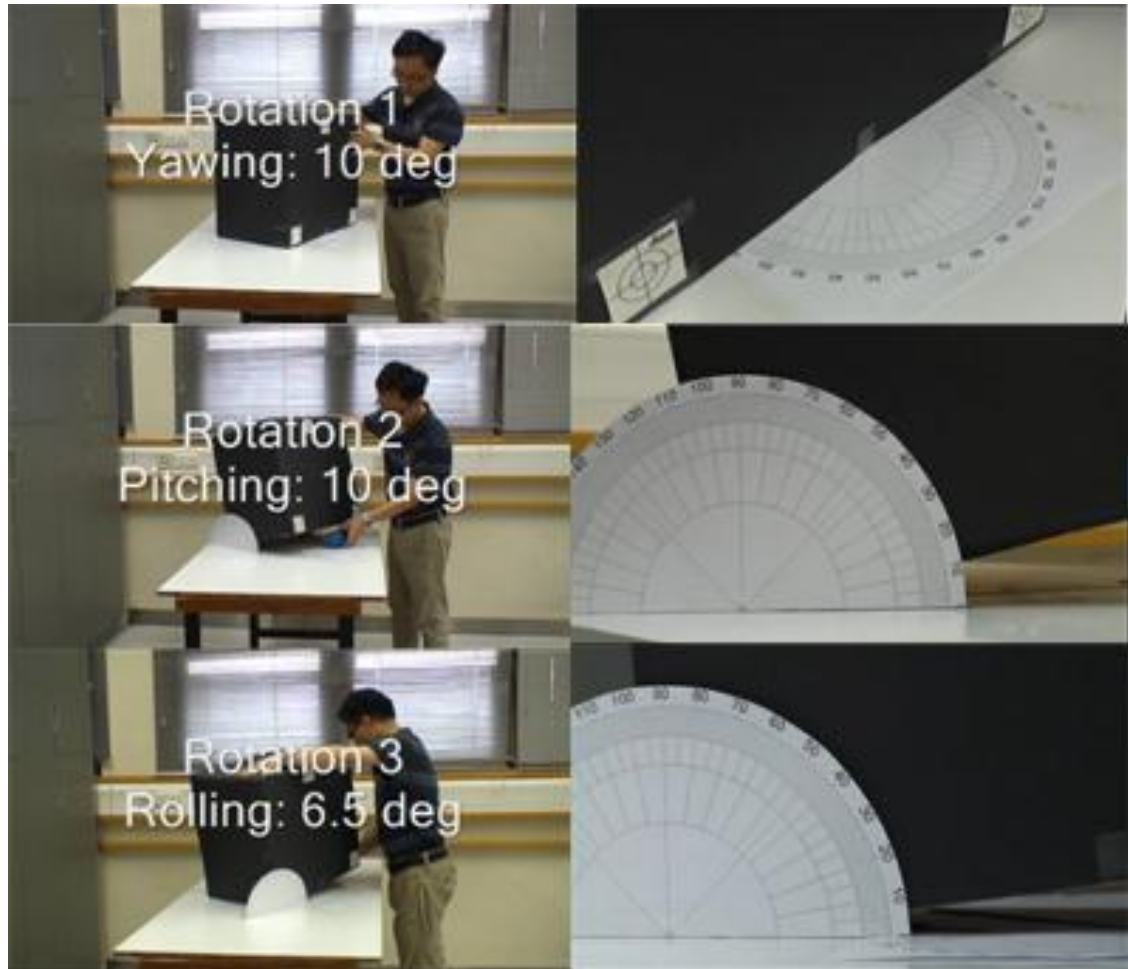


Figure 3-15: Using protractor to measure the rotation angles as bench mark

As shown in Figure 3-15, in order to verify the computing results, we used a protractor to measure the rotation angles between the “final” positioning state (black box at T0) and a simulated “actual” state of the box (T1, T2 and T3).

### ***3.9.1 Computation by using the proposed algorithm***

The raw surveying data were then transferred into the developed system through the Internet, and processed by the positioning controllers to calculate the coordinates of each point with respect to the total station’s coordinate system (Northing, Easting and

Elevator). These coordinates were then transformed with respect to the box coordinate system (shown in Figure 3-12). This transformation was based on the three rotation angles which were determined from initializing the total station at T0 (-61.99, 1.0119, -0.4058 as shown in Figure 3-14). The three rotation angles were entered in Equation (19) to generate the transformation matrix, and then the matrix was applied to transform the point coordinates with reference to the box coordinate system. The transformation results are listed in Table 3-1:

Table 3-1: Transformation of the coordinates from total station CS to Box CS

		Total station CS (m)			Box CS(mm)		
		Northing	Easting	Elevation	X	Y	Z
T0	P11	8.5050	3.6440	-0.1330	0.0000	0.0000	0.0000
	P12	8.4180	3.8220	-0.5170	-190.7074	-6.0073	-387.6901
	P13	8.6170	3.4480	-0.5200	232.9208	-6.0360	-382.6754
T1	P11	8.5000	3.6470	-0.1330	-4.9961	3.0053	-0.0884
	P12	8.3850	3.8050	-0.5160	-191.2180	31.1088	-386.6238
	P13	8.6420	3.4760	-0.5200	219.9461	-41.2576	-382.9928
T2	P11	8.5700	3.6910	-0.0810	-11.9448	-79.5651	51.6209
	P12	8.4230	3.8380	-0.4590	-203.5793	-18.0544	-329.9477
	P13	8.6210	3.4650	-0.4640	218.7344	-17.6659	-326.9574
T3	P11	8.4740	3.7000	-0.1110	-64.4037	1.0226	20.7875
	P12	8.4090	3.8400	-0.5150	-210.8598	-6.5195	-386.0721
	P13	8.6040	3.4680	-0.4720	208.2544	-4.0502	-335.1294

Next, the transformed coordinates of the three tracking points were processed by the algorithms of the proposed methodology given in Sections 6 and 7, resulting in the rotation matrices and rotation angles as followings:

Step 1: Calculation of the mean-coordinates at initial state  $T_0$  :

$$\bar{x}_{t_0} = [14.0711 \quad -4.0144 \quad -256.7885]^t \quad (1)$$

And subtract the mean-coordinates form each of the three points at state  $T_0$ :

$$\dot{x}_{p11,t0} = x_{p11} - \bar{x}_{t0} = [-14.0711 \quad 4.0144 \quad 256.7885]^t$$

$$\dot{x}_{p12,t0} = x_{p12} - \bar{x}_{t0} = [-204.7785 \quad -1.9928 \quad -130.9016]^t \quad (2)$$

$$\dot{x}_{p13,t0} = x_{p13} - \bar{x}_{t0} = [218.8497 \quad -2.0216 \quad -125.8869]^t$$

Step 2: Calculation of the pose change between states  $T_0$  and  $T_1$  :

The mean-coordinates at state  $T_1$ :

$$\bar{x}_{t1} = [7.9107 \quad -2.3812 \quad -256.5683] \quad (3)$$

And subtract the mean-coordinates form each of the three points at state  $T_1$  :

$$\dot{x}_{p12,t1} = x_{p12} - \bar{x}_{t0} = [-12.9068 \quad 5.3864 \quad 256.4799]^t$$

$$\dot{x}_{p12,t1} = x_{p12} - \bar{x}_{t0} = [-199.1287 \quad 33.4900 \quad -130.0554]^t \quad (4)$$

$$\dot{x}_{p12,t1} = x_{p12} - \bar{x}_{t0} = [212.0354 \quad -38.8764 \quad -126.4245]^t$$

Construction of the correlation matrix:

$$c = \frac{1}{3} \sum_{i=1}^3 \dot{x}_{p1i,t1} (\dot{x}_{p1i,t0})^t =$$

$$\frac{1}{3} \left( \begin{bmatrix} -12.9068 \\ 5.3864 \\ 256.4799 \end{bmatrix} [-14.0711 \quad 4.0144 \quad 256.7885] + \begin{bmatrix} -199.1287 \\ 33.4900 \\ -130.0554 \end{bmatrix} [-204.7785 \quad -1.9928 \quad -130.9016] + \begin{bmatrix} 212.0354 \\ -38.8764 \\ -126.4245 \end{bmatrix} [218.8497 \quad -2.0216 \quad -125.8869] \right) = \begin{bmatrix} 29121 & 28 & 1314 \\ 5147 & 11 & 631 \\ -1548 & 515 & 32934 \end{bmatrix} \quad (5)$$

SVD:

$$\mathbf{c} = \mathbf{u} \cdot \mathbf{w} \cdot \mathbf{v}^t =$$

$$\begin{bmatrix} 0.3438 & 0.9229 & 0.1734 \\ -0.0719 & -0.1583 & 0.9848 \\ -0.9363 & 0.3510 & -0.0120 \end{bmatrix} \begin{bmatrix} 33495 & 0 & 0 \\ 0 & 29017 & 0 \\ 0 & 0 & 0 \end{bmatrix} \begin{bmatrix} 0.3532 & 0.9355 & 0.0003 \\ -0.0147 & 0.0053 & 0.9999 \\ -0.9354 & 0.3532 & -0.0156 \end{bmatrix} \quad (6)$$

Computing the rotation matrix:

$$\mathbf{R} = \mathbf{u} \begin{bmatrix} 1 & 0 & 0 \\ 0 & 1 & 0 \\ 0 & 0 & \det(\mathbf{u}\mathbf{v}^t) \end{bmatrix} \mathbf{v}^t$$

$$= \begin{bmatrix} 0.3438 & 0.9229 & 0.1734 \\ -0.0719 & -0.1583 & 0.9848 \\ -0.9363 & 0.3510 & -0.0120 \end{bmatrix} \begin{bmatrix} 1 & 0 & 0 \\ 0 & 1 & 0 \\ 0 & 0 & 1 \end{bmatrix} \begin{bmatrix} 0.3532 & 0.9355 & 0.0003 \\ -0.0147 & 0.0053 & 0.9999 \\ -0.9354 & 0.3532 & -0.0156 \end{bmatrix} \quad (7)$$

$$= \begin{bmatrix} 0.9849 & 0.1732 & 0.0017 \\ -0.1732 & 0.9849 & -0.0040 \\ -0.0023 & 0.0037 & 1.0000 \end{bmatrix}$$

Computing the rotation angles:

$$\varphi = \tan^{-1}\left(-\frac{r_{21}}{r_{11}}\right) = \tan^{-1}\left(-\frac{-0.1732}{0.9849}\right) = 9.9751$$

$$\theta = \tan^{-1}\left(-\frac{r_{32}}{r_{33}}\right) = \tan^{-1}\left(-\frac{0.0037}{1}\right) = -0.2099 \quad (8)$$

$$\phi = \sin^{-1}(r_{31}) = \sin^{-1}(-0.0023) = -0.1329$$

Step 3: Repeat step 2 for  $\mathbf{T}_2$  and  $\mathbf{T}_3$ , and the results are:

$\mathbf{T}_2$ :

$$\varphi = \tan^{-1}\left(-\frac{r_{21}}{r_{11}}\right) = \tan^{-1}\left(-\frac{0.0030}{1.0000}\right) = -0.1712$$

$$\theta = \tan^{-1}\left(-\frac{r_{32}}{r_{33}}\right) = \tan^{-1}\left(-\frac{0.1755}{0.9845}\right) = -10.1105 \quad (9)$$

$$\phi = \sin^{-1}(r_{31}) = \sin^{-1}(-0.0041) = -0.2341$$

**T<sub>3</sub>:**

$$\phi = \tan^{-1}\left(-\frac{r_{21}}{r_{11}}\right) = \tan^{-1}\left(-\frac{0.0059}{0.9940}\right) = -0.3404$$

$$\theta = \tan^{-1}\left(-\frac{r_{32}}{r_{33}}\right) = \tan^{-1}\left(-\frac{-0.0017}{0.9941}\right) = 0.0961 \quad (10)$$

$$\phi = \sin^{-1}(r_{31}) = \sin^{-1}(0.1089) = 6.2521$$

### 3.9.2 Comparing the calculated results with the measured results

The measured rotation angles and calculated angles by the proposed methodology are given in Table 3-2. Although the calculation can give three places of decimal accuracy, the state-of-the-art physical measurements by using protractor only have one place of decimal accuracy. In order to compare the “actual results” with the calculated result, only two places of decimals are kept. From the Table 3-2, it can be concluded that the errors in the computed rotation angles are within 0.5 deg as benchmarked against the protractor measurements, and the calculated rotation changes of the box closely reflect its actual movements.

Table 3-2: the calculated results and the measured results

	Rotation angles	Measured results	Calculated results
T1	$\phi$	10.0	9.98
	$\theta$	0.0	-0.21
	$\phi$	0.0	-0.13
T2	$\phi$	0.0	-0.17
	$\theta$	-10.0	-10.11

	$\phi$	0.0	-0.23
	$\varphi$	0.0	-0.34
T3	$\theta$	0.0	0.10
	$\phi$	6.5	6.25

### ***3.9.3 Visualization of the computing results***

The rotation matrices were utilized in the 4D-PosCon to update the positioning of the 3D virtual model. Shown in Figure 3-16, the 4D-PosCon makes a copy of the black box model and changes the position of the box according to the real situation (rendered in purple).

The 3D visualization gives rise to both accurate analysis and intuitive perception of the relative position and rotation between the positioning states of the box. The proposed method is conducive to detecting some minute deviations occurring when maneuvering the box, as observed in T3. To arrive at the actual positioning state of T3, we rotated the box about the axis Y(Roll) by 6.5 deg while incidentally inducing about 0.5 deg of yawing rotation. The 4D-PosCon determines the roll and yaw to be 6.29 deg and 0.41 deg, respectively. Note the 0.5 deg yawing of the box can be easily visualized as the black portion at the left bottom corner of the box in the T3 snapshot given in Figure 3-16.

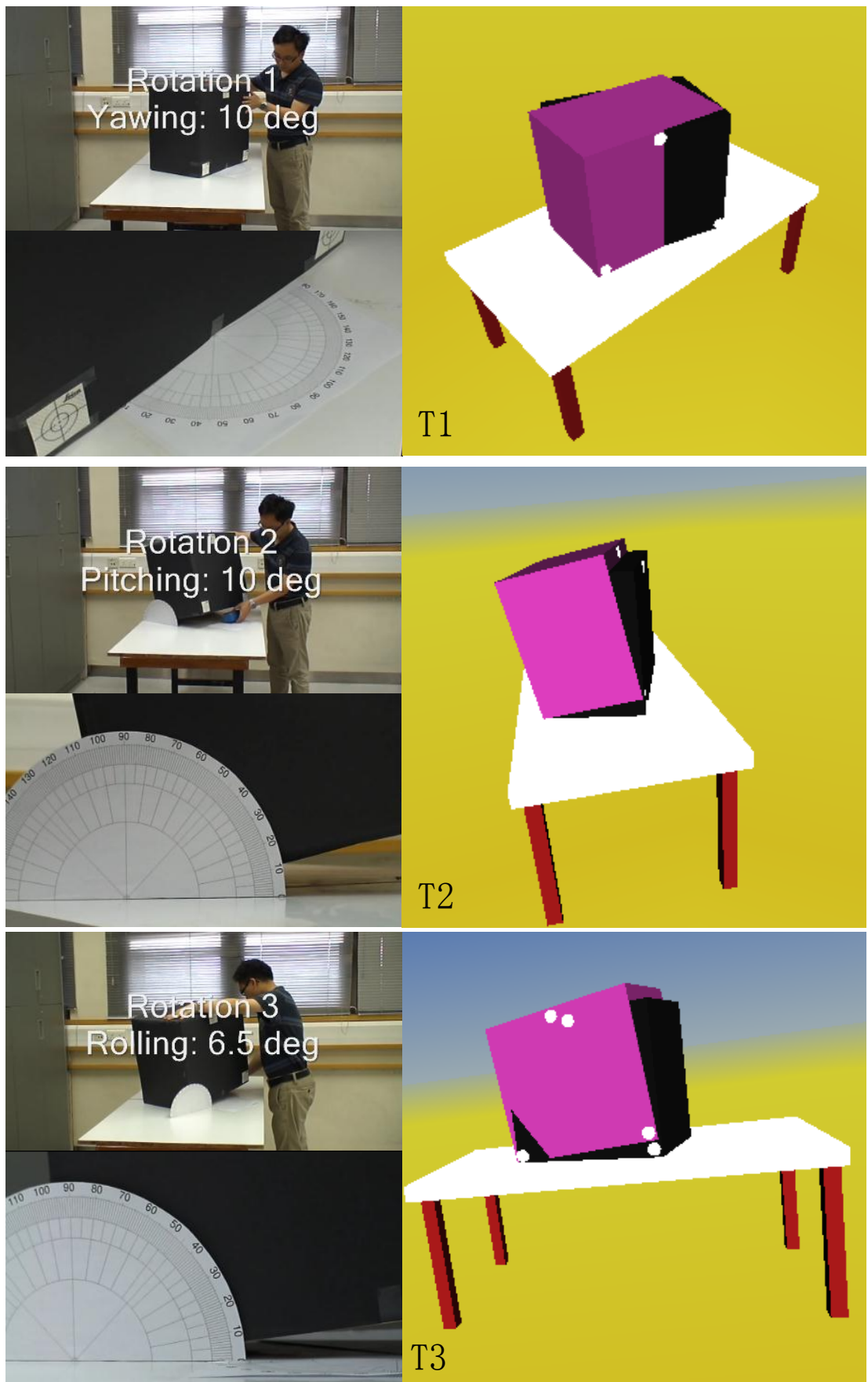


Figure 3-16: Visualization of the rotation deviations on the box

### **3.10 Summary**

This chapter has proposed a methodology for real-time 3D positioning and visualization of single solid site object by integrating automated construction surveying with 3D data models. A special algorithm has been applied to transform the coordinates of a limited quantity of tracking points into a transformation matrix, which is then used to update the position and orientation of the 3D geometric models. The real-time 3D positioning and visualization of solid site objects can improve current construction practices in terms of efficiency and accuracy.

Based on the proposed methodology, a computer system named as 4D-PosCon has been prototyped. 4D-PosCon extends the application of state-of-the-art 4D technologies to visualize the real-time position and orientation of a building component being tracked. The strategies for designing 4D-PosCon are elaborated, which are intended to provide researchers and software vendors with insights of the requirements, challenges, and opportunities in developing next generation 4D tools. With those tools, the 4D models can be readily integrated with automated data collection systems in support of both planning and operation control on a construction site.

To validate the proposed methodology and test the prototype system of 4D-PosCon, laboratory experiments were designed and carried out. The experimental results show



that the proposed methodology not only provides acceptable accuracy, but the visualization also enhances users' intuitive perceptions of any deviations between the as-designed model and the actual pose of solid objects.

## ***Chapter 4 Real-time 3D Positioning and Visualization of Articulated System***

### **4.1 Introduction**

Construction equipment plays an important role in many construction operations, such as earth moving by loaders and haulers, large-scale building components lifted by various cranes, tunnelling by tunnel boring machines. The interactions between the components/material and construction equipment characterize major construction operations on construction sites.

Chapter 3 has introduced the techniques for realizing the real-time 3D visualization of solid objects on site. However, most construction equipment is a kind of articulated system with an open kinematic chain. Compared with a solid object which is usually treated as one solid body, construction equipment is comprised of multiple solid bodies which are linked by joints (i.e. revolute joints and prismatic joints). It is not feasible to treat each component that makes up the equipment as a separate single solid object for independent 3D positioning due mainly to three considerations: (1) because the equipment may consist of many parts articulated by mechanical joints, tracking and positioning a large quantity of control points in one surveying cycle would entail

frequent interruptions to the continuous equipment operation; and (2) line of sight to particular control points on certain parts of the equipment may be unavailable or not guaranteed during dynamic site operations in order to enable the application of laser-based positioning technology; and (3) direct installation of measurement instruments (such as gyroscopes and angular sensors) for accurate real-time 3D positioning of all the components of the articulated equipment system can be too expensive to be practical in the field.

This chapter presents a methodology for efficient real-time 3D visualization of articulated construction equipment working on site. Generic data models and analytical procedures are proposed to deduce translation and rotation matrices for positioning each equipment component with respect to the base frame, thus generating the 3D model of construction equipment with an accurate pose at its current working location. The methodology minimizes the use of sophisticated sensors required to position the articulated system in the 3D space, since it does not need the direct measurement of the target points for each component. Instead, lengths of cylinder rods on the equipment, which is much easier to gauge by using linear encoders, provide input data for analytical calculation.

The following sections first describe the importance of the research of real-time 3D positioning and visualization of construction equipment working on site. Then an

overview of the proposed methodology is presented. Following the overview, the underpinning data model is discussed. Next, a kinematic modeling technique widely used in the robotics literature is introduced and adapted for mathematical representation of typical construction equipment. Sections 5 and 6 describe the position analysis technique to solve the mathematical model based on lengths of cylinder rods on a backhoe excavator. Section 7 validates the proposed methodology through 2D and 3D virtual experiments. The conclusion is given in Section 8.

## **4.2 Importance of the research**

### ***4.2.1 Improving the performance of construction equipment operations***

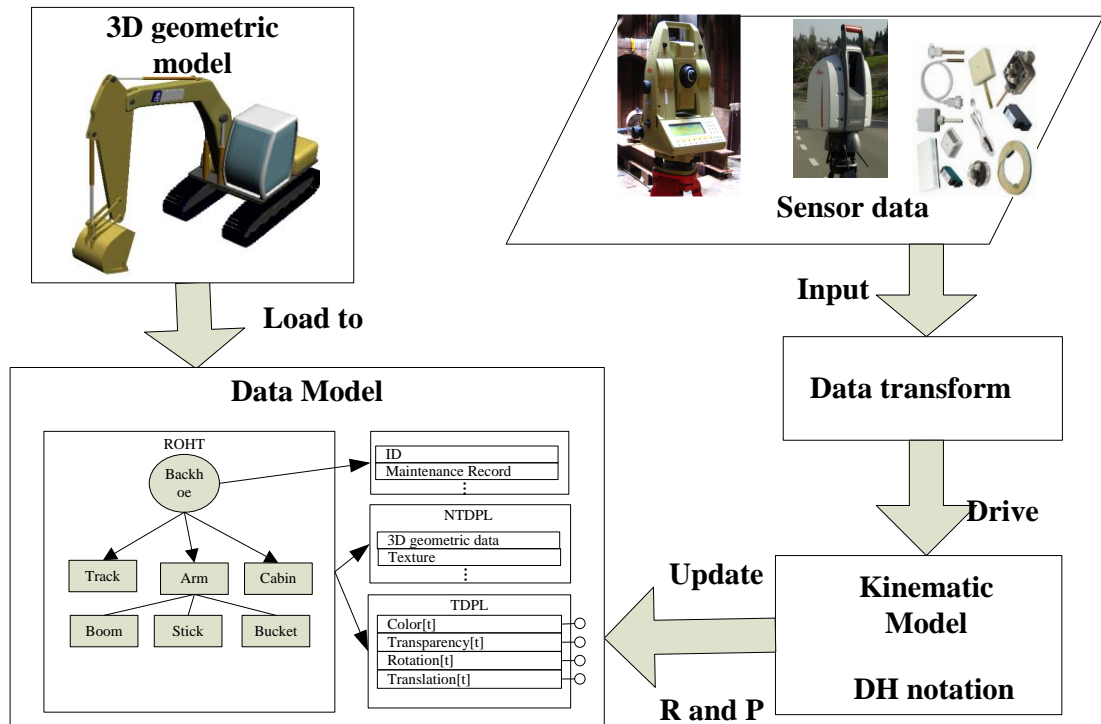
The use of real-time sensor data to update 3D virtual scenes of construction equipment provides a straightforward solution to enhance the operator's situational awareness on a construction site. Real-time 3D positioning and visualization of the construction equipment is defined as the technology that takes advantage of real-time sensor data to update the computer generated 3D virtual scenes of the construction equipment working on site. With the real-time 3D visualization, construction equipment can be correctly positioned in a geo-coordinated site system with respect to current site constraints so as to guide the desired direction of movement as per the design in the immediate future. In addition to gains in quality of work and productivity, revealing spatial relationships between the equipment and surrounding structures and facilities on a real time basis

helps the equipment operator prevent collision accidents. In the near future, real-time 3D positioning and visualization of construction equipment also provides the prerequisite to enable more effective automation control or tele-operation of construction equipment in the field.

#### ***4.2.2 Important component in construction automation system***

A 3D positioning and visualization system is an important component in any construction automation system, e.g. the Automated Steel Construction Testbed (ASCT) developed by the American National Institute of Standards and Technology (NIST) Construction Metrology and Automation Group (Lytle and Saidi 2007; Lytle et al. 2002). In their methodology, three site measurement receivers were mounted on a robotic crane named as RoboCrane to measure the crane's pose in the 3D space. The position data collected from the three receivers were used to calculate the position and orientation parameters of the RoboCrane, which was visualized in a 4D system.

### **4.3 Overview of the proposed methodology**



**Figure 4-1: The logical flow chart of the proposed methodology**

In this chapter a backhoe excavator is studied as an example for describing the whole methodology and application procedures. Nevertheless, the methodology is generic that can be adapted to other types of articulated construction equipment. Figure 4-1 gives the overview and logical flow of the proposed methodology. First, the generic data model for construction equipment is introduced, which is then specifically customized to model the backhoe. Then, 3D geometric models of the backhoe's components are prepared by using a 3D CAD tool and loaded to the data model. The data model decomposes the backhoe into components by following a hierarchical tree data structure. Note the data model is still a static model that does not reflect real construction site operations at this stage. In order to determine the correct pose of the equipment, the rotation matrices and position vectors of each solid component of the equipment must

be updated according to their real poses at a particular time on the site. This can be potentially achieved by integration of automated-data-collection sensors with the equipment kinematic model being proposed.

Kinematics is the study of the motion of objects without consideration of the causes leading to the motion (Beggs 1983). The motion of an object is described in computer by the location and orientation changes in two time frames. The kinematic analysis is about applying mathematics to define the connections between joined objects (such as different components of an equipment system) and determine the movement of real world objects in relation to one another in an analytical fashion. The kinematic model being proposed is intended to minimize the quantity of sensors required to obtain the pose data of the equipment; note the sensor data are straightforward and inexpensive to collect and will be processed through an adapter which contains essentially data transform equations defined for equipment kinematics modeling.

As mentioned in Chapter 2, six parameters are used to describe the position changes between two position states of an object, which can be viewed as the movement of the object between two time events. However, in order to correctly render 3D computer graphics, all the data in the 3D models need be transformed from the previous state to the new state. Basically, the coordinates of all the points in the 3D model are transformed into new coordinates. This is generally achieved by using a  $4 \times 4$

homogeneous transformation matrix (Grigore and Coiffet 2003). In linear algebra, a point's three coordinate values can be represented by a three dimensional vector ( $\bar{\mathbf{x}}$ ).

The homogeneous transformation matrix is applied to transform the vector to a new form that represents the new location of that point:

$$\bar{\mathbf{x}}' = \mathbf{T}\bar{\mathbf{x}} \quad (5)$$

Where  $\mathbf{T}$  is the  $4 \times 4$  homogeneous transformation matrix which can be represented as

Eq. (2):

$$\mathbf{T} = \begin{bmatrix} \cos \theta \cos \varphi & -\sin \varnothing \sin \theta \cos \varphi + \cos \varnothing \sin \varphi & \cos \varnothing \sin \theta \cos \varphi + \sin \varnothing \sin \varphi & \Delta x \\ \cos \theta \sin \varphi & \sin \varnothing \sin \theta \sin \varphi + \cos \varnothing \cos \varphi & -\cos \varnothing \sin \theta \sin \varphi + \sin \varnothing \cos \varphi & \Delta y \\ -\sin \theta & \sin \varnothing \cos \theta & \cos \varnothing \cos \theta & \Delta z \\ 0 & 0 & 0 & 1 \end{bmatrix} \quad (6)$$

Where  $\varnothing, \theta$ , and  $\varphi$  are the three rotation angles, namely, roll, pitch and yaw;  $\Delta x, \Delta y$  and  $\Delta z$  describe location translation between the two time events.

If elements of the matrix are expressed as functions of time, then the matrix represents the motion of an object along the time dimension. Multiplying the three coordinate numbers of a point in the first time frame (before moving) by the transformation matrix will yield the point coordinates in the second time frame (after moving).

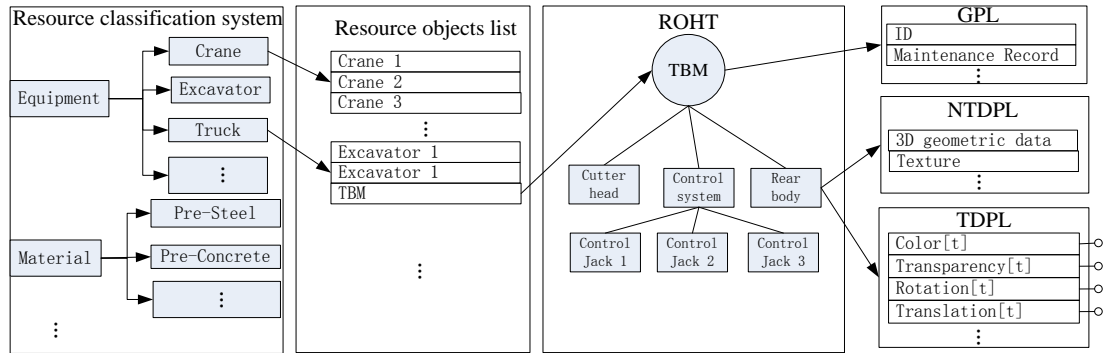
#### 4.4 The generic data models for articulated system

Development of appropriate data models for representing construction resources is vital to construction simulation modeling and applications, such as resource-constrained



scheduling and simulation (Lee and Gatton 1994; Lu et al. 2008; Shi and AbouRizk 1997), 3D visualization of simulated construction operations (Kamat and Martinez 2000; Kamat and Martinez 2004; Kamat and Martinez 2005), and tele-operations/automation in construction (Lytle et al. 2002; Seo et al. 2000; Seo et al. 2007; Yoshida and Awata 2002).

A construction project usually involves a large quantity of equipment and materials resources, each of which can be unique in terms of types, geometric shapes, functions, service time, utilization settings etc. The same resources are modeled in different ways to fit in with particular application purposes and practical site constraints. For example, in a construction scheduling system, concrete is simply treated as a notation showing its updated quantity information, while it will be modeled as a fluid object in a 3D construction operation visualization system (Kamat and Martinez 2004). Thus a resource classification system and a resource object hierarchical tree structure are introduced in the proposed data model in order to manage the diverse nature of construction equipment resources and different level-of-detail requirements in different applications, as shown in Figure 4-2.



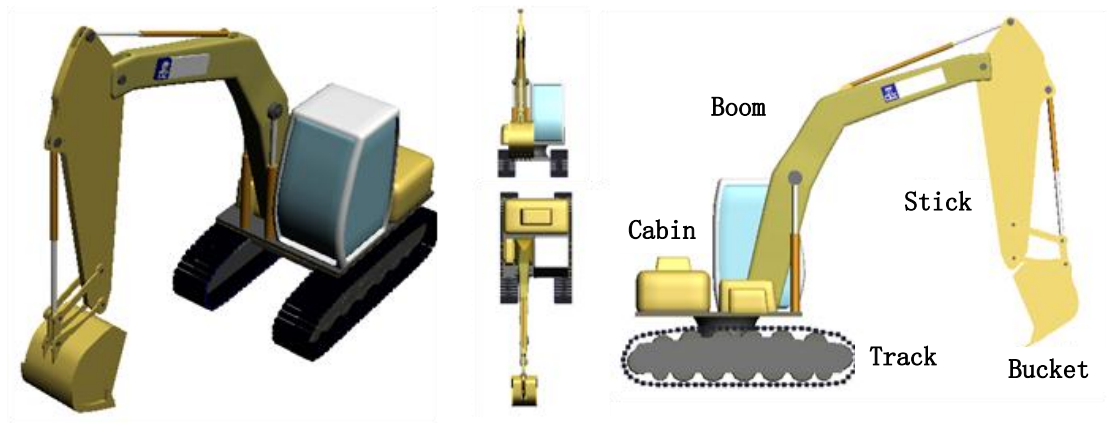
**Figure 4-2: A generic data models for articulated system**

The resource classification system is a set of trees that organize different types of construction resources in groups according to a classification system. Each type of construction resources is also linked with a resource object list that contains all the individual resource objects used in a construction project. In order to manage the different level-of-details, each object in the list is linked with a resource object hierarchical tree (ROHT), which is the same as the BOHT defined with respect to design purposes. The root node is linked with a global property list (GPL) which contains the data describing the characteristics of the particular resource, such as identification number, maintenance records (for construction equipment). Each leaf node in the tree is linked with a NTDPL and a TDPL, similar to the structures defined for the product data model mentioned in Section 3.

#### **4.4.1 Data models for backhoe**

Figure 4-3 shows the prepared 3D geometric model of a typical backhoe which is comprised of a track, a cabin, and a mechanical arm. The arm can be further divided

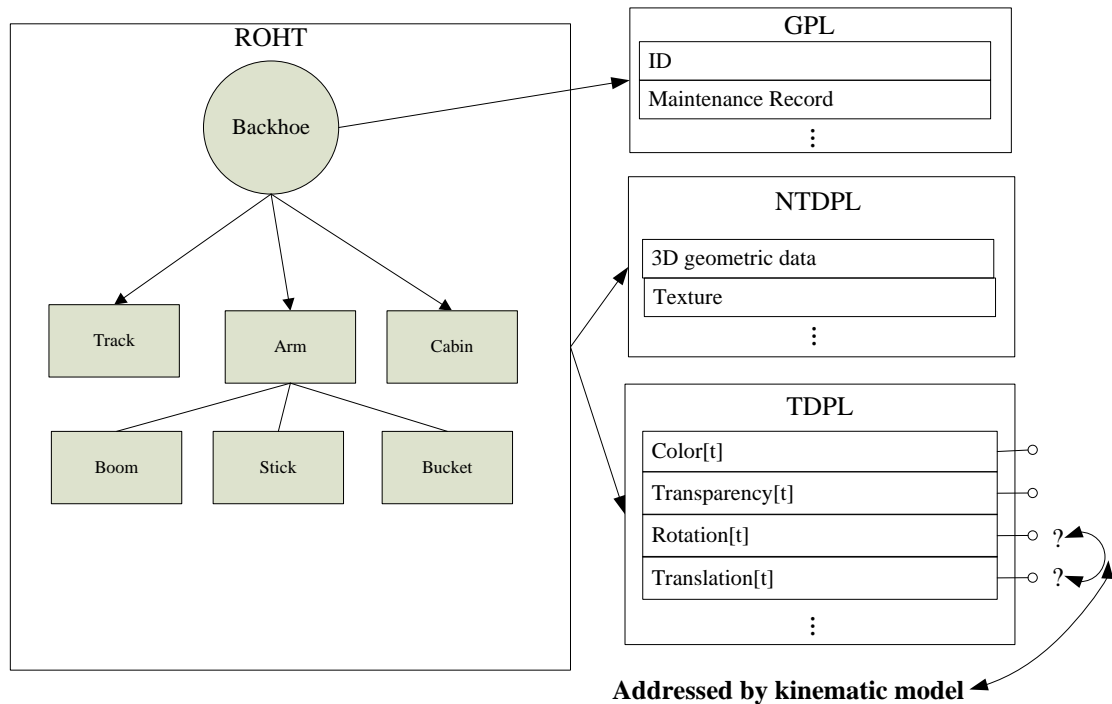
into three parts: the boom, the stick and the bucket. The cabin rotates around an axis perpendicular to the track plane. Similarly, the boom rotates around an axis on the cabin, the stick rotates around an axis on the boom, and the bucket rotates around an axis on the stick.



**Figure 4-3: The 3D model of a typical backhoe**

The 3D models of the backhoe's components are loaded into the data model, as given in Figure 4-4. The resource object hierarchical tree is designed according to the structure of the equipment mentioned above. Each node in the tree is linked with a none-time-dependent property list and a time-dependent property list. Besides, the root node is linked with a global property list that contains the descriptive information of the equipment such as the identification number, the maintenance records. It is noteworthy that the data list is scalable and can be appended with a given quantity of elements making up the equipment system. The following sections focus on addressing two

time-dependent properties in the TDPL, namely the rotation matrix and translation (position) vector for each equipment component.



**Figure 4-4: The data model of the backhoe and the problems will be addressed by kinematic model**

## 4.5 Kinematic Modeling

In this section, a kinematic modeling technique, first proposed by Denavit and Hartenberg (Denavit and Hartenberg 1995), is introduced and adapted for real-time 3D positioning and visualization of a typical articulated system that can be abstracted as an open kinematic chain. The backhoe is used to demonstrate the modeling process.

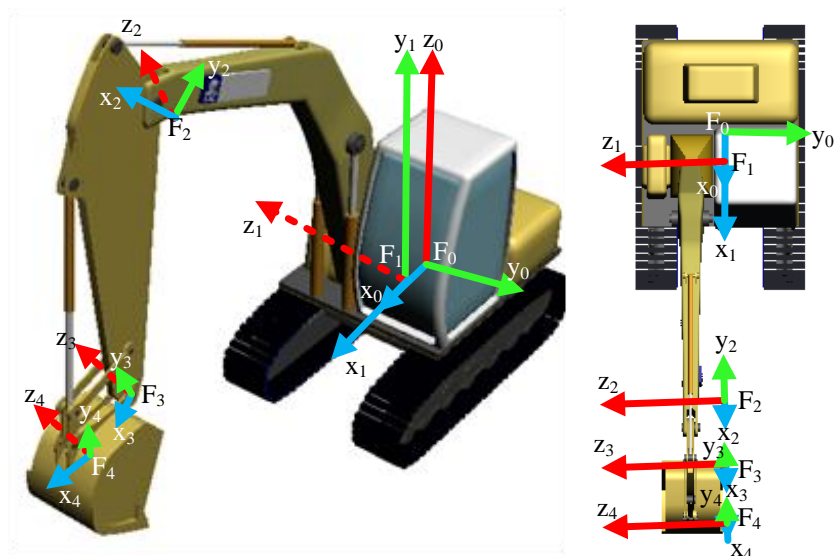
### 4.5.1 Frames assignment

The first step in the development of a kinematic model is to attach coordinate frames to each solid body of the equipment. Note that once positioning frames established, the

relative position and orientation between a frame and a solid body cannot be changed.

Thus all the assigned frames suffice to represent the position and orientation of solid bodies contained in the equipment system. A set of rules and conventions are observed in the frame assignment process as follows:

- The z-vector,  $\mathbf{z}_i$  of a frame  $\mathbf{F}_i$  coincides with the axis of a revolute joint connecting two adjacent components. The only possible exception to this rule is the last frame.



**Figure 4-5: Frame assignment on a backhoe**

As shown in Figure 4-5, the z-vector of the first frame  $\mathbf{F}_0$  (the base frame attached to the track)  $\mathbf{z}_0$  is assigned on the axis of the revolute joint connecting the track and the cabin. By the same rule,  $\mathbf{z}_1$  is assigned on the axis of the revolute joint connecting the cabin and the boom,  $\mathbf{z}_2$  on the axis of the revolute joint connecting the boom and the stick, and  $\mathbf{z}_3$  on the axis of the revolute joint connecting the stick and the bucket,

respectively. One special frame is the one attached to the end link of the articulate chain (i.e. the bucket in the backhoe case). It is the only frame that does not entail the aligning of its z axis with a revolute joint axis. However, in order to simplify the computational procedure given in the next section, it is advisable to align the z axis of the end link of the articulate chain with the z axis of the previous frame, for instance,  $\mathbf{z}_4$  is aligned with  $\mathbf{z}_3$  in the present case.

- The x-vector,  $\mathbf{x}_i$  of a frame  $\mathbf{F}_i$  must be assigned on the common perpendicular to axes  $\mathbf{z}_{i-1}$  and  $\mathbf{z}_i$  and is oriented from  $\mathbf{z}_{i-1}$  to  $\mathbf{z}_i$  (the only exception is the first frame that can point to any direction.) For simplicity, the direction of  $\mathbf{x}_0$  is usually assigned as the direction of  $\mathbf{x}_1$ .

If the axes of  $\mathbf{z}_{i-1}$  to  $\mathbf{z}_i$  are parallel, the common perpendicular can be at any point along the two axes. In this case, the axis  $\mathbf{x}_i$  is located at the point where the axis  $\mathbf{z}_i$  intersects with the axis  $\mathbf{x}_{i-1}$ . as shown in Figure 4-6, axes  $\mathbf{z}_1$  and  $\mathbf{z}_2$  are parallel, thus any axis perpendicular to  $\mathbf{z}_2$  is also perpendicular to  $\mathbf{z}_1$  (e.g. all black axes are the common perpendicular of  $\mathbf{z}_1$  and  $\mathbf{z}_2$  ). In order to unambiguously determine the axis  $\mathbf{x}_2$  , the axis  $\mathbf{x}_1$  is extended to intersect with axis  $\mathbf{z}_2$ . The intersection point is the position where axis  $\mathbf{x}_2$  is located. As shown in Figure 4-7,  $\mathbf{x}_2$ ,  $\mathbf{x}_3$  and  $\mathbf{x}_4$  are located following this rule.

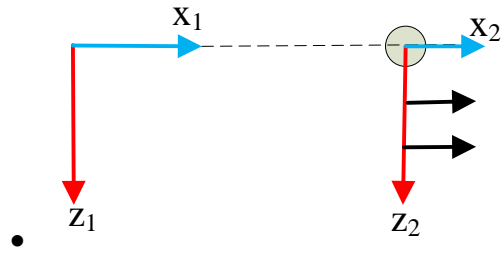


Figure 4-6: Assignments of axis X2 in the case that  $z_1$  is parallel to  $z_2$

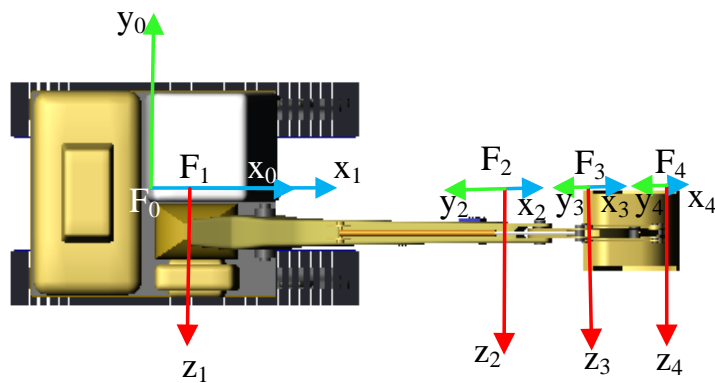


Figure 4-7: Top view of backhoe showing the frames assigned

- The  $y$ -vector,  $y_i$  of a frame  $F_i$  is determined by the right hand rule as shown in Figure 4-8: using right hand to hold the  $z$ -axis with the thumb pointing to the same direction of axis  $z$ , and the  $y$ -axis is oriented from  $x$ -axis with 90 degrees rotation.

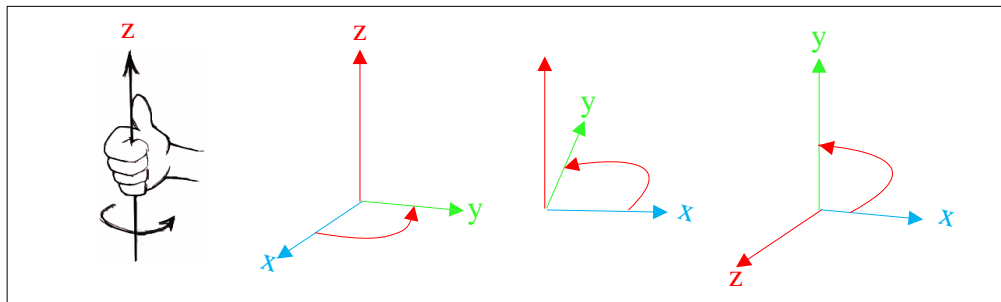


Figure 4-8: The right hand rule on the direction of axis  $y$

Following the three rules, the frames can be fully located on any construction equipment that can be represented with open kinematic chains.

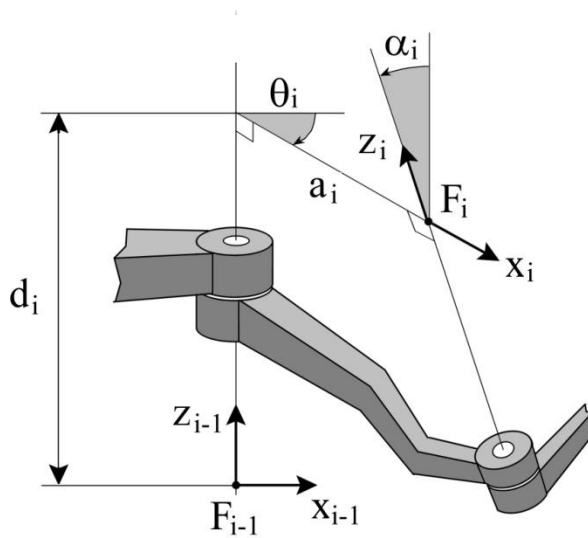
#### ***4.5.2 Representation of frame position and orientation using DH parameters***

The DH technique models the kinematic chain by describing the 3D relationship between each frame along the chain and the preceding frame. As discussed in Chapter 2, the representation of one frame to another is obtained by using a  $4 \times 4$  transformation matrix which can be obtained by using six independent parameters, namely, three rotation angles and a point position described with x, y and z coordinates. However, with all the frames established by following the frame assignment rules mentioned in the previous section, the use of four DH parameters is sufficient to determine the position and orientation of one frame (or a solid object) with respect to another.

The DH parameters are commonly denoted as  $d_i$ ,  $a_i$ ,  $\alpha_i$  and  $\theta_i$  as demonstrated in

Figure 4-9:



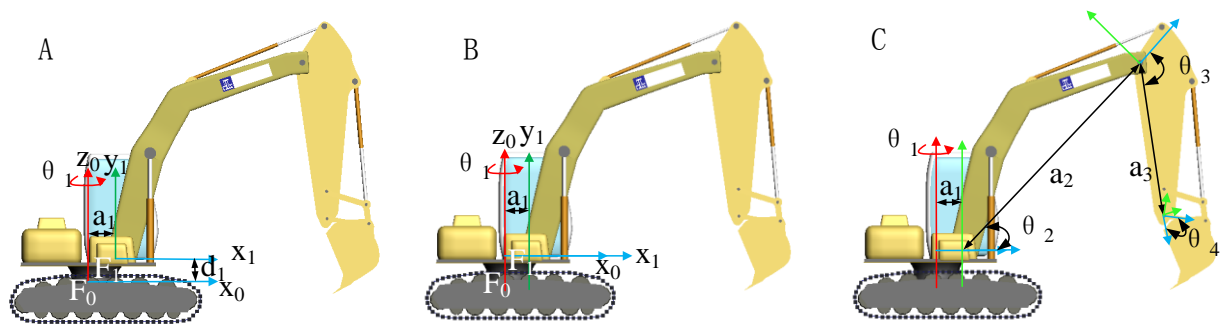


**Figure 4-9: Illustration of DH parameters from frame  $F_{i-1}$  to frame  $F_i$**

- $d_i$ , called link offset, is the length of the common perpendicular to axes  $x_{i-1}$  and  $x_i$ .
- $a_i$ , called link length, is the length of the common perpendicular to axes  $z_{i-1}$  and  $z_i$ .
- $\alpha_i$ , called link twist, is the angle around axis  $x_i$  that rotate axis  $z_{i-1}$  to direction of axis  $z_i$ .
- $\theta_i$ , called link angle, is the angle around  $z_{i-1}$  that rotate axis  $x_{i-1}$  to the direction of axis  $x_i$ .

In a practical case, not all the parameters are time dependent variables. Some parameters are invariable over time, representing the fixed dimensions and configurations of the equipment design. The dimensions of the equipment can be retrieved from equipment specifications, e.g. as shown in Figure 4-10 C,

$d_i, a_i$  and  $\alpha_i$  are invariable over time and hence can be retrieved from design specifications of the equipment. The only time dependent variable is  $\theta_i$ , the rotation angle of the revolute joint connecting two mechanical parts. The time dependent variable can be evaluated based on sensor data and computing algorithms which are addressed in next section.



**Figure 4-10: DH parameters of the backhoe example**

In order to simplify the matrix computation, if possible, the frames should be assigned on such locations that would make most of the parameters equal to zero. As shown in Figure 4-10A and Figure 4-10B, the frames  $F_0$  and  $F_1$  are both assigned according to the DH rules described in above section. However, the link length between  $F_0$  and  $F_1$  is  $d_1$  in Figure 4-10A while it equals zero in Figure 4-10B. As shown in Figure 4-10 C, the backhoe excavator has five solid bodies that are connected by four revolute joints. Thus a total of sixteen (4X4) DH parameters suffice to determine the relative position of the four frames attached on these four joints. However, proper assignment of the four frames can make eight parameters equal zero, and the remaining eight none zero

parameters are  $a_1, \alpha_1, \theta_1, a_2, \theta_2, a_3, \theta_3$  and  $\theta_4$ , among which only  $\theta_1, \theta_2, \theta_3$  and  $\theta_4$  are time dependent parameters corresponding to the rotation angles of four revolute joints, denoted as  $\theta_1^t, \theta_2^t, \theta_3^t$  and  $\theta_4^t$  in following calculations.

The kinematic model that represents the relative motion in the backhoe's components can be summarized in Table 4-1. In the next section, the kinematic model will be used to analyze the 3D position of each component of the backhoe by using mathematical equations.

Table 4-1: DH parameters of the backhoe example

Frame	d	a	$\alpha$	$\theta$	Joint Type
1	0	$a_1$	90	$\theta_1$	Revolute
2	0	$a_2$	0	$\theta_2$	Revolute
3	0	$a_3$	0	$\theta_3$	Revolute
4	0	0	0	$\theta_4$	Revolute

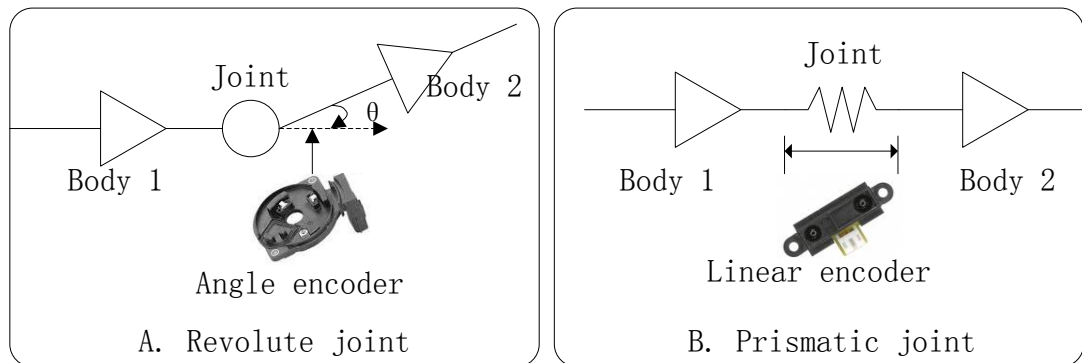
## 4.6 3D positioning analysis

The 3D positioning analysis solves the following problem: Given geometrical dimensions and configurations and mechanical joints for particular construction equipment, how to determine the position matrices for all the frames attached on the solid bodies of the equipment.

### 4.6.1 Raw data from joint sensors

There are many types of sensors can be used to collect site data, so as to drive the real-time 3D positioning and visualization of construction equipment operations. The

commonly used equipment sensors include angle encoders for revolute joints, linear encoders for prismatic joints as shown in Figure 4-11. It is noteworthy that in addition to the measurement accuracy, the effort as needed for sensor installation and implementation is another important factor to consider in applying sensor technologies for practical applications. For example, it is difficult, if not impossible, to install angle encoders on the equipment joints to sense the rotation angles directly. By contrast, it is much easier to install a linear encoder to gauge the length of the cylinder rod of a hydraulic jack that controls the rotation of the joint. Therefore, a computing algorithm is desired which deduces the precise angles from the cylindrical length data measured by linear encoder sensors.

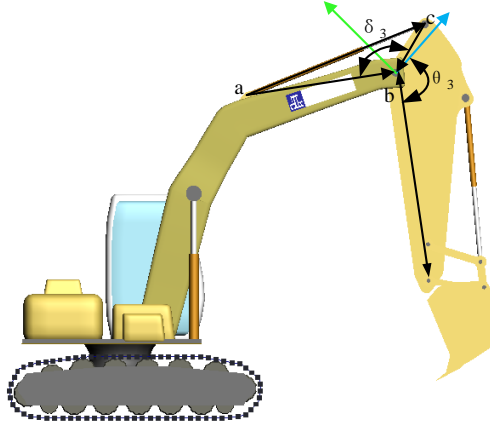


**Figure 4-11: Sensors for revolute and prismatic joints**

#### ***4.6.2 Computing the rotation angles by laws of trigonometry***

As shown in Figure 4-12, the third revolute joint is selected as the demonstration case without loss of generality. Suppose that the backhoe's initial pose (at time event  $t_0$ ) is modeled using 3D CAD and the dimensions are measured in advance, namely,

$\theta_3^{t_0}$ ,  $l_{ac}^{t_0}$ ,  $l_{ab}$  and  $l_{bc}$  are known. The following equations calculate the  $\theta_3^{t_1}$  based on the length of the cylinder rod  $l_{ac}^{t_1}$ .



**Figure 4-12: Translate the linear encoder data to the DH parameters**

The angle  $\delta_3^{t_0}$ , and  $\delta_3^{t_1}$  are calculated by the following equations:

$$\delta_3^{t_0} = \cos^{-1} \frac{l_{ab}^2 + l_{bc}^2 - (l_{ac}^{t_0})^2}{2l_{ab}l_{bc}} \quad (1)$$

$$\delta_3^{t_1} = \cos^{-1} \frac{l_{ab}^2 + l_{bc}^2 - (l_{ac}^{t_1})^2}{2l_{ab}l_{bc}} \quad (2)$$

Thus,  $\theta_3^{t_1}$  is determined by the following equation:

$$\theta_3^{t_1} = \theta_3^{t_0} + (\delta_3^{t_1} - \delta_3^{t_0}) \quad (3)$$

### **4.6.3 Principles of forward kinematics**

In order to visualize the change of the backhoe's pose during construction operations, the rotation matrices and translation vectors for each solid body of the backhoe excavator should be calculated. The first step is to develop the pose matrix by the DH parameters and the principle of forward kinematics, which represents a process to

compute the position and orientation of a frame when all the joint variables (DH parameters) are known.

At a time event  $t$ , a frame  $F_i$  is described with respect to  $F_{i-1}$  by its pose matrix using DH notations (Denavit and Hartenberg 1995):

$$A_i^t = \begin{bmatrix} c_i^t & -\gamma_i^t s_i^t & \sigma_i^t s_i^t & a_i^t c_i^t \\ s_i^t & \gamma_i^t c_i^t & -\sigma_i^t c_i^t & a_i^t s_i^t \\ 0 & \sigma_i^t & \gamma_i^t & d_i^t \\ 0 & 0 & 0 & 1 \end{bmatrix} \quad (4)$$

Where  $c_i^t = \cos(\theta_i^t)$ ,  $s_i^t = \sin(\theta_i^t)$ ,  $\gamma_i^t = \cos(\alpha_i^t)$ , and  $\sigma_i^t = \sin(\alpha_i^t)$ .

Based on the principle of forward kinematics, we can describe all the frames in Figure 4-5 with respect to frame  $F_0$  by the following equation:

$$T_i^t = A_1^t A_2^t \dots A_{i-1}^t A_i^t \quad (5)$$

And the rotation matrix and translation vector can be directly retrieved from the partitioned form:

$$T_i^t = \begin{bmatrix} R_i^t & P_i \\ 0 & 1 \end{bmatrix} \quad (6)$$

Where,  $R_i^t$  is the rotation matrix expressing the orientation of frame  $F_i$  from  $F_0$  and the vector  $P_i$  is the translation vector indicating the move of the origin from  $F_0$  to frame  $F_i$ .

#### **4.6.3.1 The backhoe example**

From the DH parameter in Table 4-1, the transformation matrix can be calculated as follows:

$$T_1^t = A_1^t = \begin{bmatrix} c_1^t & 0 & s_1^t & a_1 c_1^t \\ s_1^t & 0 & -c_1 & a_1 s_1^t \\ 0 & 1 & 0 & 0 \\ 0 & 0 & 0 & 1 \end{bmatrix} \quad (7)$$

Where,  $c_1^t = \cos(\theta_1^t)$ ,  $s_1^t = \sin(\theta_1^t)$ ,  $\gamma_i^t = \cos(90) = 0$ , and  $\sigma_1^t = \sin(90) = 1$ ,  $a_1$  is constant and other parameters equal zero. Similarly:

$$T_2^t = A_1^t A_2^t = \begin{bmatrix} c_1^t & 0 & s_1^t & a_1 c_1^t \\ s_1^t & 0 & -c_1 & a_1 s_1^t \\ 0 & 1 & 0 & 0 \\ 0 & 0 & 0 & 1 \end{bmatrix} \begin{bmatrix} c_2^t & -s_2^t & 0 & a_2 c_2^t \\ s_2^t & c_2^t & 0 & a_2 s_2^t \\ 0 & 0 & 1 & 0 \\ 0 & 0 & 0 & 1 \end{bmatrix} \quad (8)$$

$$T_3^t = A_1^t A_2^t A_3^t = T_2^t \begin{bmatrix} c_3^t & -s_3^t & 0 & a_3 c_3^t \\ s_3^t & c_3^t & 0 & a_3 s_3^t \\ 0 & 0 & 1 & 0 \\ 0 & 0 & 0 & 1 \end{bmatrix} \quad (9)$$

$$T_4^t = A_1^t A_2^t A_3^t A_4^t = T_3^t \begin{bmatrix} c_4^t & -s_4^t & 0 & 0 \\ s_4^t & c_4^t & 0 & 0 \\ 0 & 0 & 1 & 0 \\ 0 & 0 & 0 & 1 \end{bmatrix} \quad (10)$$

#### 4.6.4 The location of the base frame

The construction equipment moves around the site, thus the base frame  $F_0$  needs to be located so that the 3D equipment model can be fixed in real time in the site space. The technique discussed in Chapter 3 can be used to efficiently position the base frame assigned on the track of the equipment.

### 4.7 Validation

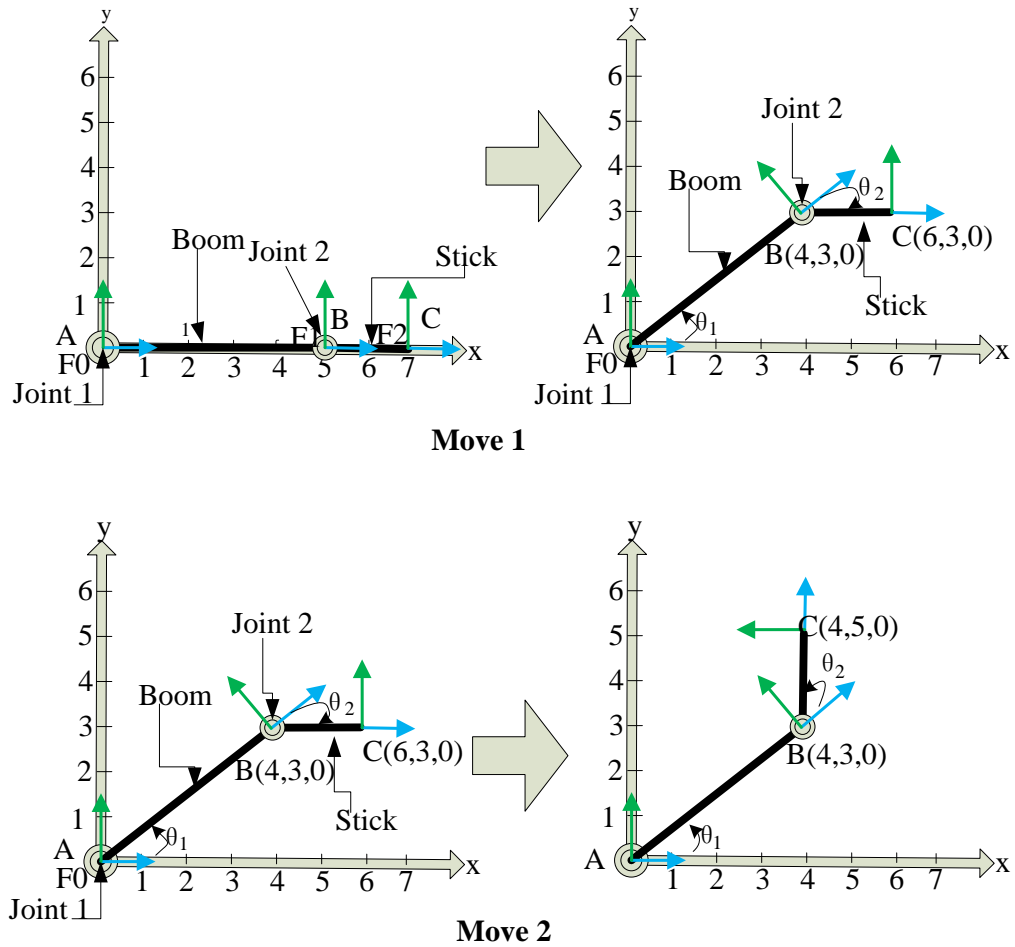
To validate the proposed methodology, we must compare the results from the proposed methodology with the actual results. The articulated system is much more complex than the single solid object, especially when it is defined as a 3D problem. Thus, we will first design a simple articulated system that consists of two solid bodies linked by a revolute

joint. This articulated system can only rotate around the revolute joint axis on a two dimensional (2D) plane, so it is easy to observe the actual movement results from 2D Cartesian Coordinates System. We can readily compare the observed results with the calculated results to validate the proposed methodology.

Validation of the articulated system that can move in the 3D space is much more complex, since it is difficult to observe and measure the actual results from the 3D Cartesian Coordinates System. To validate the proposed methodology in the 3D space, two groups of virtual experiments were designed and conducted in a computer simulation environment. In the first group of experiments, we intentionally moved an articulated system that have similar configurations of a backhoe excavator (for simplification, the bucket is not considered) at three special poses. The pose of the articulated system can be calculated by the law of trigonometry, by which we can obtain the actual position results for cross checking the proposed analytical method. In the second group of experiments, the pose of the articulated system were modeled in a 3D CAD system so as to represent and derive the actual results. The positioning results from the proposed methodology are also entered in the same 3D computer environment (the position of target points are marked in same 3D virtual space). Then we can validate the analytical results by observing the relative positions of target points in the 3D viewer. The following will elaborate on these virtual experiments in details.



### 4.7.1 Validation on 2D experiments



**Figure 4-13: A two dimensional articulated system**

As shown in Figure 4-13, a 2D articulated system is designed to validate the methodology for positioning an articulated system. This numerical example illustrates the movement of an articulated duo-bar system that simulates the boom and the stick of the backhoe excavator. As shown in the Figure 4-13, the “Joint 1” and “Joint 2” revolves around the corresponding axis  $z$  pointing outward of the figure. The upper Fig. 14 illustrates the “Move 1” while the lower Fig. 14 shows the “Move 2” between two time events. The points A, B and C are the end points of the boom and stick. Points A

and B also denote the coordinates of the two joints. The following steps demonstrates the computation procedures and validates the proposed approach by comparing analytical results with corresponding results taken directly from the x-y coordinate system.

### **Step 1: Frames assignment**

To simplify the computation, the boom and stick start from the axis x shown in left hand side figure in “move 1”, and the frames are attached based on the rules discussed in Section 5.1. As shown in Figure 4-13, the **z** axes of the three frames are on the revolute joint axes (the last frame is on the end of the stick), which points outward of the figure.

The **x** axes are assigned on the common perpendicular to axes **z**. Since all z axes are perpendicular to the boom and the stick, **x**<sub>1</sub> is assigned on the direction of boom and **x**<sub>2</sub> is assigned on the direction of stick.

### **Step 2: Determination of the DH parameters:**

The DH parameters are determined by the configurations of the articulated duo-bar system. The length of boom is 5 units and the length of stick is 2 units and both d and  $\alpha$  equals zero. The time-dependent parameters are two angles of the revolute joints, namely,  $\theta_1$  and  $\theta_2$ . The DH parameters are summarized in Table 4-2.

Table 4-2: DH parameters of the backhoe example

Frame	d	a	$\alpha$	$\theta$	Joint Type
1	0	5	0	$\theta_1$	Revolute
2	0	2	0	$\theta_2$	Revolute

**Step 3: Calculations of the transformation matrices by using equations (4) and (5):**

$$T_1^t = A_1^t = \begin{bmatrix} c_1^t & -s_1^t & 0 & 5c_1^t \\ s_1^t & c_1^t & 0 & 5s_1^t \\ 0 & 0 & 1 & 0 \\ 0 & 0 & 0 & 1 \end{bmatrix} \quad (11)$$

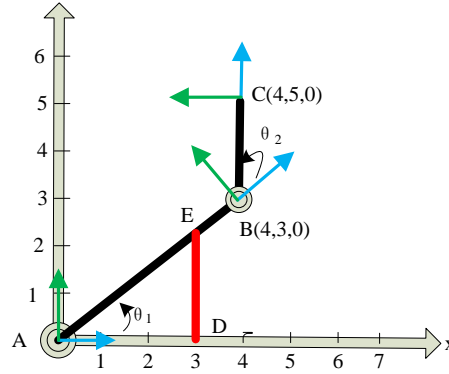
Where  $c_1^t = \cos(\theta_1^t)$ ,  $s_1^t = \sin(\theta_1^t)$ .

$$T_2^t = A_1^t A_2^t = \begin{bmatrix} c_1^t & -s_1^t & 0 & 5c_1^t \\ s_1^t & c_1^t & 0 & 5s_1^t \\ 0 & 0 & 1 & 0 \\ 0 & 0 & 0 & 1 \end{bmatrix} \begin{bmatrix} c_2^t & -s_2^t & 0 & 2c_2^t \\ s_2^t & c_2^t & 0 & 2s_2^t \\ 0 & 0 & 1 & 0 \\ 0 & 0 & 0 & 1 \end{bmatrix} \quad (12)$$

Where  $c_2^t = \cos(\theta_2^t)$ ,  $s_2^t = \sin(\theta_2^t)$ .

Note, the above angles are not spatial orientation angles of a solid body (pitch, yaw, and roll) but joint rotation angles between connected components of an articulated equipment system. As it is difficult to gauge those joint-rotation angles by directly installing instrumentation on the joints, those joint-rotation angles can be easily calculated by the law of trigonometry. For example, as shown in the following figure, if the red bar ED is the hydraulic jack. The angle can be easily calculated based on the length of the cylindrical rod. Actually, in the present case, the required input data  $\cos(\theta_1^t)$  and  $\sin(\theta_1^t)$  are determined by  $\cos(\theta_1^t) = \frac{AD}{AE}$  and  $\sin(\theta_1^t) = \frac{ED}{AE}$ . So all input data can be actually collected from using a linear encoder sensor to gauge the rod

extension length of the hydraulic jack (i.e. ED). Note AD, AE remain constant over the rotation process.



**Figure 4-14: The rotation angles can be computed from linear encoder data**

**Step 4: Validations on “move 1”:**

As shown in the “move 1” of Figure 4-13, the joint rotates an angle that:

$c_1^1 = \cos(\theta_1^1) = \frac{AD}{AE} = 0.8, s_1^1 = \sin(\theta_1^1) = -\frac{ED}{AE} = -0.6$  and  $c_2^1 = \cos(\theta_2^1) = \cos(\theta_1^1) = 0.8, s_2^1 = \sin(\theta_2^1) = -\sin(\theta_1^1) = 0.6$ , where the subscript 1 denotes the time event at which the “move 1” occurred. Note that the angle is negative when the rotation direction is counter-clockwise and positive when the rotation direction is clockwise.

Then:

$$T_1^1 = A_1^1 = \begin{bmatrix} 0.8 & 0.6 & 0 & 4 \\ -0.6 & 0.8 & 0 & -3 \\ 0 & 0 & 1 & 0 \\ 0 & 0 & 0 & 1 \end{bmatrix} \quad (13)$$

$$T_2^1 = A_1^1 A_2^1 = \begin{bmatrix} 0.8 & 0.6 & 0 & 4 \\ -0.6 & 0.8 & 0 & -3 \\ 0 & 0 & 1 & 0 \\ 0 & 0 & 0 & 1 \end{bmatrix} \begin{bmatrix} 0.8 & -0.6 & 0 & 1.6 \\ 0.6 & 0.8 & 0 & 1.2 \\ 0 & 0 & 1 & 0 \\ 0 & 0 & 0 & 1 \end{bmatrix} = \begin{bmatrix} 1 & 0 & 0 & 6 \\ 0 & 1 & 0 & -3 \\ 0 & 0 & 1 & 0 \\ 0 & 0 & 0 & 1 \end{bmatrix} \quad (14)$$

In order to validate the proposed approach, the following calculation determines the coordinates of points B and C, which are then compared against the coordinates taken directly in Figure 4-13. Note, in order to apply the transformation matrix to calculate the three coordinates the vector should be extended to four dimensions with number one appended at the end of the point coordinate vector P. The first three numbers of the resulting vector denote the three coordinate numbers:

$$P_B^1 = P_B^0 T_1^1 = [5 \ 0 \ 0 \ 1] \begin{bmatrix} 0.8 & 0.6 & 0 & 4 \\ -0.6 & 0.8 & 0 & -3 \\ 0 & 0 & 1 & 0 \\ 0 & 0 & 0 & 1 \end{bmatrix} = [4 \ 3 \ 0 \ 21] \quad (15)$$

Where  $P_B^0$  denotes the coordinates of point B at the initial position and  $P_B^1$  for the coordinates of point B at the position after “move 1” has incurred

$$P_C^1 = P_B^0 T_1^1 + P_C^0 T_1^1 T_2^1 = [5 \ 0 \ 0 \ 1] \begin{bmatrix} 0.8 & 0.6 & 0 & 4 \\ -0.6 & 0.8 & 0 & -3 \\ 0 & 0 & 1 & 0 \\ 0 & 0 & 0 & 1 \end{bmatrix} + [2 \ 0 \ 0 \ 1] \begin{bmatrix} 1 & 0 & 0 & 6 \\ 0 & 1 & 0 & -3 \\ 0 & 0 & 1 & 0 \\ 0 & 0 & 0 & 1 \end{bmatrix} = [6 \ 3 \ 0 \ 34] \quad (16)$$

The computation results in terms of the first three elements are consistent with the point coordinates of B (4, 3, 0) and C (6, 3, 0) which are taken in the x-y coordinate system in Figure 4-13.

#### Step 4: Validations on “move 2”:

As shown in the right hand side of Figure 4-13, the joints rotate angles such that:

$$c_1^2 = \cos(\theta_1^2) = \frac{AD}{AE} = 0.8, s_1^2 = \sin(\theta_1^2) = -\frac{ED}{AE} = -0.6 \text{ and } c_2^2 = \cos(\theta_2^2) =$$

$$-\sin(\theta_1^2) = 0.6, s_2^2 = \sin(\theta_2^2) = -\cos(\theta_1^2) = -0.8, \text{ Where the subscript 2 denotes the}$$

time event at the end of the “Move 2”. Note that the two joints rotate counter-clockwise, thus the rotation angles are negative.

Then:

$$T_1^2 = A_1^2 = \begin{bmatrix} 0.8 & 0.6 & 0 & 4 \\ -0.6 & 0.8 & 0 & -3 \\ 0 & 0 & 1 & 0 \\ 0 & 0 & 0 & 1 \end{bmatrix} \quad (17)$$

$$T_2^2 = A_1^2 A_2^2 = \begin{bmatrix} 0.8 & 0.6 & 0 & 4 \\ -0.6 & 0.8 & 0 & -3 \\ 0 & 0 & 1 & 0 \\ 0 & 0 & 0 & 1 \end{bmatrix} \begin{bmatrix} 0.6 & 0.8 & 0 & 1.2 \\ -0.8 & 0.6 & 0 & -1.6 \\ 0 & 0 & 1 & 0 \\ 0 & 0 & 0 & 1 \end{bmatrix} = \begin{bmatrix} 0 & 1 & 0 & 4 \\ -1 & 0 & 0 & -5 \\ 0 & 0 & 1 & 0 \\ 0 & 0 & 0 & 1 \end{bmatrix} \quad (18)$$

In order to validate the proposed approach, the following calculations will determine the coordinates of Points B and C and then the analytical results are compared against the x-y coordinate numbers directly taken in Figure 4-13:

$$P_B^2 = P_B^0 T_1^2 = [5 \ 0 \ 0 \ 1] \begin{bmatrix} 0.8 & 0.6 & 0 & 4 \\ -0.6 & 0.8 & 0 & -3 \\ 0 & 0 & 1 & 0 \\ 0 & 0 & 0 & 1 \end{bmatrix} = [4 \ 3 \ 0 \ 21] \quad (19)$$

Where  $P_B^0$  denotes the coordinates of point B at the initial position and  $P_B^2$  denotes the coordinates of point B at the end of “move 2”.

$$P_B^2 = P_B^0 T_1^2 + P_C^0 T_1^2 T_2^2 = [5 \ 0 \ 0 \ 1] \begin{bmatrix} 0.8 & 0.6 & 0 & 4 \\ -0.6 & 0.8 & 0 & -3 \\ 0 & 0 & 1 & 0 \\ 0 & 0 & 0 & 1 \end{bmatrix} + [2 \ 0 \ 0 \ 1] \begin{bmatrix} 0 & 1 & 0 & 4 \\ -1 & 0 & 0 & -5 \\ 0 & 0 & 1 & 0 \\ 0 & 0 & 0 & 1 \end{bmatrix} = [4 \ 5 \ 0 \ 30] \quad (20)$$

The computation results are consistent with the point coordinates of B (4, 3, 0) and C (4, 5, 0) which can also be easily taken in Figure 4-13.

#### **4.7.2 Validation on 3D experiments**

As show in Figure 4-15, the articulated system simulating the backhoe excavator is designed to validate the proposed methodology in the 3D space. In order to simplify the calculation and validation processes, the bucket of the excavator is not considered in the experiments. The system has three revolute joints that enable the movements of the stick (DE) in the 3D space.

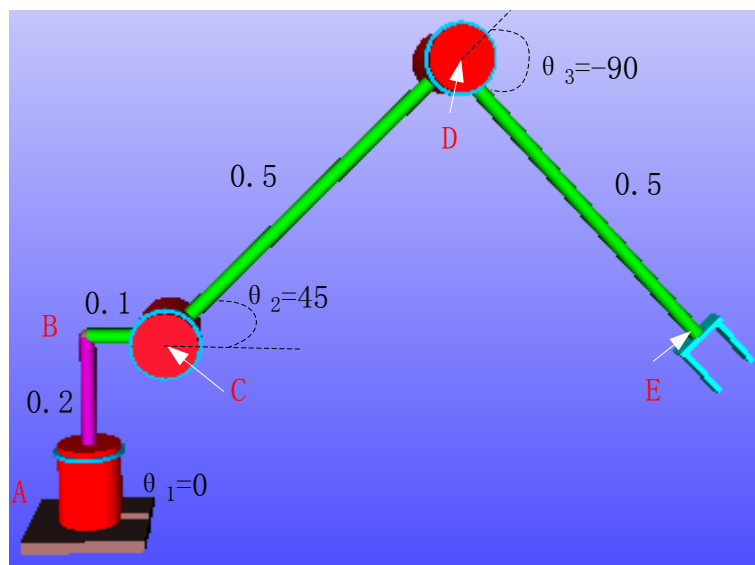


Figure 4-15: The configuration of the articulated system simulating the backhoe excavator

The input data are summarized in Table 4-3 and Table 4-4. The time dependent variables  $\theta_1, \theta_2$  and  $\theta_3$  determine the position of the whole system. Total of six experiments are designed to validate the proposed methodology. The joints angles are given in Table 4-4 that simulate the data collected from the field.

Table 4-3: The input configuration of the articulated system:

Joint	d	a	$\alpha$	$\theta$	Joint Type
1	0.2	0.1	90	$\theta_1$	Revolute
2	0	0.5	0	$\theta_2$	Revolute
3	0	0.5	0	$\theta_3$	Revolute

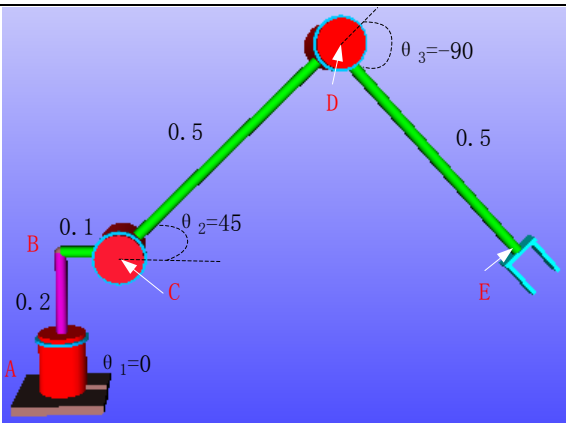
Table 4-4: The input data for the six experiments

Test no.	Joint angles	C1	S1	C2	S2	C3	S3
1	0,45,-90	1	0	0.7071	0.7071	0	-1
2	45,45,-90	0.7071	0.7071	0.7071	0.7071	0	-1
3	45,90,-90	0.7071	0.7071	0	1	0	-1
4	45,30,-90	0.7071	0.7071	0.866	0.5	0	-1
5	-30,10,-90	0.866	0.5	0.9848	0.1736	0	-1
6	-30,10,-45	0.866	0.5	0.9848	0.1736	0.7071	-0.7071

#### 4.7.2.1 Experiments with actual results calculated by law of trigonometry:

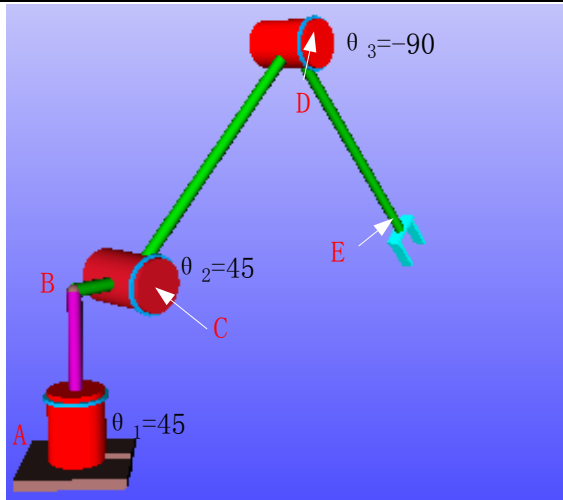
As shown in Table 4-4, in order to validate the proposed methodology, three virtual experiments are conducted. In these experiments, three joint angles are intentionally set so as to make it possible to apply the law of trigonometry to calculate the 3D position of point E, which provides the actual results.

Table 4-5: Three experiments and the actual results by the law of trigonometry

Exp. no.	Joint angles	Figure	Expected point "E" by trigonometry
1	0,45,-90		$X=0.8071$ $Y=0$ $Z=0.2$

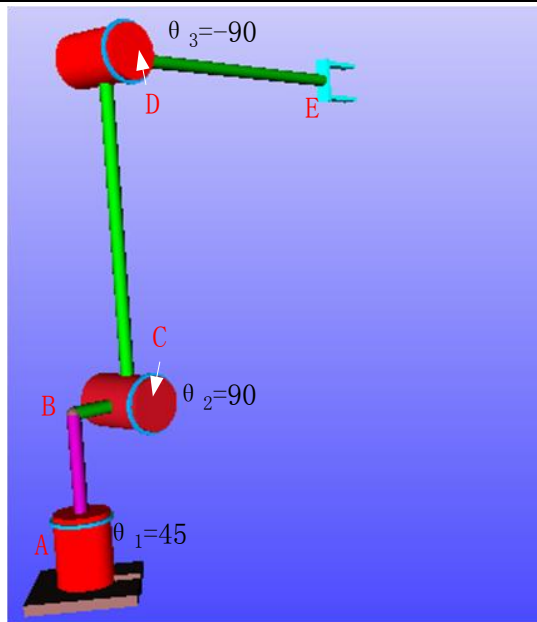


2 45,45,-90



X=0.5707  
Y=0.5707  
Z=0.2

3 45,90,-90



X=0.4243  
Y=0.4243  
Z=0.7

**Firstly**, the actual results will be calculated by the law of trigonometry:

The first experiment:  $\theta_1 = 0, \theta_2 = 45$  and  $\theta_3 = -90$

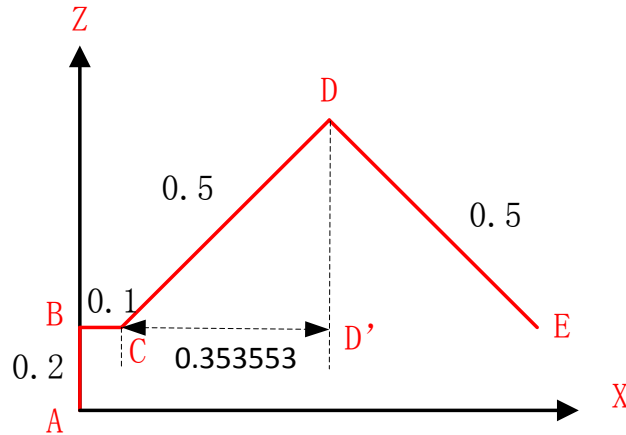


Figure 4-16: Calculate the position of point E by law of trigonometry

As shown in Figure 4-16, since  $\theta_1$  equals zero, there is no rotation about axis Z, and the coordinates of point E can be calculated as following:

$$\begin{aligned} X = BE &= BC + CD' + D'E = 0.1 + 2 * 0.5 * \cos(45) = 0.8071 \\ Y &= 0 \\ Z &= AB = 0.2 \end{aligned} \quad (21)$$

The second experiment:  $\theta_1 = 45, \theta_2 = 45$  and  $\theta_3 = -90$

Based on the first experiment, we rotate the joint 1 about axis Z with 45 degrees. The coordinates of point E can be calculated as follows:

$$\begin{aligned} X &= BE * \cos(45) = 0.8071 * \cos(45) = 0.5707 \\ Y &= BE * \sin(45) = 0.8071 * \sin(45) = 0.5707 \\ Z &= AB = 0.2 \end{aligned} \quad (22)$$

The third experiment:  $\theta_1 = 45, \theta_2 = 90$  and  $\theta_3 = -90$

Based on the second experiment, we rotate Joint 2 about axis Z by 90 degrees. The coordinates of point E can be calculated as follows:

$$\begin{aligned} X &= (BC + DE) * \cos(45) = 0.6 * \cos(45) = 0.4243 \\ Y &= (BC + DE) * \sin(45) = 0.6 * \sin(45) = 0.4243 \\ Z &= AB + CD = 0.2 + 0.5 = 0.7 \end{aligned} \quad (23)$$

**The next step** is to use the proposed methodology to calculate the position of point E:

$$T_C = \begin{bmatrix} C1 & 0 & S1 & 0.1C1 \\ S1 & 0 & -C1 & 0.1S1 \\ 0 & 1 & 0 & 0.2 \\ 0 & 0 & 0 & 1 \end{bmatrix} \quad (24)$$

$$T_D = \begin{bmatrix} C1 * C2 & C1 * -S2 & S1 & C1 * 0.5 * C2 + 0.1 * C1 \\ S1 * C2 & S1 * -S2 & -C1 & S1 * 0.5 * C2 + 0.1 * S1 \\ S2 & C2 & 0 & 0.5 * S2 + 0.2 \\ 0 & 0 & 0 & 1 \end{bmatrix} \quad (25)$$

$$T_E = \begin{bmatrix} C1 * C2 * C3 + (C1 * -S2) * S3 & C1 * C2 * -S3 + (C1 * -S2) * C3 & S1 & E(1,4) \\ S1 * C2 * C3 + (S1 * -S2) * S3 & S1 * C2 * -S3 + (S1 * -S2) * C3 & -C1 & E(1,4) \\ S2 * C3 + C2 * S3 & S2 * -S3 + C2 * C3 & 0 & E(1,4) \\ 0 & 0 & 0 & 1 \end{bmatrix} \quad (26)$$

Where  $C1 = \cos(\theta_1)$ ,  $C2 = \cos(\theta_2)$ ,  $C3 = \cos(\theta_3)$ ,  $S1 = \sin(\theta_1)$ ,  $S2 = \sin(\theta_2)$ ,  $S3 = \sin(\theta_3)$ , and

$$E(1,4) = C1 * C2 * 0.5 * C3 + (C1 * -S2) * 0.5 * S3 + (C1 * 0.5 * C2 + 0.1 * C1)$$

$$E(2,4) = S1 * C2 * 0.5 * C3 + (S1 * -S2) * 0.5 * S3 + (S1 * 0.5 * C2 + 0.1 * S1)$$

$$E(3,4) = S2 * 0.5 * C3 + C2 * 0.5 * S3 + (0.5 * S2 + 0.2)$$

Assume that we have obtained the joint movement parameters by using linear sensors, so the  $C1$ ,  $C2$ ,  $C3$ ,  $S1$ ,  $S2$ , and  $S3$  in Equation 26 can be obtained by the law of trigonometry, for example, as shown in Figure 4-16,  $S2 = \frac{DD'}{CD}$ , where the length of  $CD$  can be obtained from equipment design specification and the length of  $DD'$  can be sourced from linear encoders. Thus, Equation 26 can be solved. The final results are summarized in Table 4-6. Comparing the calculation results (bold in Table 4-6) with the actual results, we can conclude that the proposed methodology can be used to position the articulated system since the two methods produce the same results.

Table 4-6: The calculated results from the proposed methodology

Test no.	C1	S1	C2	S2	C3	S3	Transformation matrix of solid body "DE"
1	1	0	0.7071	0.7071	0	-1	$\begin{bmatrix} 0.7071 & 0.7071 & 0 & \mathbf{0.8071} \\ 0 & 0 & -1 & \mathbf{0} \\ -0.7071 & 0.7071 & 1 & \mathbf{0.2} \\ 0 & 0 & 0 & 1 \end{bmatrix}$
2	0.7071	0.7071	0.7071	0.7071	0	-1	$\begin{bmatrix} 0.5 & 0.5 & 0.7071 & \mathbf{0.5707} \\ 0.5 & 0.5 & -0.7071 & \mathbf{0.5707} \\ -0.7071 & 0.7071 & 1 & 0.2 \\ 0 & 0 & 0 & 1 \end{bmatrix}$
3	0.7071	0.7071	0	1	0	-1	$\begin{bmatrix} 0.7071 & 0 & 0.7071 & \mathbf{0.4243} \\ 0.7071 & 0 & -0.7071 & \mathbf{0.4243} \\ 0 & 1 & 0 & \mathbf{0.7} \\ 0 & 0 & 0 & 1 \end{bmatrix}$

#### 4.7.2.2 Validation by visualization

In previous experiments, the actual results are calculated by the law of trigonometry. However, the validation method is only applicable to some special poses of the articulated system. In order to validate the methodology for random poses, we need an alternative method to obtain the actual results. Visualization is an efficient approach for verification and validation of computing algorithms (Kamat et al. 2005), by which computer graphics can be used to generate the actual results in the 3D virtual environment. Given any random input of joint rotation angles, it is possible to manually create the articulated system in the 3D computer graphics based on a parametric 3D computer aided design (CAD) system such as 3D Max and SketchUp. The created 3D model represents the actual pose resulting from the movements. On the other hand, we can use the proposed method to calculate the position of target points on the articulated system (such as the point "E"). Then the position of the target points can also be marked

and visualized in the same 3D environment. If the actual result and the result from the proposed methodology converge in the same 3D environment, the computing algorithm can be validated by such visual inspection. The validation procedures are discussed in the followings:

Step 1: First, the proposed methodology (Equation 26) is applied to calculate the position of target point E and summarized in Table 4-7:

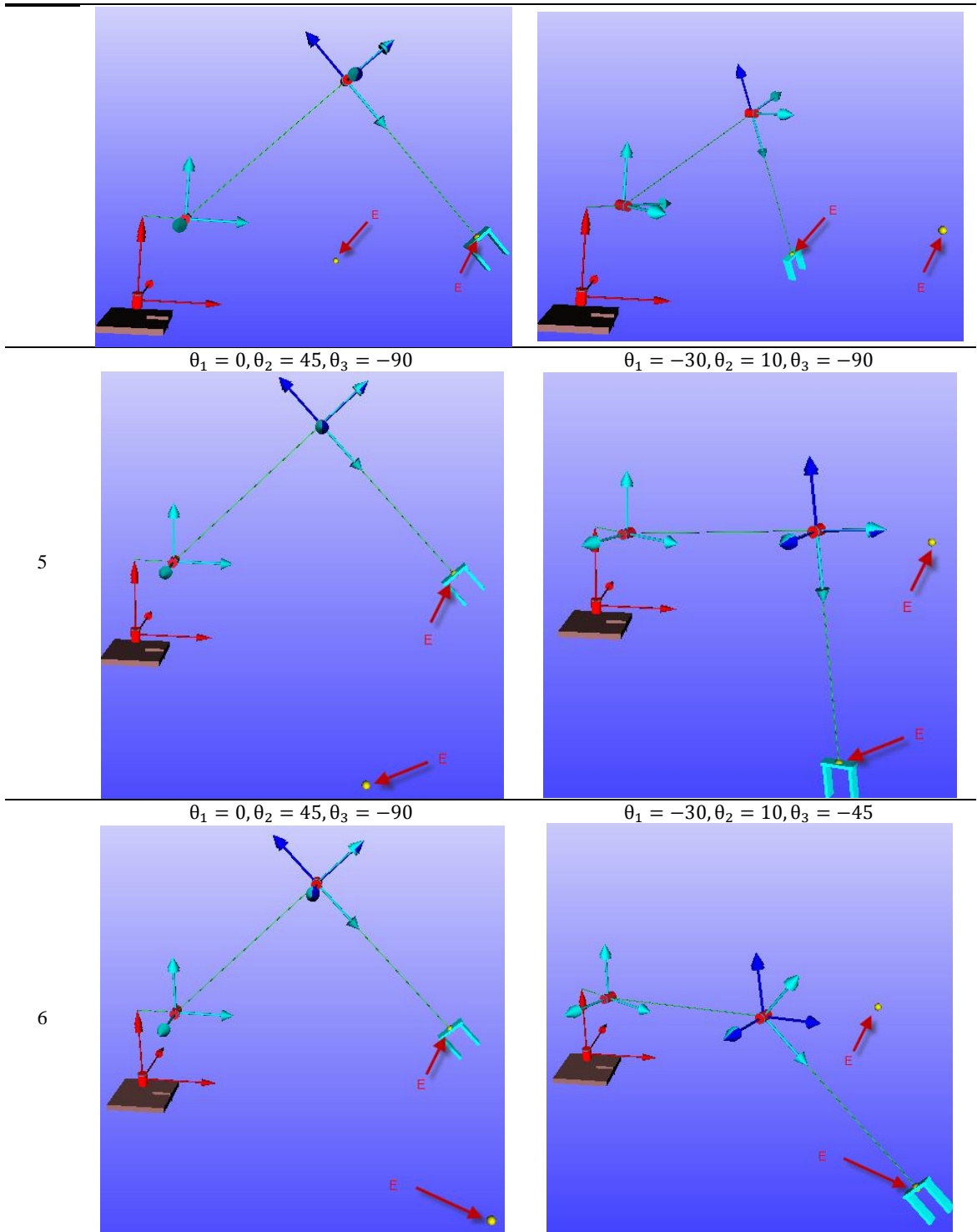
Table 4-7: The calculated results from the proposed methodology

Test no.	C1	S1	C2	S2	C3	S3	Transformation matrix of solid body "DE"
4	0.7071	0.7071	0.866	0.5	0	-1	$\begin{bmatrix} 0.3536 & 0.6124 & 0.7071 & \mathbf{0.5537} \\ 0.3536 & 0.6124 & -0.7071 & \mathbf{0.5537} \\ -0.8660 & 0.5 & 0 & \mathbf{0.0170} \\ 0 & 0 & 0 & 1 \end{bmatrix}$
5	0.866	0.5	0.9848	0.1736	0	-1	$\begin{bmatrix} 0.1504 & 0.8529 & -0.5000 & \mathbf{0.5882} \\ -0.0868 & -0.4924 & -0.8660 & \mathbf{-0.3396} \\ -0.9848 & 0.1736 & 0 & \mathbf{-0.2056} \\ 0 & 0 & 0 & 1 \end{bmatrix}$
6	0.866	0.5	0.9848	0.1736	0.7071	-0.7071	$\begin{bmatrix} 0.7094 & 0.4967 & -0.5000 & \mathbf{0.8677} \\ -0.4096 & -0.2868 & -0.8660 & \mathbf{-0.5010} \\ -0.5736 & 0.8192 & 0 & \mathbf{0} \\ 0 & 0 & 0 & 1 \end{bmatrix}$

Step 2: Visualize the actual pose of the backhoe and expected target points (yellow dots) determined by the proposed method:

Table 4-8: Validation by visualizing the actual pose and the calculated target point "E"

Test no.	Initial pose and target points	Final pose
4	$\theta_1 = 0, \theta_2 = 45, \theta_3 = -90$	$\theta_1 = 45, \theta_2 = 30, \theta_3 = -90$



As shown in Table 4-8, in the three virtual experiments, the actual pose and the calculated target point “E” converge in the 3D virtual environment, which validates that

the proposed methodology is effective to position an articulated system by using some joint movement parameters.

## **4.8 Summary**

This chapter has described the methodology for real-time 3D positioning and visualization of typical articulated construction resources (largely include but not limited to the construction equipment) working on site. The expression of each equipment component as a solid body in the 3D virtual world is the same as the single solid object, which requires a rotation matrix and a translation vector to uniquely determine the location and orientation in the 3D space. However, the proposed real-time 3D positioning and visualization technique of articulated system is different to the one used for single solid site object in that a kinematic model is introduced to make the proposed methodology practical by minimizing the use of sensors required to locate the solid bodies of the equipment.

The kinematic model is a mathematical representation of the relative position and orientation between two conjoint solid bodies which are normally linked with revolute joint or prismatic joint for typical construction equipment. The DH notation which is widely used in the robotic literature is applied to develop the kinematic model for a typical articulated system with open kinematic chains.

In order to clearly express the whole procedure, a backhoe excavator is chosen to illustrate the modeling process, including the 3D geometric modeling, the data structure modeling, the kinematical modeling and the real time positioning analysis.

The proposed methodology is well structured and can be coded in software in an ad hoc manner with ease. However, it requires construction practitioners, who may not have strong programming skills, to develop the software tackle different equipment systems, which may hinder them to adopt the visualization technique on their daily management and/or engineering works.

In order to eliminate the barrier arising from software development, a graphic network modeling technique, originally applied in mechanical engineering for mechanical system simulation and design, will be developed for construction application in next chapter.



## ***Chapter 5***

# ***Graphic Network Modeling for 3D Positioning and Visualization of Construction Resources***

### **5.1 Introduction**

Chapter 4 has described the methodology for 3D positioning and visualization of articulated equipment systems in construction. In order to derive the 3D position information for each solid part in the articulated equipment system, the dimensions and configurations of the equipment are required as input parameters for the mathematic equations. Thus, construction equipment with different configurations has different sets of mathematic equations in order to realize 3D positioning of the equipment in the field.

Construction technology is a perennially evolving science. New methods of construction, advanced equipment systems, and new materials and tools are continually being developed and adopted on construction sites (Kamat and Martinez 2008). For each type of equipment, developing the kinematic model and coding the 3D positioning algorithms in a computer system in an ad hoc manner requires tremendous programming efforts, which will hinder the wide application of the developed 3D positioning and visualization techniques in the construction domain.

As envisioned by Abourizk et al.(1992), solutions which appear to be too theoretical or analytical tend not to be easily accepted or utilized by construction practitioners (Abourizk et al. 1992). Thus, real-time 3D positioning and visualization technologies need to be presented in very simple and graphical interfaces so as to enable application. This chapter will introduce the technique that enables users to build the real-time 3D positioning and visualization system using the so-called “link node” graphic network modeling technique. This technique provides user-friendly graphic interfaces that facilitate construction practitioners, without the requirement of programming skills, to build real-time 3D positioning and visualization systems that can be easily adapted to a variety of construction applications.

## **5.2 Background**

The graphic network modeling technique provides basic graphic elements that can be linked with each other to form powerful applications. It is essentially pictorial or schematic emphasizing graphic input of the parameters required, leading to the generation of graphics based on the 3D positioning information of the articulated system.

The graphic network modeling technique is based on the network theory, which is an area of applied mathematics and part of the graph theory. Network theory has been applied in many disciplines including project management, logistics, computer science,

operations research, and sociology. Network theory concerns itself with the study of graphs as a representation of relations between discrete elements. Examples of which include Critical Path Method (CPM), Program Evaluation & Review Technique (PERT), Construction Simulation Network like CYCLONE (Halpin 1977) (Abourizk et al. 1992), and logistical networks, etc.

A graphic network modeling environment generally provides two basic elements, namely: links and nodes. Various nodes are linked with each other to form a more sophisticated and powerful network topology. Network topology is arrangement (or mapping) of the elements (links, nodes, etc.) of a network, especially expressing the physical (real) and logical (virtual) interconnections between nodes. Any particular network topology is determined only by the graphical mapping of the configuration of physical and/or logical connections between nodes.

### ***5.2.1 Simulink environment***

Simulink<sup>®</sup> is a kind of powerful graphic network modeling software environment for multi-domain simulations and model-based designs of dynamic and embedded systems. It provides an interactive graphical environment and a customizable set of block libraries that enable users to design, simulate, implement, and test a variety of time-varying systems, including communications, controls, signal processing, video processing, and image processing (MathWorks<sup>®</sup> 2010b).

SimMechanics™ is a toolbox for modeling 3D mechanical systems within the Simulink® environment. Instead of deriving and programming equations, users can use this simulation tool to build a model composed of bodies, joints, constraints, and force elements that reflect the structure and functionality of the system (MathWorks® 2010a).

The graphic network modeling tools in Simulink® provide flexible ways for representing various mechanical systems of construction equipment. The following sections will describe the methodology to apply and extend the SimMechanics™ for real-time 3D positioning and visualization of the articulated system discussed in Chapter 4.


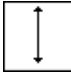
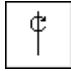

## **5.3 Methodology**

The objective of the research on graphic network modeling is to study the feasibility of using reusable graphic elements to model the real-time 3D positioning and visualization applications. The SimMechanics tool in the Simulink environment provides a set of basic graphic elements for modeling the mechanical system. Moreover, the Simulink environment provides three types of mechanism for creating custom blocks that can be reused to model the application system. Thus the Simulink is selected as an ideal platform for conducting this research.

### ***5.3.1 Built-in graphic blocks***

The SimMechanics provides a set of graphic elements (blocks) for modeling the mechanical system. However, some of them are used for dynamic analysis (such as force, inertial, moment of inertia tensor etc.) which will not be used for the 3D positioning and visualization in this research. Table 5-1 lists the graphic elements used for modeling the kinematics of construction equipment in this research.

Table 5-1: Graphic elements for kinematic modeling of construction equipment

Name	Block Icon	Description
Body		The block represents a rigid body, e.g. the components of construction equipment. The coordinates for the body's center of gravity, one or more body coordinate systems (frames) should be specified
Prismatic joint		The Prismatic block represents a single translational degree of freedom along a specified axis between two bodies.
Revolute joint		The Revolute block represents a single rotational degree of freedom about a specified axis between two bodies. The rotational sense is defined by the right-hand rule.
Spherical joint		The Spherical block represents three rotational degrees of freedom at a single pivot point, a "ball-in-socket" joint. Two rotational degree of freedoms specify a directional axis, and a third rotational degree of freedom specifies rotation about that directional axis. The sense of each rotational degree of freedom is defined by the right-hand rule, and the three rotations together form a right-handed system

---

A joint between two bodies represents relative degrees of freedom between the bodies. The Joint Actuator block actuates a Joint block connecting two Bodies with one of these signals:

A generalized force:

Force for translational motion along a prismatic joint primitive

Joint



Actuator

Torque for rotational motion about a revolute joint primitive

A motion (used in this research):

Translational motion for a prismatic joint primitive, in terms of linear position, velocity, and acceleration.

Rotational motion for a revolute joint primitive, in terms of angular position, velocity, and acceleration.

---


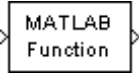
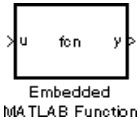
### **5.3.2 Custom graphic blocks**

Simulink provides three approaches that enable users to create their own block libraries as a way to reuse the functionality of software procedures in one or more models, namely, 1. MATLAB function blocks, 2. Subsystem blocks, 3. S-Function blocks. Each of these blocks has advantages in particular modeling applications.

MATLAB function blocks allow users to use MATLAB functions to define custom blocks. These blocks serve as a good starting point for creating a custom block that incorporate the algorithms developed in Chapter 3 and Chapter 4. Users can create a

custom block from a MATLAB function using one of the three types of MATLAB function blocks listed in Table 5-2.

Table 5-2: The three types of MATLAB function blocks for developing custom blocks

Name	Block Icon	Description
Fcn block		The Fcn block applies the specified mathematical expression to its input.
MATLAB Fcn		The MATLAB Fcn block applies the specified MATLAB function or expression to the input. The output of the function must match the output dimensions of the block or an error occurs.
Embedded MATLAB Function		With an Embedded MATLAB Function block, users can write a MATLAB function for use in a Simulink model. The MATLAB function users create executes for simulation and generates code for a Real-Time Workshop target.

The “Fcn block” allows users to use a MATLAB expression to define a single-input, single-output (SISO) block. Thus, the “Fcn block” will be used to define the equations (1) (2) and (3) developed in Section 6.2 of Chapter 4, which compute the rotation angles from the lengths of hydraulic jack rods.

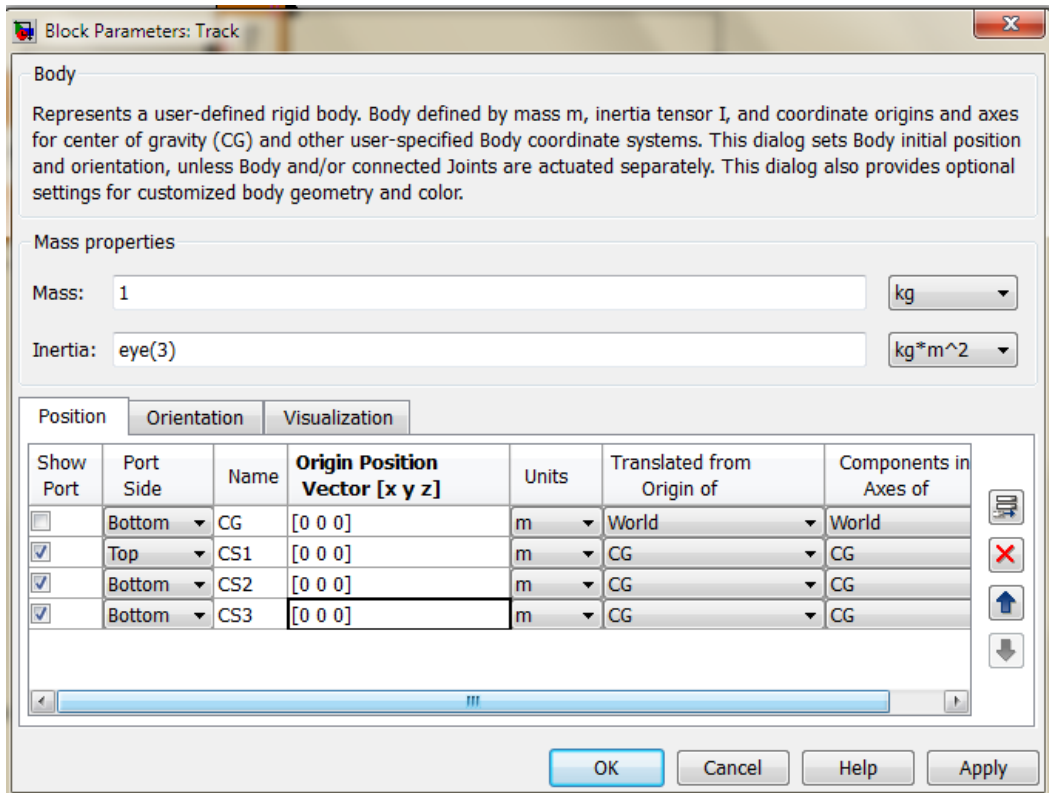
The Embedded MATLAB Function block allows users to define a custom block with multiple inputs and outputs. Thus, the Embedded MATLAB Function block is ideal for the “points to matrix” algorithm developed in Section 6 of Chapter 3.

### ***5.3.3 Modeling process***

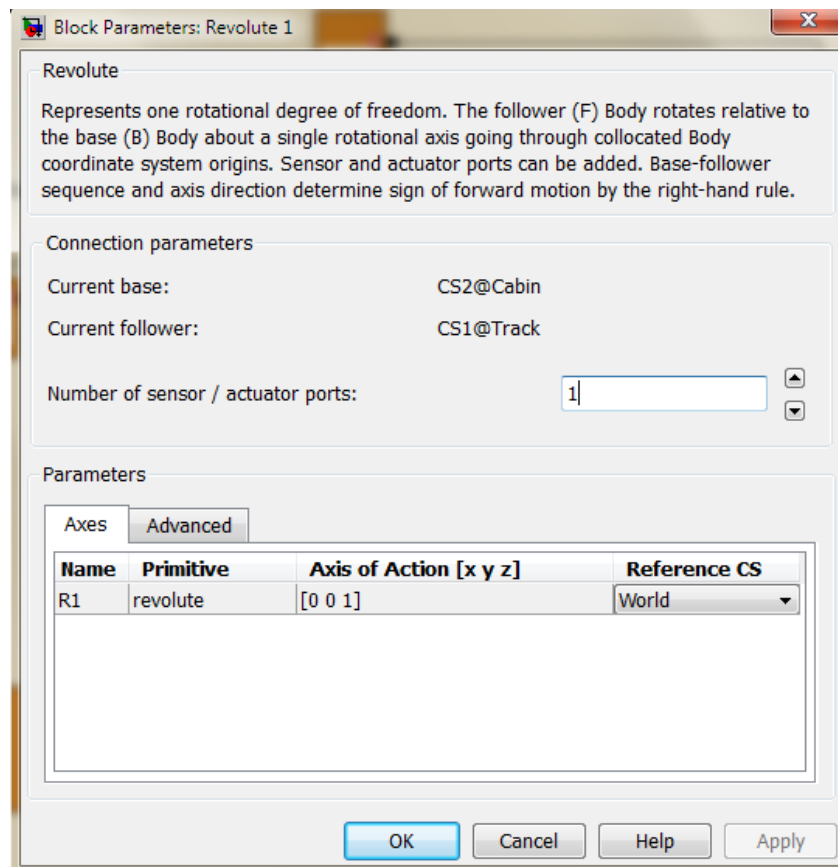
Modeling a 3D positioning and visualization application using the above graphic elements is a three-step process. The following paragraphs will list the three steps, and introduce the related modeling knowledge. In the following Section 4, a backhoe excavator will be used to illustrate the whole modeling process.

First, site engineers or equipment operators who may understand the equipment configurations, create the kinematic model by linking body blocks with joint blocks. As shown in Figure 5-1, the initial position and orientation should be entered in the Body block parameters dialog. The coordinates of ports that connect joints also need to be specified in this dialog. These data are provided by the configuration of the equipment. Similarly, the axes of joints should be defined in their parameter dialogs as shown in Figure 5-2.





**Figure 5-1: The parameters dialog of Body Block**



**Figure 5-2: The parameters dialog of Revolute Joint Block**

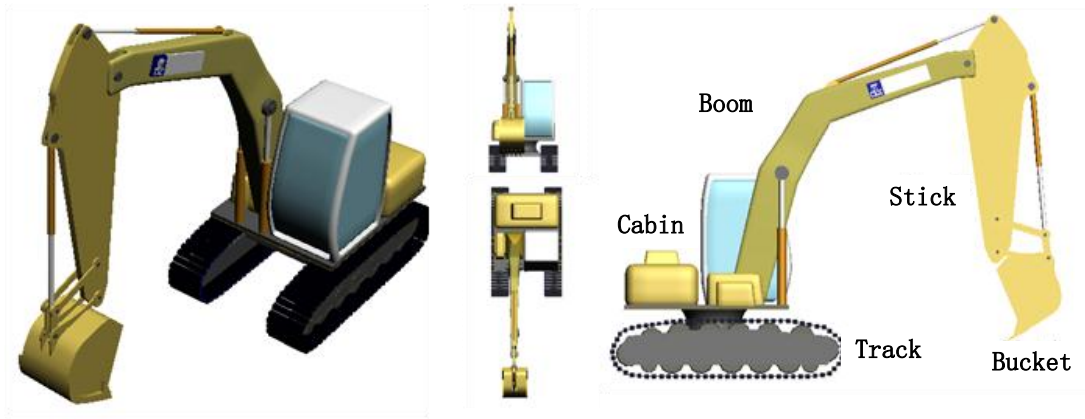
Second, the above equipment kinematic model is then linked with real-time sensor signals by using the two custom blocks “Length to Angle” and “Points to Matrix” and the actuator blocks.

Then, the real-time 3D positioning system has been modeled by using the graphic blocks. However, in order to visualize the 3D positioning data, the data model developed in Section 4 of Chapter 4 should be linked with the 3D positioning system.

This step can be achieved by using the virtual reality tool box provided by the Simulink environment or other virtual reality tools as long as they provide interface to link with the 3D positioning data.

## **5.4 Application**

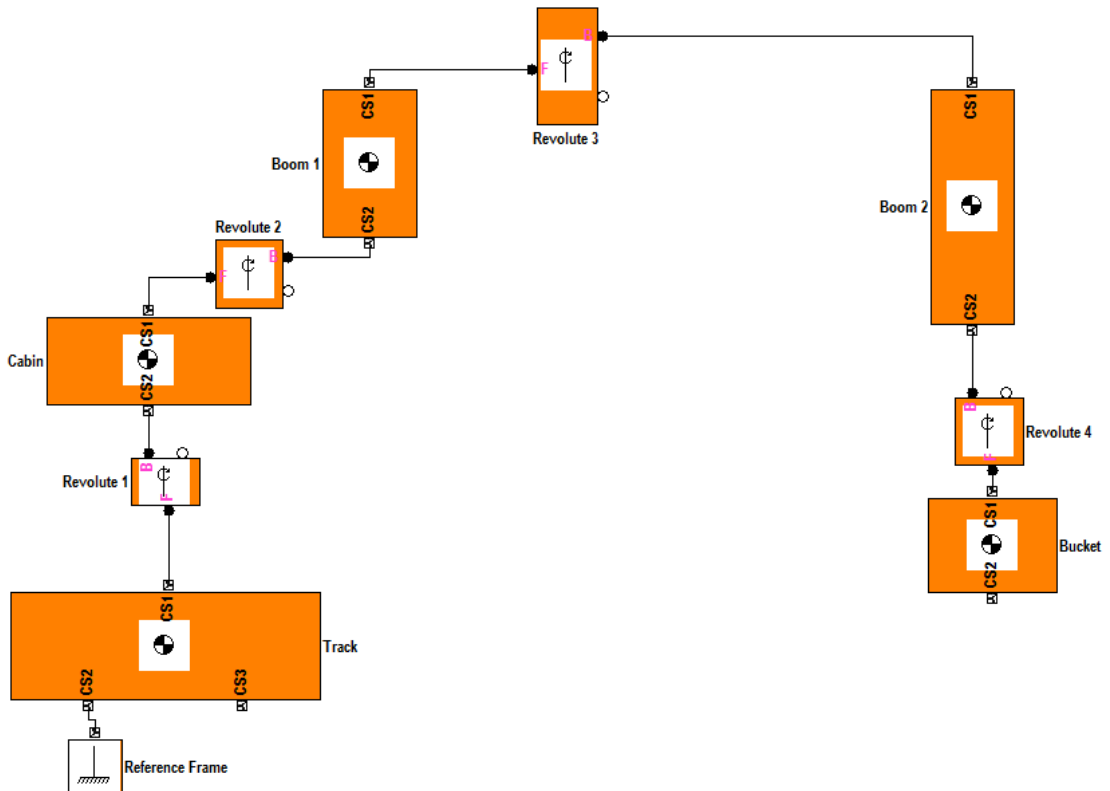
In this section, the example of backhoe excavator, which has been used to illustrate the DH method in Chapter 4, is now used to demonstrate the graphic modeling techniques in real-time 3D positioning and visualization modeling applications. For the ease of reading, the configurations of the backhoe are again represented in Figure 5-3. The backhoe excavator is comprised of five parts: Track, Cabin, Boom, Stick and Bucket.



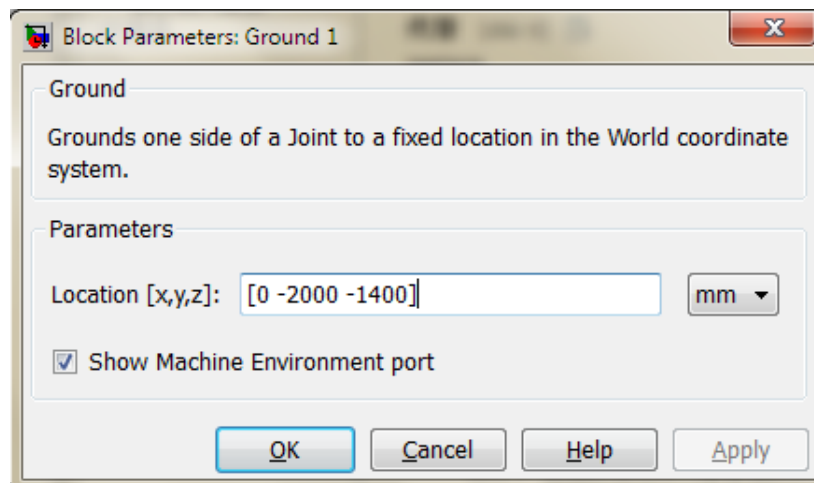
**Figure 5-3: The configurations of the backhoe excavator**

The first step is to model the backhoe based on its configurations. As shown in Figure 5-6, the backhoe can be modeled using the provided graphical elements discussed in Section 3.1. However, only two types of graphical elements are needed, namely, the body blocks and revolute joint blocks. For each body block, the coordinates of the joint should be defined, while for each revolute joint, the axis vector that links with two bodies should be indicated. There are four revolute joints that link the five bodies. Except the joint that links the track and cabin whose axis points upside, all other three joints' axes point outward as shown in Figure 4-5.

As discussed in Chapter 2, a reference frame is needed for 3D positioning of objects in the field. Although the Simulink environment does not provide a reference coordinate block, we can use the "Ground Block", which is used to represent the ground in SimMechanics, as the reference frame. The location of the Ground Block can be defined in its parameter dialog as shown in Figure 5-5. The location may be given in the local coordinates of a construction site or in the world coordinates system.



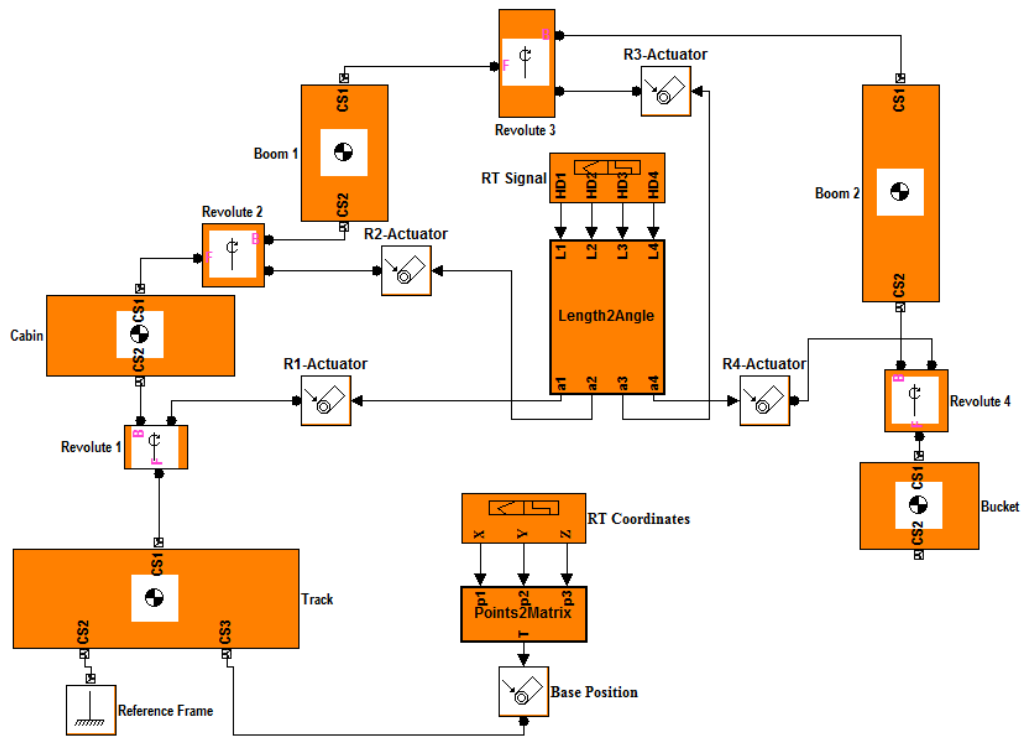
**Figure 5-4: Modeling the backhoe excavator using body blocks and joint blocks.**



**Figure 5-5: The parameters dialog of Ground Block.**

The above kinematic model defines the initial 3D position of the backhoe and the DH parameters required to calculate the 3D position of the backhoe. The next step is to extend the model with custom blocks to link the real-time data that drive the movement of model. As shown in Figure 5-6, two custom blocks are used to transform the real-

time data captured by sensors to the 3D positioning information. The 3D positioning information is then transferred to the kinematic model by linking the “Actuator Blocks” with the four joints and the track.



**Figure 5-6: Extend the kinematic model with custom blocks to link the real-time data**

The model now can compute the 3D position of the backhoe based on the real-time data.

The pose matrices of the five bodies can be automatically retrieved by using Equations

(7), (8), (9) and (10). The last step is to link the pose matrices with the data model

developed in Section 4 of Chapter 4. As shown in Figure 5-7, the 3D geometry data are

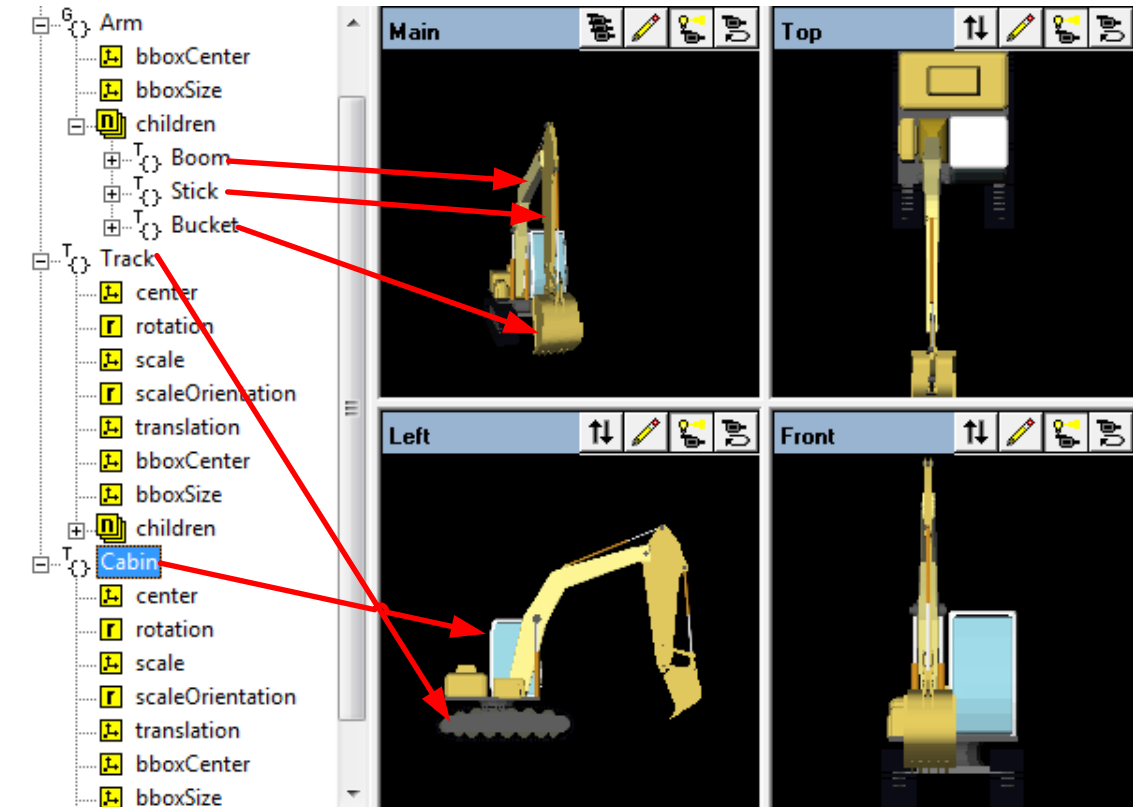
stored in the Resource Object Hierarchical Tree discussed in Chapter 4. Besides the

geometry data, there are many other properties, such as rotation, scale, translation etc.

The most important properties about 3D positioning and visualization are the rotation

and translation. As shown in Figure 5-8, the computation results from the above model

are linked with the ROHT data model. This completes the whole process of using graphic elements to model the 3D positioning and visualization application based on the backhoe excavator example.



**Figure 5-7: The data model developed for real-time 3D positioning and visualization of backhoe excavator**

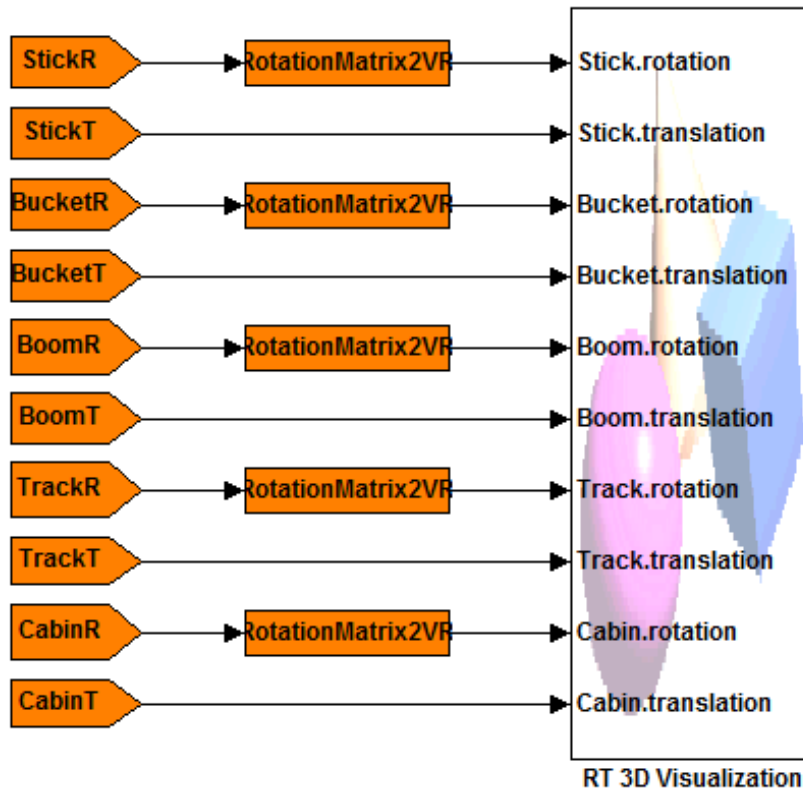


Figure 5-8: 3D visualization by linking the computation result with the ROHT data model

## 5.5 Summary

Technologies that appear to be too theoretical or analytical tend not to be accepted or utilized by construction practitioners (Abourizk et al. 1992). This chapter provides a graphic modeling technique to enable real-time 3D positioning and visualization of articulated equipment systems in construction.

This technique can efficiently solve two problems, they are: (1). All the theoretical and analytical equations can be concealed in the graphic blocks, and users do not need to understand the theories underneath in order to use the real-time 3D positioning and visualization technology; (2). Various articulated systems, especially the construction

equipment, can be easily modeled by reusing or reorganizing the developed graphic blocks. Users who do not have any programming skill still can model their own applications for 3D positioning and visualization of various equipment systems working in the field.



## ***Chapter 6***

### ***Application Possibility in Positioning Tunnel Boring Machines***

#### **6.1 Introduction**

In previous chapters, the methodologies for 3D positioning of an articulated equipment system are presented and validated with a backhoe example. This chapter will discuss the possibility of synthesizing the methodologies for real-time 3D positioning and visualization of tunnel boring machines (TBM). Tunnel boring machines are the key construction equipment on tunneling projects. The positioning and visualization of TBM is very useful for tunneling alignment control and TBM steering in the invisible underground space.

This chapter is organized as follows: first, the practical industrial needs and the related knowledge obtained from previous research are discussed. Then, an outline of the application procedure is given, and evaluation of the possibility to apply the proposed methodology in microtunneling and pipe-jacking operations is elaborated in regard to two aspects, namely, (1) the input: the site data, simulation data and the geometric data model, and (2) the controller for graphic kinematics modeling of TBM which generates a kinematic model; the base frame is determined by using the “point-to-matrix” algorithm and coded in a graphical application block. Finally, results from the

evaluation of practical application simulation in a computer simulation environment are presented, and the applicability and limitation of the proposed methodology in tunneling project are discussed.

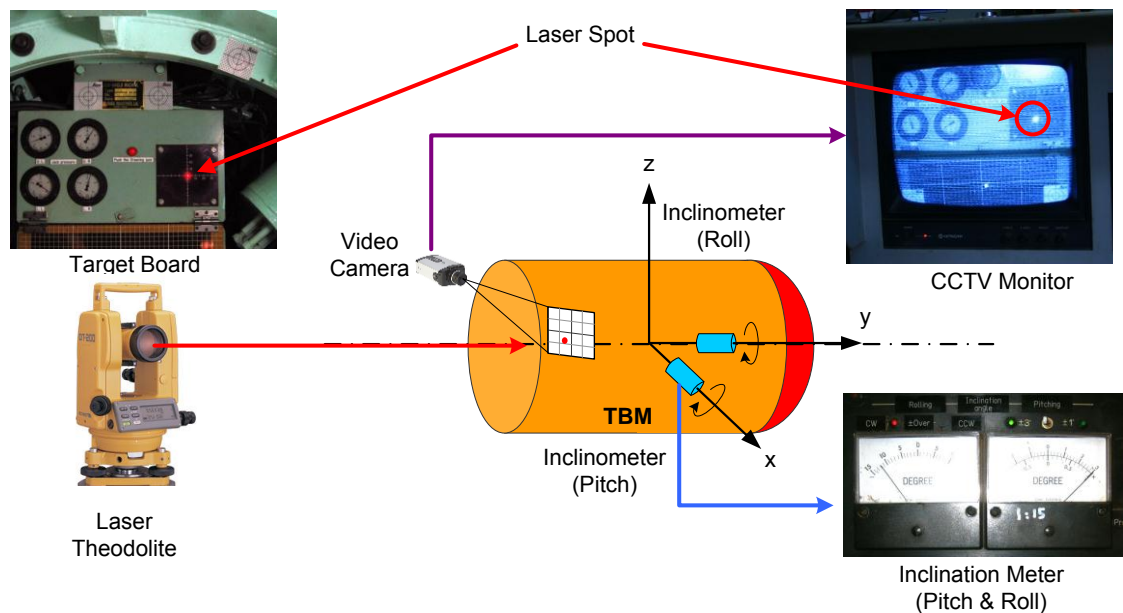
## **6.2 Background**

### ***6.2.1 The practical industrial needs***

In recent years, TBMs have been increasingly adopted by the construction industry for developing urban underground pipeline systems, minimizing the disruption to traffic, businesses, and other aspects of the social equity. Micro-tunnel boring machines (MTBM, with the diameters generally ranging from 0.61 to 1.5 meters) are commonly used in microtunneling projects. The main differences between MTBM and large diameter TBM are: (1) MTBM is operated remotely; (2) MTBM usually has the tunnel liner pushed behind the machine (the process known as “pipe-jacking”). On a typical microtunneling project, the MTBM advances from a jacking shaft to a receiving shaft. Due to the nature of small diameters, the visual information on MTBM operations is very limited. It is a challenging task for operators to steer the MTBM and control the tunnel alignment in practice.

As shown in Figure 6-1, the TBM operators count on the visual information obtained from a closed-circuit television (CCTV) and instrument panels to steer advancing of the

MTBM along the designed tunnel alignment. A laser theodolite set up in the jacking shaft projects a laser beam on the target board fixed at the rear of the MTBM. The displacement of the laser point indicates the alignment deviations. Two inclinometers are installed in the MTBM to gauge the roll and pitch angles information. The operators watch the CCTV and the inclinometer readings in order to make decisions on how to steer the MTBM.



**Figure 6-1: The commonly used visualization approach for MTBM remote control**

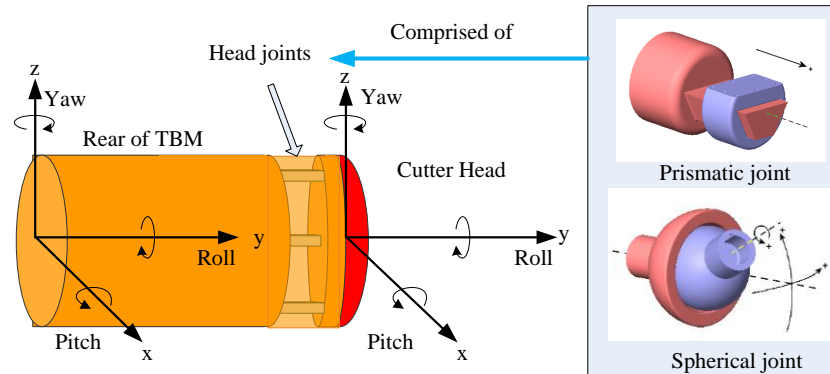
Nonetheless, tele-operation systems enabled with a conventional CCTV are unable to generate perfect tele-existence (Hirabayashi et al. 2006). Additionally, the traditional visual feedback does not provide the visual information of the cutter head orientation. Thus, operators only count on their experiences to steer the cutter head through “push or pull” operations on control jacks so as to correct any deviations as detected from CCTV.

It has been reported that construction equipment operators tend to concentrate on processing visual information because they rely on the visual sense as their main means of perceiving the working environment (Hirabayashi et al. 2006). The insufficient visual feedback to TBM operators may cause numerous problems including misalignment, trapping TBM underground, and damage of existing utility pipe in the close proximity, which would result in project delays and significantly drive up project costs. It was reported that problems with TBM operation and alignment check on average account for 24% and 20% delay time respectively in trenchless projects (Hegab and Smith 2007). And the performance of the microtunneling largely depends on the skill of the TBM operators (Yoshida and Haibara 2005).

### ***6.2.2 Kinematics of MTBM***

In general, most articulated construction equipment systems can be viewed as open kinematic chains consisting of a finite number of components that are joined together with simple prismatic or revolute joints, each of which typically allows only one degree of freedom in connection with the next component down the hierarchy (Kamat and Martinez 2005). However, the kinematic chain of a MTBM is a kind of special closed kinematic chain known as parallel robot (Khalil and Dombre 2002). Figure 6-2 shows the kinematic chains of a typical MTBM that consists of a rigid rear body linked with a rigid cutter head by three hydraulic cylinders. A hydraulic cylinder can be viewed as a

combination of a prismatic joint and a spherical joint. Note that different MTBM may have different mechanical configurations as mentioned in the introduction section.



**Figure 6-2: The kinematic chains of MTBM**

At the control station the operators manipulate buttons to push or pull the piston rods of the hydraulic cylinders in order to adjust the orientation of the cutter head. To update the equipment model based on sensor data, the motion of equipment components should be defined by kinematic models (Seo et al. 2000) which are mathematical representations (i.e. linear equations and differential equations) of relative motions between solid components linked by joints. The kinematic model should be developed to represent the pose of the cutter head based on the length of the piston rods.

### ***6.2.3 Virtual reality in construction applications***

Virtual reality (VR) is a generic term for describing technologies about creating a real-time visual/audio/haptic experience. Essentially, virtual reality is about the navigation, animation and manipulation of 3D computer-generated environments, and can be categorized into “Immersive VR” and “Non-immersive VR” (Vince 2004).

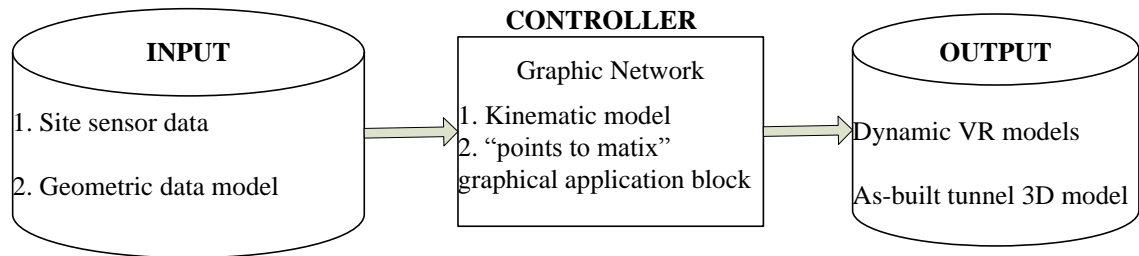
Virtual reality technologies have been extensively embraced by construction practitioners and researchers in the application areas of dynamic 3D visualization of simulated construction operations (Kamat and Martinez 2001), 4D visualization of construction process/schedule (McKinney et al. 1996), 3D/4D based constructability review (Hartmann and Fischer 2007). However, these applications are largely confined to the design/planning purposes. There is still a lack of documented evidences as well as efficient methodologies for VR applications in the construction stage, aimed to improve construction tasks at the operational level such as construction equipment operations.

One important impeditive factor is attributable to the enormous effort as needed to build the kinematic model reflecting site operations in the VR world. Without a kinematic model, it is very difficult to visualize the dynamic construction site at the operational level. The majority of previous approaches for construction equipment visualization need to derive a set of equations and code specific kinematic models in customizing particular visualization systems (Kamat and Martinez 2005; Seo et al. 2007).

### **6.3 Preparation for the evaluation**

The main goal is to evaluate the possibility of applying proposed methodologies for 3D positioning and visualization of MTBM during pipe-jacking operations, aimed at assisting operators in making more informed decisions in steering MTBM remotely.

Figure 6-3 gives an overview of the procedure that applies the proposed methodology to position the MTBM.



**Figure 6-3: Overview of the application procedure**

The most important part in the procedure is to develop a controller based on the proposed methodology, which integrates the kinematic model and “points to matrix” transformation algorithm. The controller performs like a computing engine that translates the input data to the position and orientation information of each equipment component. Thus the equipment 3D geometric models can be updated using the computing results, which generates dynamic virtual reality models to reflect the actual pose of the MTBM working on a site, including the position and orientation of the rear part and the orientation of the cutter head. As a by-product of the dynamic 3D visualization, the as-built tunnel model can be approximately obtained in 3D by connecting the TBM’s states on consecutive time points of positioning.

### ***6.3.1 Preparation of input data***

Preparation of input data is the first step to apply the proposed methodologies. As discussed in Section 6.2.2, a MTBM is composed of a rear part (main body), a cutter

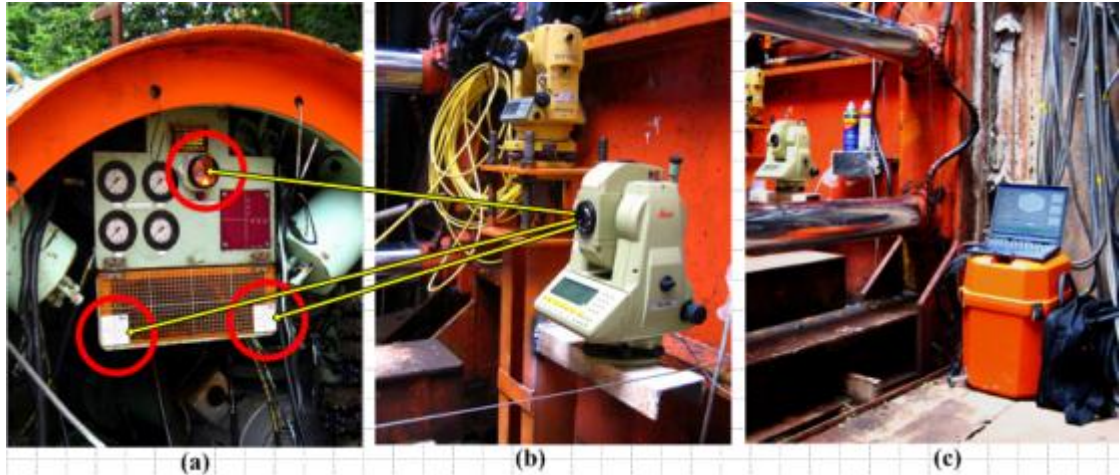
head and a control system that consists of several hydraulic cylinders. In order to test the applicability of the proposed methodology for positioning MTBM, we need to obtain the position of target points fixed on the rear part of the MTBM along with the lengths of each hydraulic cylinder.

As shown in Figure 6-4, the coordinates of target points fixed on the rear part of MTBM were collected by a system which was originally developed for automatically tracking and guiding TBM during micro-tunnelling and pipe jacking operations (Shen et al. 2010). In this system, a computer controlled total station (Figure 6-4 b) automatically measures the coordinates of targets (Figure 6-4 a) mounted on the rear end of a MTBM.

As shown in Table 6-1, the data collected by the positioning system mainly consist of two parts, namely, the primary data which are the coordinates of positioning points; and the metadata which describe the primary data in terms of the tracking time and the point ID. The controller uses the time information to synchronize dynamic VR models with site data, and processes point coordinates to calculate the position and orientation of the rear part of the MTBM by using the “points to matrix” transformation algorithm. Note the lengths of hydraulic cylinders can be readily collected from the existing MTBM mechanical control system. The goal of the experiments is to verify the applicability of the proposed methodology, so we generate simulation data to simulate the operations of



hydraulic jacks, which is sufficient for the purpose of concept proving and applicability evaluation.



**Figure 6-4: The configuration of the point coordinates collection system**

Table 6-1: The coordinates of target points

Date	Time	North	East	Elevator
20090908	182848	825844.5330	817632.3755	-4.0139
20090908	182751	825844.5339	817632.3758	-4.0139
20090910	172746	825826.6349	817626.1330	-3.9820
20090910	172639	825826.6418	817626.1347	-3.9806
20090910	172530	825826.6474	817626.1367	-3.9807
20090910	172424	825826.6522	817626.1384	-3.9800
20090910	172317	825826.6588	817626.1407	-3.9787
20090910	172211	825826.6642	817626.1434	-3.9795

---

20090910	172105	825826.6701	817626.1448	-3.9796
20090910	171960	825826.6760	817626.1461	-3.9782
20090910	171855	825826.6814	817626.1488	-3.9790
20090910	171750	825826.6814	817626.1488	-3.9790
20090910	171644	825826.6927	817626.1528	-3.9792
20090910	171454	825826.7023	817626.1555	-3.9786
20090910	171349	825826.7106	817626.1592	-3.9780
20090910	171245	825826.7223	817626.1619	-3.9796
20090910	171001	825826.7339	817626.1653	-3.9791
20090910	170858	825826.7339	817626.1653	-3.9783
20090910	170754	825826.7341	817626.1646	-3.9783
20090910	170650	825826.7360	817626.1653	-3.9777
20090910	170548	825826.7398	817626.1666	-3.9770
20090910	170444	825826.7493	817626.1700	-3.9757
20090910	170341	825826.7580	817626.1723	-3.9751
20090910	170238	825826.7646	817626.1747	-3.9766
20090910	170136	825826.7737	817626.1787	-3.9753

---

---

20090910	170034	825826.7813	817626.1814	-3.9754
20090910	165930	825826.7907	817626.1848	-3.9756
20090910	165828	825826.7992	817626.1878	-3.9764
20090910	165726	825826.8074	817626.1915	-3.9758
20090910	165624	825826.8156	817626.1952	-3.9752
20090910	165522	825826.8232	817626.1979	-3.9768
20090910	165420	825826.8307	817626.2006	-3.9776
20090910	165319	825826.8372	817626.2029	-3.9806
20090910	165217	825826.8459	817626.2053	-3.9814
20090910	165115	825826.8525	817626.2076	-3.9815
20090910	165013	825826.8596	817626.2117	-3.9809
20090910	164912	825826.8669	817626.2151	-3.9782
20090910	164812	825826.8714	817626.2174	-3.9804
20090910	164711	825826.8801	817626.2197	-3.9819
20090910	164609	825826.8876	817626.2224	-3.9813
20090910	164508	825826.8952	817626.2251	-3.9793
20090910	164407	825826.9031	817626.2295	-3.9808

---

---

20090910	164306	825826.9116	817626.2325	-3.9831
20090910	164205	825826.9163	817626.2342	-3.9846
20090910	164103	825826.9210	817626.2359	-3.9847
20090910	164003	825826.9255	817626.2382	-3.9840
20090910	163902	825826.9259	817626.2399	-3.9841
20090910	163802	825826.9325	817626.2423	-3.9827
20090910	163700	825826.9373	817626.2440	-3.9821
20090910	163559	825826.9429	817626.2460	-3.9822
20090910	163459	825826.9486	817626.2480	-3.9815
20090910	163357	825826.9573	817626.2504	-3.9795
20090910	163256	825826.9648	817626.2531	-3.9796
20090910	163044	825826.9860	817626.2591	-3.9813
20090910	160541	825827.1960	817626.3371	-3.9880
20090910	160440	825827.2007	817626.3387	-3.9881
20090910	160339	825827.2075	817626.3404	-3.9896
20090910	160238	825827.2122	817626.3421	-3.9896
20090910	160137	825827.2174	817626.3424	-3.9904

---

---

20090910	160037	825827.2223	817626.3434	-3.9919
20090910	155936	825827.2279	817626.3455	-3.9927
20090910	155835	825827.2376	817626.3481	-3.9928
20090910	155734	825827.2423	817626.3498	-3.9936
20090910	155633	825827.2498	817626.3525	-3.9937
20090910	155532	825827.2583	817626.3555	-3.9939
20090910	155431	825827.2677	817626.3589	-3.9940
20090910	155330	825827.2821	817626.3633	-3.9935
20090910	155229	825827.2972	817626.3687	-3.9937
20090910	155128	825827.3167	817626.3764	-3.9940
20090910	155027	825827.3365	817626.3834	-3.9936
20090910	154926	825827.3532	817626.3902	-3.9931
20090910	154647	825827.3928	817626.4043	-3.9930
20090911	183329	825814.6198	817621.9237	-3.9571
20090911	183228	825814.8491	817622.0041	-3.9569
20090911	183128	825815.0796	817622.0841	-3.9568
20090911	183027	825815.1535	817622.1093	-3.9567

---

---

20090911	182653	825815.1538	817622.1114	-3.9567
----------	--------	-------------	-------------	---------

20090911	182552	825815.1538	817622.1114	-3.9567
----------	--------	-------------	-------------	---------

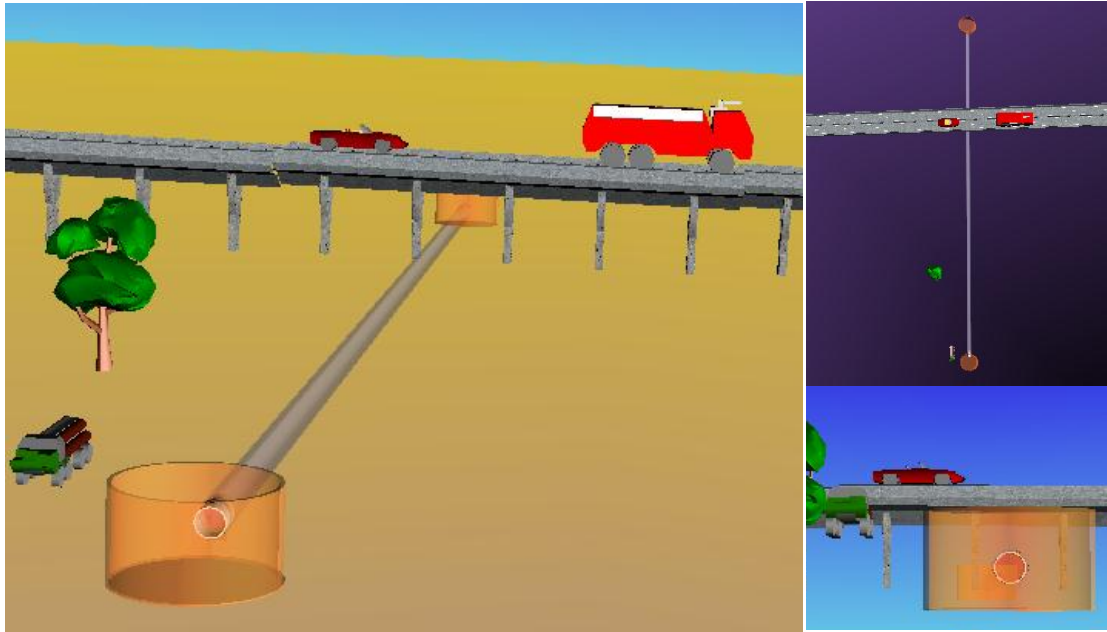
---

### ***6.3.2 3D Geometric modeling***

Design of a graphical representation is of great importance for the effective delivery of information of the equipment and the working environment to enable remote control (Seo et al. 2000). The geometric modelling maps the real construction site layout to the 3D virtual world. Geometric modelling describes the 3D shape and dimensions of objects as well as their appearances, such as texture, surface reflection coefficients, and colour.

There are two types of objects to be modelled, namely, the static objects (i.e. the existing facilities, jacking shaft, receiving shaft, the designed tunnel and surrounding environments like trees), and the moving objects (i.e. the MTBM). Any commonly used 3D CAD modelling tools (e.g. AutoCAD, 3D MAX, and SketchUp) can be applied to model these objects. It is important to note each component of a moving object should be modelled separately, while their relative position and orientation will be dynamically determined by the kinematic model. As shown in Figure 6-5, the designed tunnel, the jacking pit, the receiving pit, and the adjacent existing infrastructure are modelled as static objects in the virtual world. The MTBM is modelled as five standalone sub-

models, namely the rear part, the hydraulic cylinders of three push jacks and the cutter head.



**Figure 6-5: The static 3D models for a micro-tunneling project**

### ***6.3.3 Kinematic modeling***

The geometric modeling generates the static 3D geometry which is not sufficient for expressing the motion of objects in the real world. The kinematic modelling mathematically represents the dynamic position and orientations (pose) of site objects in the time-dependent 3D virtual world. The kinematic model can be built by using techniques discussed in Chapter 5.

Figure 6-6 shows the kinematic model of MTBM modeled using the graphic blocks. A body block represents a user-defined rigid body, which is defined by mass, inertia tensor, coordinate origins and axes for center of gravity and other user-specified body

coordinate systems. As shown in Figure 6-6 , the five body blocks represent the rear part of TBM, the cutter head and the three hydraulic cylinders, respectively. The rear part of TBM is linked with the hydraulic cylinders by prismatic joints, while the cutter head is linked with the hydraulic cylinders by spherical joints. A prismatic joint represents one translational degree of freedom. The follower body (F) translates relative to the base body (B) along a single translational axis connecting the origins of two body coordinate systems. A spherical joint represents three rotational degrees of freedom. The follower body pivots freely relative to the base body at the collocated origin of the two body coordinate systems.

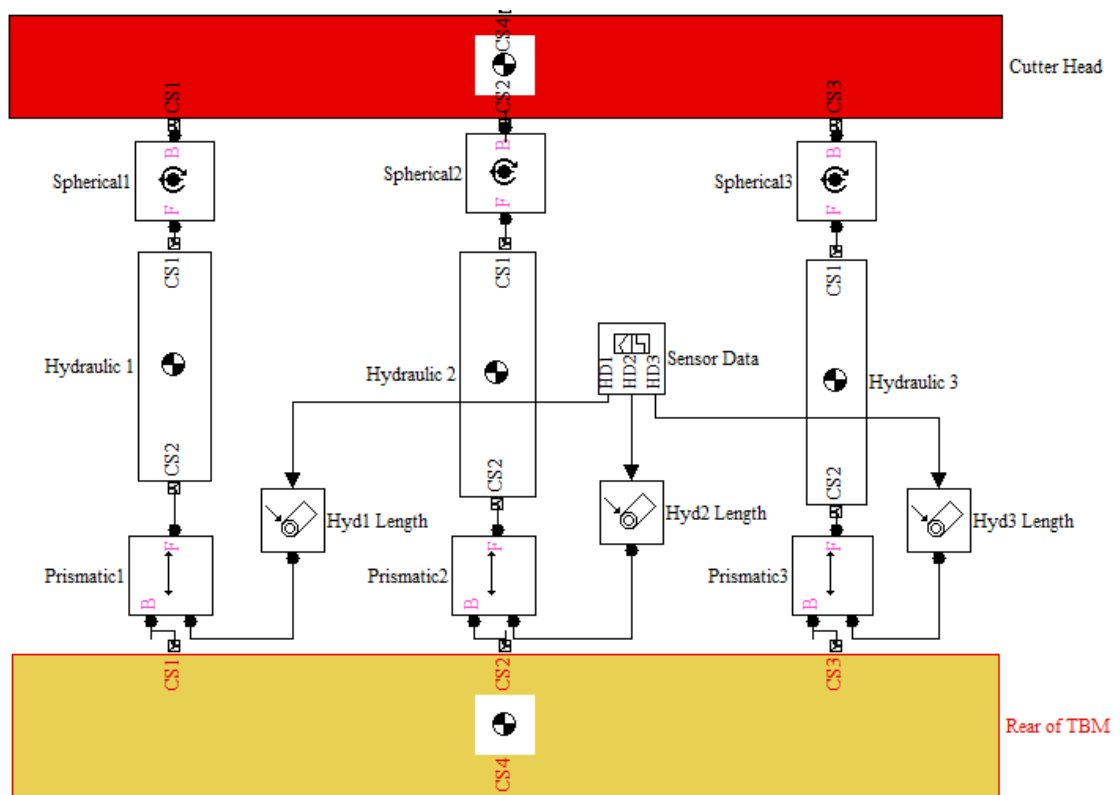


Figure 6-6: The kinematic model of MTBM in Simulink environment



The push or pull operations on the hydraulic cylinders induce the pose changes of the head cutter, which provides a mechanism to adjust the drilling direction. The kinematic model provides an interface for inputting the length information of the piston rods of hydraulic cylinders.

### 6.3.4 “Points to matrix” transformation

The “points to matrix” transformation algorithm proposed in Chapter 3 is coded as a user-defined function (as discussed in Chapter 5). The input parameters of the function are the coordinates of three tracking points on MTBM, while the output is the position and orientation information in the form of a  $4 \times 4$  homogeneous transformation matrix.

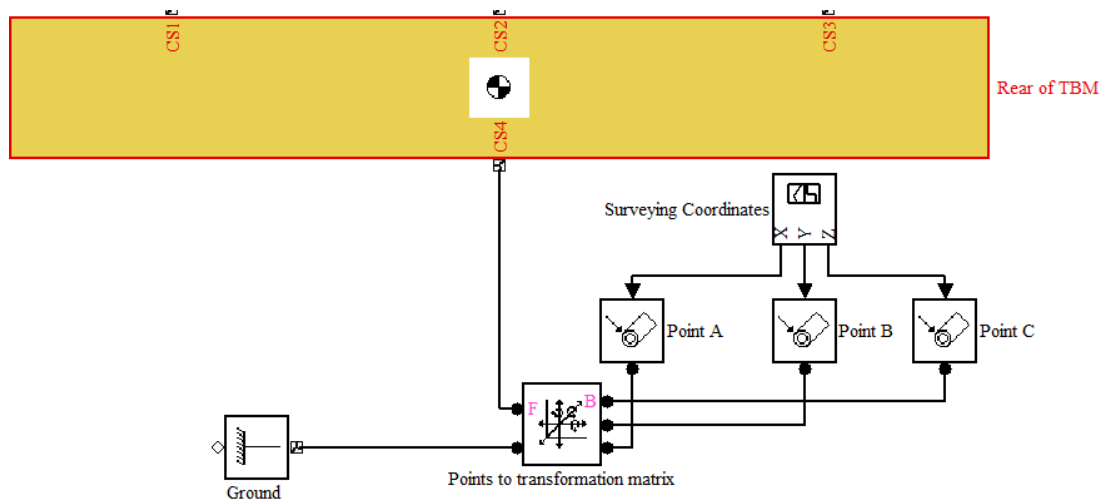


Figure 6-7: Coding the “points to matrix” transformation algorithm in user-defined application blocks

## 6.4 Potential benefits and limitations

Based on the prepared input data and the developed “Controller”, two virtual experiments were conducted in a computer simulation environment in order to evaluate

the applicability of the proposed methodology. The first experiment was to evaluate the possibility of applying the proposed methodology for 3D positioning and visualization of the rear part of the MTBM to support tunnelling alignment control. Then, a second experiment was conducted to evaluate the possibility to apply the methodology for 3D positioning and visualization of the articulated cutter head control system in order to support the TBM steering control.

#### ***6.4.1 Positioning and visualization of MTBM's position and orientation***

As shown in Figure 6-8, the collected data (coordinates of three tracking points) are transferred by the “points to matrix” transformation algorithm which generates the position and orientation definitions (“**RT**” in Figure 6-8) of the rear part of the MTBM.

The VR graphic engine uses the computing results to update the position of the rear part of the MTBM model. In order to visualize the positioning result, a “tracer application block” is used to simulate the 3D models of installed tunnel segments. The “tracer application block” is a built-in block in the Simulink environment that provides the function of placing small 3D segment behind a moving object to visualize the object's moving path. The tracer block also provides an interface to change the color of the tunnel segments into yellow during the drilling process, symbolizing the actually completed tunnel.

Figure 6-8 illustrates the results from the experiments, alignment deviations can be visualized based on the input of the point coordinate data. We can also navigate in the virtual world to examine the details of the alignment and spatial relationships between the tunnel being installed and any existing underground facilities. The visualization results show that the proposed methodologies have significant potentials to be applied for tunneling alignment guidance and “as-built” tunnel surveying. The underground situation, which is invisible in current industry practices, can be visualized with high accuracy and in real time on computer screens.

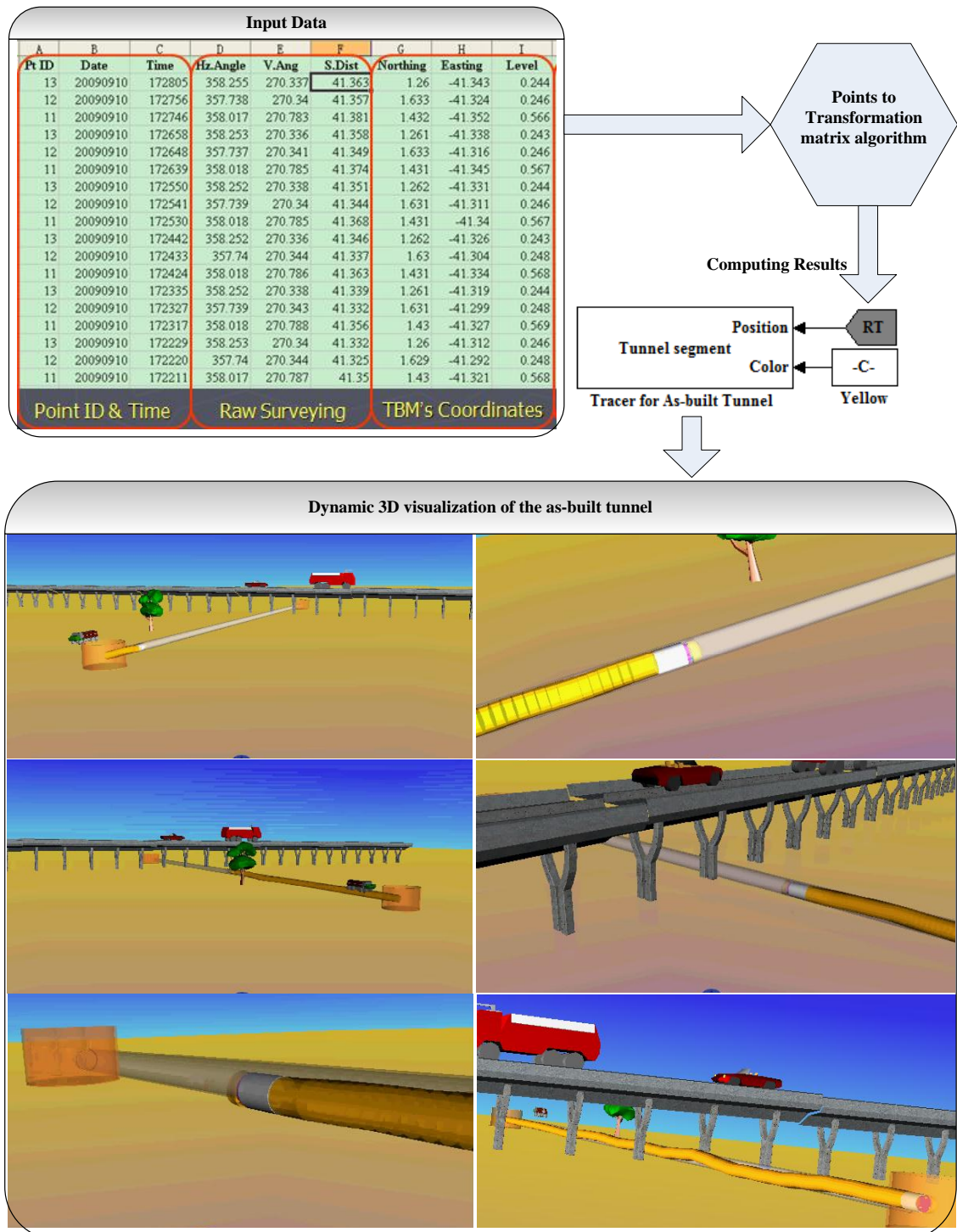
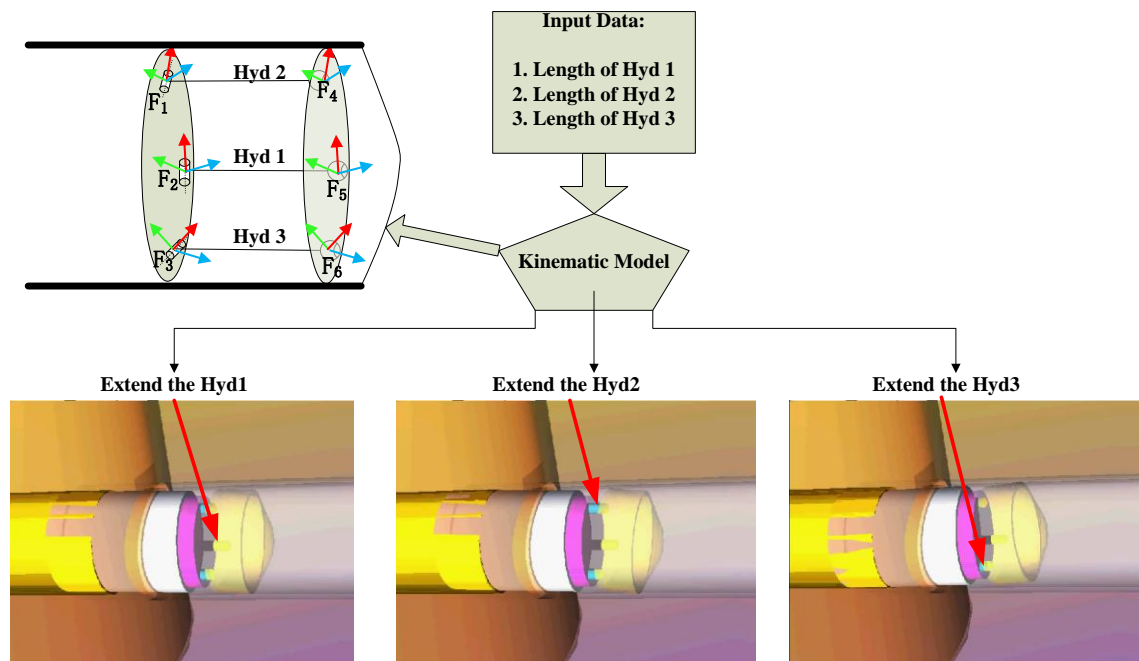


Figure 6-8: The data flow and visualization result of the first experiment

### 6.4.2 Positioning and visualization of cutter head control system

Based on the position and orientation information (“RT” and “RR” in Figure 6-9) from the first experiment and the piston rods’ length data, the kinematic model generates the

position (translation vector) and orientation (rotation matrix) of the five body elements of the TBM. The computing results are used to update the 3D geometric models in the virtual reality environment. The data flow of the second experiment is given in Figure 6-9.



**Figure 6-9: The data flow and visualization results of the second experiment**

As shown in Figure 6-9, the changes of the piston rods' lengths can be exactly reflected in the virtual reality environment. Any change of the control jacks will result in the position and orientation changes on the cutter head. We can navigate (rotate and scale the 3D view, zoom in and out) in the virtual world to check the orientation of the cutter head. The visualization results show the significant potential of the proposed approach to support operators in making fast and sound decisions during steering MTBM in the invisible working space.

### ***6.4.3 Limitations and future work***

The above virtual experiments demonstrate the possibility to apply the proposed methodologies for positioning a MTBM during pipe-jacking operations. However, there are some limitations that should be addressed in planning for field application of the methodologies on real tunneling projects.

Positioning and visualization of the rear part of the MTBM entails the surveying of several target points on the TBM, which requires the line-of-sight between the total station and TBM working in the underground space. Thus, the proposed methodologies cannot be reliably applied in the tunnel with curved alignment design, in which case the line-of-sight between the total station and the TBM cannot be guaranteed. However, for the large diameter tunnel project, where the total station can be installed in the tunnel, it is still possible to apply the proposed methodologies by moving the total station with the advancement of the TBM in order to maintain the line-of-sight availability.

Due to the time and site constraints, this research only evaluated the application possibility of the proposed methodologies for positioning and visualization of TBM based on computer simulations. Future research should apply and validate the proposed methodologies in the real construction field subject to practical site constraints before implementing the proposed methodologies in practical tunneling construction.

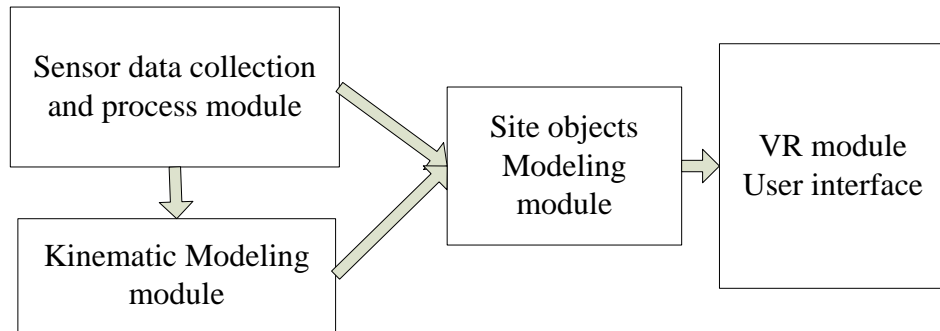
## **6.5 Future development of visualization system**

The evaluation is conducted by using the visualization tool in the Simulink environment.

The tool is originally developed for mechanical system design, which lacks effective interfaces for real-time data communication. Thus, it is difficult to synchronize automated data collection system and the visualization system for real-time updating. Thus, the future research needs to develop a customized real-time construction operation 3D positioning visualization system in order to facilitate the wide application of the proposed methodologies.

The fundamental mechanisms under the real-time 3D positioning and visualization of construction resources are not different from the 4D visualization. Both must provide functions to update the time-dependent properties of corresponding data models. Thus it is straightforward to implement the framework based on the state-of-the-art 4D techniques. The implementation may extend the current 4D applications into the construction process level in order to support both virtual management and physical engineering tasks.

As shown in Figure 6-10, four modules need to be developed to implement the proposed framework, namely, (1) sensor data collection and process module, (2) kinematic modeling module, (3) site objects modeling module, and (4) virtual reality (VR) module.



**Figure 6-10: The modules and data flow of next generation 4D system for real-time 3D visualization of construction operations**

The sensor data collection and process module is responsible for controlling various sensors for positioning the equipment. The raw data collected should be verified and filtered in this module to facilitate follow-up computations. There are generally two types of data: the first type of data can be directly used to update site object models, while the second type of data is used by the kinematic modeling module.

The kinematic modeling module should be developed based on the graphical network modeling technique introduced in Chapter 5. The core of the module is mathematical equations described in Chapter 4. Thus a computation engine should be developed in this module to solve the equations based on the input parameters from the data collection system. The computational results are in terms of the rotation matrix and translation vectors which will be used to update the position and orientation of site object models.



The site objects modeling module is used to create and organize the data models of construction resources. It is not necessary to provide functions to model the 3D geometric models, since there are many powerful commercially available 3D CAD tools in the market place. This module only needs to provide the interface to import the geometric data from the data files generated by these 3D CAD tools. The commonly used 3D geometric data file formats include Autodesk DWG, DXF, VRML file WRL, COLLADA and 3DS. Regardless of the file formats, the geometric data should be organized and stored according to the proposed data models.

The virtual reality (VR) module contains a 3D graphic engine which renders data models in computer displays. In order to facilitate the application, it must provide user friendly interfaces that allow users to manipulate the virtual reality environment (such as navigation, zoom in and zoom out.)

## **6.6 Summary**

Positioning and visualization of a MTBM that is working underground is useful for tunneling alignment control and MTBM steering control. This chapter discusses the application procedure and the possibility to apply the proposed methodologies for 3D positioning and visualization of MTBM during microtunneling and pipe-jacking operations.

The virtual experiments show that the proposed methodology can build dynamic and real-time 3D virtual reality scenes that can be utilized to support tele-operations of the MTBM as well as tunnel alignment control. The limitation of the methodologies in positioning TBM has also been discussed and future work as needed to overcome practical site constraints and to realize field implementation of the proposed methodologies has been proposed.

## ***Chapter 7***

### ***Conclusions***

Real-time 3D positioning and visualization of construction resources entails frequently updating the position and orientation of the 3D design models based on positioning and sensor data fed back from site in real time. This provides construction engineers with accurate spatial information about the building component being handled and the construction equipment in operation. The frequently updated positioning information and 3D models also produce cost effective and accurate virtual references for locating and positioning building components and construction equipment in the field.

#### **7.1 Contributions**

This research first classifies construction resources into two categories, namely: solid object and articulated system. Generic data models are proposed for storing and organizing the two types of construction resources. Then a “points to matrix” algorithm is developed to compute the 3D positioning parameters of solid object. The 3D positioning parameters are defined as time-dependent transformation matrices resulting from the coordinate values (x, y, and z) of a limited quantity of control points, which can be tracked by sensor technology or surveying technology like a robotic total station.

The proposed methodology was validated through a laboratory test by utilizing a robotic total station.

In contrast with the building component which can generally be treated as a single solid object, an articulated equipment system normally consists of a set of rigid bodies connected by joints, which is termed as a kinematic chain. The relative motion and constraints between articulated bodies of the chain make the real-time 3D positioning and visualization a challenge. It is vital to address how to collect field data from equipment by using inexpensive nonintrusive and unconstructive sensors while minimizing the quantity of sensors as needed by applications on practical construction sites. The Denavit-Hartenberg (DH) technique, which is widely used in robotics research, is introduced and adapted for computing the relative motions of various components in the equipment system based on a minimal quantity of input variables. The proposed methodology is applied for visualizing a backhoe excavator in a 3D computer environment. The location of the backhoe excavator's track is computed by using the "points to matrix" algorithm, while the 3D position matrices for the cabin, boom, stick and bucket are deduced by combining the DH technique and hydraulic jacks' length data which can be readily obtained from linear encoders.

Considering the dynamic nature of the construction industry, where new construction methods and equipment are being continuously adopted, coding the proposed

methodologies in the computer system in an “ad hoc” manner requires long time and major programming efforts, thus making the application prohibitively expensive and practically infeasible. In response to the construction application needs, a graphic network modeling technique which is used in mechanical simulation systems has been adapted to tackle the real-time 3D positioning and visualization of articulated equipment systems in construction.

In short, this research has contributed three aspects of new knowledge in the field of construction engineering. First, instead of using expensive devices, the 3D position of solid objects can be analytically fixed by tracking a limited quantity of control points. The resulting analytical method has been successfully validated by numerical analysis and laboratory experiments. Second, the 3D position of articulated construction equipment can be analytically fixed by processing input data of tracking point coordinates and joint movement parameters. This analytical method is validated by simulating a backhoe excavator in the computer environment, where the location of the backhoe’ tracks is computed by using the “points to matrix” algorithm, and the positioning states of the cabin, boom, stick and bucket are deduced by using the DH technique. Last, the possibility of applying the developed methodologies in real-time 3D visualization of microtunneling operations has been evaluated. The kinematic chain of the tunnel boring machine (TBM) is modeled by a straightforward graphic network

modeling approach instead of undertaking major computer programming development.

The positioning of TBM's cutter head which is not visible in most TBM guidance systems can be visualized in computer 3D graphics. Thus, a TBM operator in a remote control station can make more informed decisions as regards how to steer the TBM drilling in the complicated underground space along the as-designed tunnel alignment.

This research has also revealed the needs for developing a graphic network modeling tool for complicated construction equipment system modeling. The Simulink tool adopted in this research is for prototyping and validating the graphic modeling techniques proposed for real-time 3D positioning and visualization of construction resources. However, the Simulink tool lacks the functionality for real-time data capturing and processing. It is still very difficult to apply the Simulink tool directly on a construction project in order to materialize the intended benefits. Thus, based on the methodologies developed in this research, a customized tool, which is analogous to Simulink but caters for real-time 3D positioning and visualization of construction equipment, need to be developed in the future based on proposed methodologies. This would be crucial and conducive to the development of next generation 4D application systems in construction.

## **7.2 Directions for future research**

This research has investigated the methodologies required to generate real-time 3D virtual reality environment reflecting ongoing construction operations on site. The thesis, while significantly advancing the state of the art in research, has revealed following important issues for future research to address.

### ***7.2.1 Interaction between solid objects and articulated systems***

This research has looked into 3D positioning and visualizing single solid objects and articulated systems without considering their interactions. However, the interaction between them (e.g. interaction between building elements and mobile cranes) is an interesting research topic. For example, knowing the position and orientation of a building element and given the contact position, it is possible to deduce the pose of the mobile crane by using the principles of inverse kinematics. The interaction between single solid objects and articulated systems, can bring about the benefits of reducing the requirements of sensor data as input, facilitating the trajectory planning in large-scale building components lifting operations, and will eventually lead towards the development of automated assembly by using robotic cranes in the construction field.

### ***7.2.2 Automated as-built modeling***

Since the construction operations can be fully tracked and visualized in a virtual reality environment, it is straightforward to realize the automated as-built modeling by using the collected data. In Chapter 6, the TBM can be treated as a *probe* for realizing

constructed tunnel as-built 3D modeling. The as-built modeling has been simplified, which is sufficient for the microtunneling application. However, more sophisticated methodologies for as-built modeling are desired to address construction component installation with more complicated configuration and higher measurement accuracy.

### ***7.2.3 Considering dynamics***

In contrast with kinematics, dynamics studies the forces and the results of the forces such as motion and object deformation. Essentially, construction operations are physical processes that evolve over time which are governed by physical laws (e.g. Newton's second law of motion.) More benefits can be gained by studying the dynamics through real-time monitoring of deformations and stresses on the construction element as well as the construction equipment. The accidents during construction operations, such as rollover due to the overload of lifting equipment, can be minimized by real-time monitoring of such dynamical features of construction resources in the virtual reality environment.



**Appendix A. Matlab function of the “point to matrix” custom block**

% “dp” is the coordinates of three points at time event one, “bp” is the coordinates of the three points at time event two %

Function [R, T, D] = points2TransPara (bp, DP)

n=3; %number of points

x1\_bar= (DP (1) +DP (4) +DP (7))/n;

y1\_bar= (DP (2) +dp (5) +dp (8))/n;

z1\_bar=(dp(3)+dp(6)+dp(9))/n;

x1\_p=[x1\_bar y1\_bar z1\_bar]; %mean coordinates

%point coordinates at time event one.

x11\_p=dp(1:3)'-x1\_p;

x12\_p=dp(4:6)'-x1\_p;

x13\_p=dp(7:9)'-x1\_p;

x2\_bar=(bp(1)+bp(4)+bp(7))/n;

```

y2_bar=(bp(2)+bp(5)+bp(8))/n;

z2_bar=(bp(3)+bp(6)+bp(9))/n;

x2_p=[x2_bar y2_bar z2_bar];

%point coordinates at time event two.

x21_p=bp(1:3)'-x2_p;

x22_p=bp(4:6)'-x2_p;

x23_p=bp(7:9)'-x2_p;

%constructs the cross-dispersion matrix

c=(x21_p'*x11_p+x22_p'*x12_p+x23_p'*x13_p)/n;

[u,w,v]=svd(c); %SVD decomposition

temp=[1 0 0;0 1 0;0 0 det(u*v)];

R_temp=u*temp*v'; %Rotation matrix

Yaw=atan(-R_temp(2,1)/R_temp(1,1));

Roll=asin(R_temp(3,1));

Pitch=atan(-R_temp(3,2)/R_temp(3,3));

```

```
D=[Yaw,Pitch,Roll]*180/pi; % Three rotation angles
```

```
R=R_temp(:); % Three rotation angles
```

**Appendix B. Data collected by the total station**

Movement	Point ID	Date	Time	Hz Angle	V Angle	Distance
	<b>11</b>	<b>20100520</b>	<b>161336</b>	<b>66.808</b>	<b>90.822</b>	<b>9.254</b>
	<b>12</b>	<b>20100520</b>	<b>161407</b>	<b>65.583</b>	<b>93.2</b>	<b>9.259</b>
	<b>13</b>	<b>20100520</b>	<b>161427</b>	<b>68.19</b>	<b>93.207</b>	<b>9.296</b>
	11	20100520	161624	66.808	90.821	9.255
	12	20100520	161633	65.583	93.2	9.26
	13	20100520	161642	68.191	93.206	9.296
	11	20100520	161731	66.808	90.821	9.255
Initial Position	12	20100520	161739	65.583	93.2	9.26
	13	20100520	161748	68.191	93.205	9.296
	11	20100520	161836	66.808	90.821	9.254
	12	20100520	161845	65.583	93.199	9.26
	13	20100520	161854	68.191	93.207	9.296
	11	20100520	162059	66.806	90.83	9.249
	12	20100520	162109	65.61	93.21	9.226
	13	20100520	162119	68.114	93.193	9.322

	<b>11</b>	<b>20100520</b>	<b>162421</b>	<b>66.778</b>	<b>90.825</b>	<b>9.251</b>
	<b>12</b>	<b>20100520</b>	<b>162431</b>	<b>65.59</b>	<b>93.211</b>	<b>9.222</b>
	<b>13</b>	<b>20100520</b>	<b>162442</b>	<b>68.088</b>	<b>93.192</b>	<b>9.33</b>
	11	20100520	162530	66.725	90.818	9.253
Position 1	12	20100520	162539	65.501	93.197	9.259
	13	20100520	162550	68.106	93.206	9.294
	11	20100520	162638	66.725	90.819	9.253
	12	20100520	162648	65.501	93.198	9.259
	13	20100520	162656	68.106	93.206	9.294
	<b>11</b>	<b>20100520</b>	<b>162746</b>	<b>66.698</b>	<b>90.498</b>	<b>9.331</b>
	<b>12</b>	<b>20100520</b>	<b>162755</b>	<b>65.502</b>	<b>92.838</b>	<b>9.268</b>
	<b>13</b>	<b>20100520</b>	<b>162805</b>	<b>68.105</b>	<b>92.86</b>	<b>9.303</b>
	11	20100520	162855	66.729	90.819	9.254
Position 2	12	20100520	162904	65.505	93.197	9.259
	13	20100520	162915	68.111	93.206	9.295
	11	20100520	163004	66.729	90.819	9.254
	12	20100520	163013	65.504	93.197	9.259

	13	20100520	163022	68.111	93.205	9.295
	<b>11</b>	<b>20100520</b>	<b>163112</b>	<b>66.411</b>	<b>90.69</b>	<b>9.248</b>
	12	20100520	163124	65.455	93.186	9.259
	13	20100520	163134	68.048	92.912	9.289
	11	20100520	163447	66.425	90.682	9.248
Position 3	12	20100520	163458	65.485	93.184	9.259
	13	20100520	163511	68.074	92.895	9.29
	11	20100520	163560	66.426	90.682	9.248
	12	20100520	163609	65.485	93.183	9.259
	13	20100520	163620	68.075	92.895	9.289

## ***References:***

Abourizk, S. M., Halpin, D. W., and Lutz, J. D. (1992). "State-of-the-Art in Construction Simulation." 1992 Winter Simulation Conference Proceedings, 1271-1277.

Aoshima, S., Takeda, K., and Yabuta, T. (1993). "Autotuning of Feedback Gains Using a Neural-Network for a Small Tunneling Robot." *Jsmc International Journal Series C-Dynamics Control Robotics Design and Manufacturing*, 36(4), 435-441.

Beggs, J. S. (1983). *Kinematics*, Taylor & Francis.

Behzadan, A. H., Aziz, Z., Anumba, C. J., and Kamat, V. R. (2008). "Ubiquitous location tracking for context-specific information delivery on construction sites." *Automation in Construction*, 17(6), 737-748.

Beliveau, Y. J., Williams, J. M., King, M. G., and Niles, A. R. (1995). "Real-Time Position Measurement Integrated with Cad - Technologies and Their Protocols." *Journal of Construction Engineering and Management*, 121(4), 346-354.

Bernold, L. E. (2002). "Spatial integration in construction." *Journal of Construction Engineering and Management*, 128(5), 400-408.

Blaauw, G. A., Brooks, J., and P, F. (1997). *Computer Architecture-Concepts and Evolution*, Addison-Wesley.

Black, P. E. (2004). " "data structure", in Dictionary of Algorithms and Data Structures", U.S. National Institute of Standards and Technology.

Caldas, C. H., Torrent, D. G., and Haas, C. T. (2006). "Using global positioning system to improve materials-locating processes on industrial projects." *Journal of Construction Engineering and Management*, 132(7), 741-749.

Carlson, W. (2003). "A Critical History of Computer Graphics and Animation", The Ohio State University.

Carman, A. B., and Milburn, P. D. (2006). "Determining rigid body transformation parameters from ill-conditioned spatial marker co-ordinates." *Journal of Biomechanics*, 39(10), 1778-1786.

Challis, J. H. (1995). "A Procedure for Determining Rigid-Body Transformation Parameters." *Journal of Biomechanics*, 28(6), 733-737.

Cheng, T., and Teizer, J. (2010). "Real-time data collection and visualization technology in construction." *Construction Research Congress, Banff, Canada.*

Chin, S., Yoon, S., Choi, C., and Cho, C. (2008). "RFID+4D CAD for progress management of structural steel works in high-rise buildings." *Journal of Computing in Civil Engineering*, 22(2), 74-89.



Cho, Y. K., and Haas, C. T. (2003). "Rapid geometric modeling for unstructured construction workspaces." *Computer-Aided Civil and Infrastructure Engineering*, 18(4), 242-253.

Cho, Y. K., Haas, C. T., Liapi, K., and Sreenivasan, S. V. (2002). "A framework for rapid local area modeling for construction automation." *Automation in Construction*, 11(6), 629-641.

CompHist.org. (2004). "A Brief History of Computer Graphics." [http://www.comphist.org/computing\\_history/new\\_page\\_6.htm](http://www.comphist.org/computing_history/new_page_6.htm).

Dai, F., and Lu, M. (2008). "Photo-Based 3d Modeling of Construction Resources for Visualization of Operations Simulation: Case of Modeling a Precast Facade." 2008 Winter Simulation Conference, Vols 1-5, 2439-2446.

Dai, F., and Lu, M. (2010). "Assessing the Accuracy of Applying Photogrammetry to Take Geometric Measurements on Building Products." *Journal of Construction Engineering and Management*, 136(2), 242-250.

Denavit, J., and Hartenberg, R. S. (1995). "A kinematic notation for lower-pair mechanisms based on matrices." *Journal of Applied Mechanics*, 22, 215-221.

Ergen, E., Akinci, B., East, B., and Kirby, J. (2007a). "Tracking components and maintenance history within a facility utilizing radio frequency identification technology." *Journal of Computing in Civil Engineering*, 21(1), 11-20.

Ergen, E., Akinci, B., and Sacks, R. (2007b). "Tracking and locating components in a precast storage yard utilizing radio frequency identification technology and GPS." *Automation in Construction*, 16(3), 354-367.

Ghilani, C. D., and Wolf, P. R. (2008). *Elementary surveying: an introduction to geomatics*, Pearson Prentice Hall, New Jersey, U.S.

Grigore, B., and Coiffet, P. (2003). *Virtual reality technology*, Hoboken, N.J.: Wiley-Interscience.

Halpin, D. W. (1977). "CYCLONE: Method for Modeling of Job Site Processes." *Journal of the Construction Division, ASCE*, 103(3), 489-499.

Hartmann, T., and Fischer, M. (2007). "Supporting the constructability review with 3D/4D models." *Building Research and Information*, 35(1), 70-80.

Hartmann, T., Gao, J., and Fischer, M. (2008). "Areas of application for 3D and 4D models on construction projects." *Journal of Construction Engineering and Management*, 134(10), 776-785.

Hegab, M. Y., and Smith, G. R. (2007). "Delay time analysis in microtunneling projects." *Journal of Construction Engineering and Management-Asce*, 133(2), 191-195.

Hirabayashi, T., Akizono, J., Yamamoto, T., Sakai, H., and Yano, H. (2006). "Teleoperation of construction machines with haptic information for underwater applications." *Automation in Construction*, 15(5), 563-570.

Kamat, V. R., and Martinez, J. C. (2000). "3D visualization of simulated construction operations." *Proceedings of the 2000 Winter Simulation Conference*, Vols 1 and 2, 1933-1937.

Kamat, V. R., and Martinez, J. C. (2001). "Visualizing simulated construction operations in 3D." *Journal of Computing in Civil Engineering*, 15(4), 329-337.

Kamat, V. R., and Martinez, J. C. (2004). "Dynamic three-dimensional visualization of fluid construction materials." *Journal of Computing in Civil Engineering*, 18(3), 237-247.

Kamat, V. R., and Martinez, J. C. (2005). "Dynamic 3D visualization of articulated construction equipment." *Journal of Computing in Civil Engineering*, 19(4), 356-368.

Kamat, V. R., and Martinez, J. C. (2008). "Software mechanisms for extensible and scalable 3D visualization of construction operations." *Advances in Engineering Software*, 39(8), 659-675.

Khalil, W., and Dombre, E. (2002). *Modeling, identification & control of robots*, HPS, London.

Khoury, H. M., and Kamat, V. R. (2009). "Evaluation of position tracking technologies for user localization in indoor construction environments." *Automation in Construction*, 18(4), 444-457.

Kiziltas, S., Akinci, B., Ergen, E., Tang, P., and Gordon, C. (2008). "Technological assessment and process implications of field data capture technologies for construction and facility/infrastructure management." *Journal of Information Technology in Construction* 13, 134-154.

Lee, Y., and Gatton, T. M. (1994). "Construction scheduling based on resource constraints." *AACE Trans*, 3, 1-6.

Liang, X. (2011). " On-site visualization of building component erection enabled by integration of four-dimensional modeling and automated surveying " *Automation in Construction*.

Lu, M., Chen, W., Shen, X. S., Lam, H. C., and Liu, J. Y. (2007). "Positioning and tracking construction vehicles in highly dense urban areas and building construction sites." *Automation in Construction*, 16(5), 647-656.

Lu, M., Lam, H. C., and Dai, F. (2008). "Resource-constrained critical path analysis based on discrete event simulation and particle swarm optimization." *Automation in Construction*, 17(6), 670-681.

Lytle, A. M., and Saidi, K. S. (2007). "NIST research in autonomous construction." *Autonomous Robots*, 22(3), 211-221.

Lytle, A. M., Saidi, K. S., Bostelman, R. V., Stone, W. C., and Scott, N. A. (2004). "Adapting a teleoperated device for autonomous control using three-dimensional positioning sensors: experiences with the NIST RoboCrane." *Automation in Construction*, 13(1), 101-118.

Lytle, A. M., Saidi, K. S., Stone, W. C., and Gross, J. L. "Report of the NIST Workshop on Automated Steel Construction." 19th International Symposium on Automation and Robotics in Construction (ISARC), Gaithersburg, MD, 247-254.

Mahalingam, A., Kashyap, R., and Mahajan, C. (2010). "An evaluation of the applicability of 4D CAD on construction projects." *Automation in Construction*, 19(2), 148-159.

Manseur, R. (2006). Robot modeling and kinematics, Hingham, Mass. : Da Vinci Engineering Press.

MathWorks®. (2010a). "SimMechanics 3.2-Model and simulate mechanical systems."  
<http://www.mathworks.com/products/simulink/>.

MathWorks®. (2010b). "Simulink - Simulation and Model-Based Design."  
<http://www.mathworks.com/products/simulink/>.

McKinney, K., Kim, J., Fischer, M., and Howard, C. (1996). "Interactive 4D-CAD."  
Computing in Civil Engineering, 383-389.

Navon, R., Goldschmidt, E., and Shpatnisky, Y. (2004). "A concept proving prototype of automated earthmoving control." Automation in Construction, 13(2), 225-239.

OSG-Community. (2010). " OpenSceneGraph." <http://www.openscenegraph.org/projects/osg>.

Papachristou, A., Valsamos, H., and Dentsoras, A. (2010). "Optimal initial positioning of excavators in digging processes." Proceedings of the Institution of Mechanical Engineers Part I-Journal of Systems and Control Engineering, 224(I7), 835-844.

Rojas, E. M., and Lee, N. "Visualization of Project Control Data: A Research Agenda."  
Pittsburgh, Pennsylvania, USA, 4-4.

Seo, J., Haas, C. T., Saidi, K., and Sreenivasan, S. V. (2000). "Graphical control interface for construction and maintenance equipment." *Journal of Construction Engineering and Management*, 126(3), 210-218.

Seo, J. W., Haas, C., and Saidi, K. (2007). "Graphical modeling and simulation for design and control of a tele-operated clinker clearing robot." *Automation in Construction*, 16(1), 96-106.

Shen, X. S., Lu, M., and Chen, W. (2010). "Automatically Tracking and Guiding Underground Tunnel Boring Machines during Microtunneling and Pipe Jacking Operations." *Construction Research Congress, Banff, Canada*.

Shi, J. S., and AbouRizk, S. M. (1997). "Resource-based modeling for construction simulation." *Journal of Construction Engineering and Management-Asce*, 123(1), 26-33.

Shin, D. H., and Dunston, P. S. (2008). "Identification of application areas for Augmented Reality in industrial construction based on technology suitability." *Automation in Construction*, 17(7), 882-894.

Song, J., Haas, C. T., Caldas, C., Ergen, E., and Akinci, B. (2006). "Automating the task of tracking the delivery and receipt of fabricated pipe spools in industrial projects." *Automation in Construction*, 15(2), 166-177.

Song, J., Haas, C. T., and Caldas, C. H. (2007). "A proximity-based method for locating RFID tagged objects." *Advanced Engineering Informatics*, 21(4), 367-376.

Staub-French, S. (2007). " 3D and 4D modeling for design and construction coordination: issues and lessons learned." *Journal of Information Technology in Construction*, 12, 381-407.

Teizer, J., Venugopal, M., and Walia, A. (2008). "Ultrawideband for Automated Real-Time Three-Dimensional Location Sensing for Workforce, Equipment, and Material Positioning and Tracking." *Transportation Research Record*(2081), 56-64.

Torrent, D. G., and Caldas, C. H. (2009). "Methodology for Automating the Identification and Localization of Construction Components on Industrial Projects." *Journal of Computing in Civil Engineering*, 23(1), 3-13.

Tsai, L. W. (1999). "Systematic enumeration of parallel manipulators." *Parallel Kinematic Machines*, 33-49.

Vince, J. (2004). *Introduction to Virtual Reality*, Springer London, New York.

Wang, L. C. (2008). "Enhancing construction quality inspection and management using RFID technology." *Automation in Construction*, 17(4), 467-479.



Wavering, A. J. (1998). "Parallel Kinematic Machine Research at NIST: Past, Present, and Future." First European-American Forum on Parallel Kinematic Machines, Milan, Italy.

Web3d.org. (1997). "The Virtual Reality Modeling Language."

Yoshida, K., and Awata, T. (2002). "Heading control model of a center-articulated micro-tunnelling robot." Sice 2002: Proceedings of the 41st Sice Annual Conference, Vols 1-5, 2418-2423.

Yoshida, K., and Haibara, T. (2005). "Turning behavior modeling for the heading control of an articulated micro-tunneling robot." Ieee Transactions on Robotics, 21(3), 513-520.